UNLV | UNIVERSITY LIBRARIES

UNLV Theses, Dissertations, Professional Papers, and Capstones

12-1-2015

Dissolution of Nontronite in Low Water Activity Brines and Implications for the Aqueous History of Mars

Michael Henry Steiner
University of Nevada, Las Vegas

Follow this and additional works at: https://digitalscholarship.unlv.edu/thesesdissertations

 Part of the Geochemistry Commons, and the Geology Commons

Repository Citation

Steiner, Michael Henry, "Dissolution of Nontronite in Low Water Activity Brines and Implications for the Aqueous History of Mars" (2015). *UNLV Theses, Dissertations, Professional Papers, and Capstones*. 2585.
http://dx.doi.org/10.34917/8220166

This Thesis is protected by copyright and/or related rights. It has been brought to you by Digital Scholarship@UNLV with permission from the rights-holder(s). You are free to use this Thesis in any way that is permitted by the copyright and related rights legislation that applies to your use. For other uses you need to obtain permission from the rights-holder(s) directly, unless additional rights are indicated by a Creative Commons license in the record and/or on the work itself.

This Thesis has been accepted for inclusion in UNLV Theses, Dissertations, Professional Papers, and Capstones by an authorized administrator of Digital Scholarship@UNLV. For more information, please contact digitalscholarship@unlv.edu.

DISSOLUTION OF NONTRONITE IN LOW WATER ACTIVITY BRINES AND IMPLICATIONS FOR THE AQUEOUS HISTORY OF MARS

by

Michael Henry Steiner

Bachelor of Science – Geoscience
University of Nevada, Las Vegas
2013

A thesis submitted in partial fulfillment
of the requirements for the

Master of Science - Geoscience

Department of Geoscience
College of Science
The Graduate College

University of Nevada, Las Vegas
December 2015

Copyright by Michael H. Steiner, 2015
All Rights Reserved

UNLV | GRADUATE COLLEGE

Thesis Approval

The Graduate College
The University of Nevada, Las Vegas

August 11, 2015

This thesis prepared by

Michael Henry Steiner

entitled

Dissolution of Nontronite in Low Water Activity Brines and Implications for Aqueous History of Mars

is approved in partial fulfillment of the requirements for the degree of

Master of Science – Geoscience
Department of Geosciences

Elisabeth Hausrath, Ph.D.
Examination Committee Chair

Kathryn Hausbeck Korgan, Ph.D.
Graduate College Interim Dean

Oliver Tschauner, Ph.D.
Examination Committee Member

Megan Elwood Madden, Ph.D.
Examination Committee Member

Brian Hedlund, Ph.D.
Graduate College Faculty Representative

Abstract

Dissolution of Nontronite in Low Water Activity Brines and Implications for the Aqueous History of Mars

Steiner, M.

Keywords: Mars, brines, clay minerals, astrobiology

Water is essential to life on Earth and is likely to play a role in determining the habitability of other planets. Pure liquid water is not stable on the surface of Mars but brines can temporarily remain liquid, and increasing evidence suggests the presence of recent liquid water, including brines, on Mars. Brines can host life at temperatures as low as -30 ºC and some organisms can live at activities of water as low as 0.61. Therefore, if brines have been present on Mars, they may act as habitable environments.

The Fe-rich smectite nontronite, $(CaO_{0.5},Na)_{0.3}Fe^{3+}_2(Si,Al)_4O_{10}(OH)_2 \cdot nH_2O$, has been detected on the surface of Mars, particularly in ancient terrains. If the surface of Mars experienced brine solutions throughout its history, those brines have likely impacted nontronite. Therefore, understanding alteration of nontronite in brines can help interpret past aqueous, and potentially habitable, conditions on Mars.

To interpret interactions of nontronite with brines, duplicate batch experiments were used to measure the dissolution rates of nontronite at 25 ºC at activities of water (aH_2O) of 1.00 (0.01 M $CaCl_2$ or NaCl representative of dilute waters), 0.75 (saturated NaCl and 3.00 mol kg^{-1} $CaCl_2$), and 0.50 (5.00 mol kg^{-1} $CaCl_2$). Experiments at aH_2O = 1 (0.01 M $CaCl_2$) were also conducted at 4 ºC, 25 ºC, and 45 ºC to calculate an apparent activation energy for dissolution of nontronite.

Results indicate that with decreasing activity of water the dissolution rate of nontronite also decreases. Dissolution rates at 25 ºC in $CaCl_2$-containing solutions decreased with decreasing activity of water as follows: $1.18x10^{-12} \pm 9.30\ x10^{-14}$ moles mineral $m^{-2}\ s^{-1}$($aH_2O = 1$)> $2.36x10^{-13} \pm 3.07\ x10^{-14}$ moles mineral $m^{-2}\ s^{-1}$(aH_2O = 0.75)> $2.05x10^{-14} \pm 2.87\ x10^{-15}$ moles mineral $m^{-2}\ s^{-1}$ ($aH_2O = 0.50$). Similar results were observed at 25 ºC in NaCl-containing solutions with dissolution rates as follows: $1.89x10^{-12} \pm 9.59\ x10^{-14}$ moles mineral $m^{-2}\ s^{-1}$ ($aH_2O = 1$)> $1.98x10^{-13} \pm 2.26x10^{-14}$ moles mineral $m^{-2}\ s^{-1}$($aH_2O = 0.75$). An apparent activation energy of 54.6 ± 1.0 kJ/mol was calculated from the following dissolution rates in dilute $CaCl_2$- containing solutions at temperatures of 4 ºC, 25 ºC, and 45 ºC: $2.33x10^{-13} \pm 1.25x10^{-14}$ moles mineral $m^{-2}\ s^{-1}$(4 ºC), $1.18x10^{-12} \pm 9.30\ x10^{-14}$ moles mineral $m^{-2}\ s^{-1}$(25 ºC), and $4.98x10^{-12} \pm 3.84\ x10^{-13}$ moles mineral $m^{-2}\ s^{-1}$(45 ºC).

These results suggest that martian nontronite perceptibly altered by brines at low temperatures may have experienced very long periods of water-rock interaction, with important implications for the paleoclimate and long-term potential habitability of Mars.

Acknowledgements

Credit for this thesis does not rest solely on the author as it has been influenced by more people than I can list on these pages.

I am lucky to have a supportive family who has always allowed me to pursue my interests. Mom and Dad, thank you for your countless sacrifices and support through all the years, I promise I will call more now that grad school is over. Ethan and Max, I could not ask for better brothers. When life gets tough, I know you are both there to make things easier. Uncle Chip and Aunt Debbi, thank you for opening your doors when I first came to Las Vegas. Grama, thank you for always thinking about me even when I am far away and lighting all of those candles after church to help me with school. Helen, you will always be my number one fan, thank you for all the reminders to put my heart and soul into everything I do.

Without my friends I would not be where I am today. Lauren, thank you for never letting me settle for less than my best, I am truly lucky to have you in my life. Greg, Taylor, Chris, and Joe, they say the best geologist is the one who has seen the most rocks, I think we have seen quite a few during our countless trips to Red Rock. Michael, Amanda, Jake, Victoria, Mike, Bannigan, Lince, and Jason, thanks for grabbing a drink, playing some hockey, hanging out or anything else to help me unwind.

Lastly, thank you to my advisor and officemates. Libby, my career path would be significantly different had you not hired me as an undergrad. Thank you for all of the opportunities you have provided and pushing me to succeed. Kirellos, without your next level training, I would not be the scientist I am today. Chris and Seth, the time in our office would not be the same without the countless debates, occasional video games, and

weekend burrito runs. Thanks Val for putting up with me when I started in the lab and Courtney for putting up with an office full of dudes. Thank you Renee and Angela for all of your hard work in the lab. Lastly to Jebediah Kerman for fueling my passion for planetary science.

Table of Contents

List of Tables

List of Figures

Chapter 1 Introduction

Liquid water is a necessary ingredient for life on Earth and its history on Mars is therefore essential to understanding the potential habitability of that planet. High ionic strength solutions (up to ~6.15 *m*) like brines are also able to host life at a wide range of temperature and water activities (Jones and Lineweaver, 2010). While current surface conditions on Mars are not able to sustain pure liquid water, brines may exist temporarily (Henderson-Sellers and Meadows, 1976; Brass, 1980; Haberle et al., 2001; Jones and Lineweaver, 2010; Martín-Torres et al., 2015). Chloride and chloride plus sulfate brines could be stable at present day temperatures on Mars (Brass, 1980) and increasing evidence points to their presence. Recurring Slope Lineae (RSL) growth observed by the Mars Reconnaissance Orbiter are attributed to seasonal flow suggestive of liquid brines (McEwen et al., 2011; Martínez and Renno, 2013). Correlation of Mg with S and enrichment of S, Cl, and Br measured by the MER Spirit Rover at Gusev crater suggests transport by saline solutions through soils (Haskin et al., 2005; Wang et al., 2006; Ming et al., 2008). Relative humidity and temperature measurements from the Rover Environmental Monitoring Station on the Curiosity Rover has also detected conditions capable of supporting perchlorate brines (Martín-Torres et al., 2015), and perchlorate measurements at the Phoenix landing site suggests thin films of perchlorate solutions (Cull et al., 2010). The Phoenix Lander has also measured oxygen isotopes that indicate influences by modern liquid water (Niles et al., 2010), and ice excavated by the Phoenix Lander has also been argued to have formed from a frozen brine because of its relative softness (Rennó et al., 2009; Smith et al., 2009). Therefore, over the course of martian history, a significant proportion of exposed land surfaces have likely been impacted by

interaction with liquid water and, at least recently, that water is likely to have been a brine.

The Fe-rich smectite nontronite has been detected on the surface of Mars, particularly in ancient terrains (Poulet et al., 2005; Thomson et al., 2011). Nontronite has been found intimately mixed with sulfates at Gale Crater (Milliken et al., 2010) and it has also been found beneath Al-rich silicates at Mawrth Vallis (Bibring et al., 2006; Bishop et al., 2008; Wray et al., 2008; McKeown et al., 2009; Loizeau et al., 2010; Noe Dobrea et al., 2010). Fe-Mg-rich phyllosilicates have also been documented in multiple locations on the surface of Mars by the Compact Reconnaissance Imaging Spectrometer for Mars (CRISM) on the Mars Reconnaissance Orbiter and the Observatoire pour la Mineralogie, L'Eau, les Glaces et l'Activite (OMEGA) spectrometer on the Mars Express orbiters (Poulet et al., 2005; Bishop et al., 2008; Mustard et al., 2008; Murchie et al., 2009). If brines have been active throughout Mars history, it is likely that at least some of the observed nontronite deposits have been altered by brines.

Few studies have examined mineral dissolution rates in brines (Hausrath and Brantley, 2010; Pritchett et al., 2012; Dixon et al., 2015; Olsen et al., 2015), and none that we know of have analyzed nontronite dissolution rates in brines. In previous work, dissolution of basaltic glass, forsterite, and fayalite in a near-eutectic Ca-Na-Cl brine was significantly slower than dissolution in dilute and ionic strength = 0.7 m solutions (Hausrath and Brantley, 2010). Forsterite dissolution has been shown to slow in high ionic strength Mg-sulfate brines (Olsen et al., 2015). Jarosite dissolution rates in batch reactors are also decreased relative to dilute rates, although slower initial rates increase in longer term experiments due to Cl^- complexation after gypsum precipitation occurs

(Pritchett et al., 2012). Similarly, jarosite dissolution rates in brines measured in flow-through reactors are slightly slower than the initial rates measured in brines in batch reactors (Dixon et al., 2015). Previous work therefore suggests that mineral dissolution slows significantly in high-ionic strength brines, and we therefore propose to test the importance of that effect on nontronite likely exposed for billions of years on Mars. Dissolution rates of nontronite were measured as a function of activity of water ($a$$H_2O$) at $a$$H_2O$ = 1.00, 0.75 and 0.5, and temperature at 4º, 25º, and 45 ºC, and reacted material was examined to analyze alteration resulting from brine dissolution. The results of this work can help interpret past aqueous conditions on Mars and provide a better understanding of the possible habitability of past martian environments.

Chapter 2 Materials and Methods

Materials

The Clay Mineral Society nontronite standard NAu-1 ($M^{+}_{1.05}[Si_{6.98}Al_{1.02}][Al_{0.29}Fe_{3.68}Mg_{0.04}]O_{20}(OH)_4$) was used in all mineral dissolution experiments. NAu-1 was mined from Uley Graphite Mine, Australia (Keeling et al., 2000) and has been previously characterized as predominantly nontronite with traces of kaolin, quartz, biotite and goethite totaling approximately 10% (Keeling et al., 2000). It has also previously been used in dissolution experiments to examine the effect of pH on nontronite dissolution (Gainey et al., 2014).

Nontronite was crushed using an agate mortar and pestle and sieved to a size fraction of 40-125 μm (120-325 mesh). Powdered and sieved nontronite was then ultrasonicated in ethanol at two minutes intervals until the supernatant was clear. A significant decrease in fine particles was observed when mineral surfaces were examined by Scanning Electron Microscopy (SEM) using a JSM-5600 Scanning Electron Microscope after washing, although occasional fine particles remained. Surface area of the washed nontronite was determined using a Quantachrome NOVA 2000e Surface area and Pore Size Analyzer. Nontronite was outgassed under vacuum at 50 ºC for 24 hours before measuring a six-point BET (Brunauer-Emmett-Teller) nitrogen adsorption isotherm (Brunauer et al., 1938). Dissolution rates were normalized to the measured nontronite surface area (30.865 ± 1.54 $m^2\ g^{-1}$).

Batch Dissolution Experiments

To test the effect of activity of water on nontronite dissolution, batch experiments were performed in $CaCl_2$- and NaCl-containing solutions with activities of water equal to

1.00, 0.75 and 0.5, and 1.00 and 0.75, respectively. The 1.00 dilute solutions contained 0.01M NaCl and 0.01M $CaCl_2$, which had an activity of water = 0.999 calculated using PhreeqC (Parkhurst and Appelo, 1999), similar to the ionic strength of natural soil waters (Harter and Naidu, 2001). Dissolution experiments are commonly performed in low ionic strength solutions rather than pure water to prevent rapid changes in the activity of water as the mineral dissolves. The 0.75 $a H_2O$ $CaCl_2$ brine was made by adding 166.66 g of anhydrous $CaCl_2$ to 500 g of 18.2 MΩ water, and the 0.50 $a H_2O$ $CaCl_2$ brine was made by adding 360.68g of anhydrous $CaCl_2$ to 500 g of 18.2 MΩ water (Rard and Clegg, 1997). The NaCl brine was made by adding 150 g of NaCl to 356 g of 18.2 MΩ water (Chirife and Resnik, 1984).

All solutions were adjusted to an initial pH = 2.0 using high purity HCl. Previous measurements of pH in brines have employed multiple techniques, and double junction fast flow pH electrodes have been commonly used (Bowen and Benison, 2009; Hausrath and Brantley, 2010). Although dissolution behavior as a function of pH is not the primary concern of this work, as changing nontronite dissolution rates as a function of pH under acidic conditions was previously measured by Gainey et al. (2014), it was necessary to ensure that the initial pH was the same in all conditions. To ensure this, all pH measurements were made with the same Mettler Toledo InLab® Expert Pro pH electrode. This electrode has a double junction and temperature sensor, both of which increase accuracy when measuring pH in brines. We also measured the starting pH of the brines with a VWR sympHony™ High-flow pH electrode designed for hard-to-measure samples and measured values within 0.1 pH units of the target pH of 2. We therefore make the assumption that although uncertainties on pH measurements are higher in brines, these

measurements are sufficiently precise to allow comparison between activities of water and with previous data.

For each experimental condition except the 0.50 activity experiments, which contained 5.0g of nontronite to increase solution concentrations, 0.5-1.0g of powdered, washed nontronite was combined with 200ml of solution in an acid-washed Low Density Polyethylene (LDPE) batch reactor. To test the effect of activity of water and brine composition, experiments were performed with $CaCl_2$- and NaCl-containing solutions with activities of water described above. To test the effect of temperature and calculate an apparent activation energy of dissolution, experiments were performed in 0.01M $CaCl_2$ solutions at 4 ºC, 25 ºC, and 45 ºC on an orbital shaker in a temperature-controlled cold-room (4.0 ± 0.1 ºC), or in temperature-controlled shaking water baths (25.0±0.1 ºC and 45.0 ±0.1 ºC). All solutions were equilibrated to the correct temperature for 24 hours prior to the addition of nontronite. In all cases, batch reactors were agitated at 100 strokes per minute.

To sample the reactors, ten ml of sample were removed at regular time intervals that varied depending on the temperature and solution composition and were based on preliminary experiments. A minimum of 13 samples was collected during the short initial period of the experiments, and then batch reactors were allowed to react for an additional 1-4 months to collect long term points under steady conditions. The pH of each sample was measured on a separate aliquot of unfiltered sample at room temperature, with the remainder of the sample filtered through a 0.45 μm polypropylene syringe filter, acidified to 1% v/v with high purity HNO_3, and stored at 20º C until analysis. Each condition was

run in duplicate, with at least one blank for each condition. A complete list of experimental conditions, including duplicates, is shown in Table 1.

Analytical Methods

Silica concentrations were measured with a Thermo Genesys 10S UV-Vis spectrophotometer at a wavelength of either 700nm (dilute solutions and NaCl brines) or 400 nm ($CaCl_2$ brines) using methods slightly modified from the ASTM and USGS methods to optimize analysis in high ionic strength solutions (ASTM D859-10; Fishman and Friedman, 1989). The silica analysis consists of two steps: 1) the addition of an acid and ammonium molybdate to form silicomolybdate which produces a yellow color the intensity of which reflects the concentration of available silica (ASTM D859-10) and 2) the reduction of silicomolybdate which produces a blue color the intensity of which reflects the concentration of available silica (Fishman and Friedman, 1989). Performing both steps increases the measurement range to 0.1-100 ppm measured at 700 nm, compared to a measurement range of 0.1-1.0ppm when only performing the first step measured at 400nm (ASTM D859-10; Govett, 1961). The first step is from ASTM D859-10 and the second step from the USGS test method I-1700-85 to avoid interference caused by precipitation of Ca sulfites within the brines, which occurs during the second reducing step of the ASTM D859-10 method after adding an amino-naphthol-sulfonic acid solution (ASTM D859-10; Fishman and Friedman, 1989). Both steps were used for samples from all dilute experiments at all temperatures and NaCl brines with $a H_2O$ = 0.75. Only the first step was used for $a H_2O$ = 0.75 $CaCl_2$ and $a H_2O$ = 0.50 $CaCl_2$ brines because precipitation occurred when adding sodium sulfite as a reducing agent in part two. In order to match the solution matrices for the standards and the samples, standards

were prepared in 18.2 MΩ water and then combined with a solution matching the composition of the sample solution in a 1:1 ratio, and samples were diluted 1:1 with 18.2 MΩ water. The average standard error of thirteen silica calibration curves measured on the Thermo Genesys 10S UV-Vis spectrophotometer was found to be 4 ± 3%, with the highest value = 8%. Based on that, we assume a maximum uncertainty of 10% on silica measurements.

Iron concentrations were measured using a Thermo Scientific iCE 3000 series Atomic Absorption spectrometer for all samples for which sufficient solution remained after silica measurements. All samples were treated with a $CaCO_3$ solution to reduce interference following the method described by Eaton et al. (2005). Samples from experiments with $a H_2O = 1.00$ were analyzed for iron concentrations without dilution. Brine samples require dilution 1:8 to prevent damage to the AA (Pritchett et al., 2012). Uncertainty of analysis for Fe concentrations is ±0.0164 ppm (Tu et al., 2014).

Characterization of Reacted Material

After collection of the long-term solution chemistry point(s) for each experiment (~3-6 months), solutions were decanted and the remaining material was rinsed with 18.2 MΩ water. Rinsed reacted material was frozen for at least 24 hours, and then freeze dried for 24 hours to remove all ice. Reacted material and unreacted NAu-1 for comparison was carbon coated, and observed using a JSM-5600 Scanning Electron Microscope using Energy Dispersive Spectroscopy (EDS) with a working distance between 18-20 mm, a 40 μm spot size, and 20kV acceleration voltage. Samples were also analyzed using Visible Near Infrared (VNIR) and Infrared (IR) reflectance spectroscopy to further constrain alteration and to be able to make a direct comparison to Mars. VNIR spectra were

measured at the California Institute of Technology using an Analytical Spectra Devices (ASD) VNIR and InfraRed (IR) reflectance spectra were measured using a Fourier Transform Infrared Spectrometer. Spectra were measured over a range of 0.4 to 2.5 μm and 2.5 to 25 μm. ENVI version 4.7 was used to remove the continuum and to identify the absorption wavelengths. SEM, VNIR, and IR analysis also included reacted nontronite removed from a set of experiments within a saturated $CaCl_2$ brine. Those experiments provided sufficient reacted material for analysis but had Fe and Si concentrations below detection for all samples and were not included in the kinetic portion of this study.

Chapter 3 Results

Solution Chemistry

The pH of each experiment typically remained relatively steady, increasing somewhat over time (see Supplemental Material). In general, experiments in dilute solutions remained most stable with measured pH values for $a\mathrm{H_2O} = 1.00$ conditions ranging from 1.84 to 2.54 at 25 ºC, 1.92 to 2.43 at 45 ºC, and 1.98 to 2.08 at 4 ºC. Experiments performed in lower activity solutions had larger changes with measured pH values for $a\mathrm{H_2O} = 0.75$ ranging from 1.90 to 3.05 and $a\mathrm{H_2O} = 0.5$ ranging from 1.78 to 2.6 (see Supplemental Material).

Moles released of silica and iron were corrected for solution volume removed during sampling after Welch and Ullman (2000):

$$m_t = m_{t-1} + (c_{(t)} - c_{(t-1)})V_{(t-1)} \qquad (Eq.\ 1)$$

where m is moles of silica or iron released, $c_{(t)}$ and $c_{(t-1)}$ are the concentrations of silica or iron in moles•liter^{-1} at time intervals t and $t\text{-}1$, and V is volume in liters.

All samples with sufficient solution remaining after measurement of silica were analyzed for Fe concentrations but only experiments at $a\mathrm{H_2O} = 1.0$ had detectable concentrations after dilution. Fe release increased over time, approaching steady state (Supplemental Materials) In all cases, Fe: Si ratios were below the Fe: Si ratio in nontronite, indicating incongruent dissolution and/or precipitation in experiments at $a\mathrm{H_2O} = 1.0$ (Figure 1). This is consistent with previous work (Metz et al., 2005; Gainey et al., 2014), which concluded that that Fe is not released stoichiometrically during smectite dissolution because of preferential Fe reabsorption and precipitation.

Similarly, silica concentrations in samples collected during the initial short-term period of the experiments showed a non-linear relationship indicative of an approach to steady state or equilibrium (Appendix figures 1-14). Silica release from a Na-smectite has been attributed to release from the tetrahedral site, and is therefore considered the rate-limiting step (Marty et al., 2011). Although Al is present in nontronite, Si occupies 90% of the tetrahedral sites (Velde, 1995; Keeling et al., 2000; Gainey et al., 2014). We therefore calculated dissolution rates from silica release.

Due to the effect of the opposing precipitation reaction affecting silica release, it was important to measure long term steady state conditions when the forward and opposing reaction are assumed to be equal. Therefore, several approaches were followed to ensure that there was at least one steady state point for all experiments. Unless steady state was obviously reached during the first measured 13points (aH$_2$O = 0.5 conditions only), at least one point was measured after a significantly longer time period than the duration of the initial shorter-term experiments (1-4 months). For experiments in solutions with activity of water = 1.00 and 0.75, that point, or the average of multiple such points, was used as the steady state condition for calculation of dissolution rates. For the aH$_2$O = 0.5 experiments, the average of the last 5 points was used as the steady state value – steady state conditions were defined as unchanged concentrations for three or more days. The earlier approach to steady state in the aH$_2$O = 0.50 brines is not unexpected as silica solubility is lower in brines than in dilute solutions and silica precipitation rates increase with increasing ionic strength (Iler, 1979; Icopini et al., 2005).

In all cases but the experiments performed at 4 ºC, silica release had clearly approached steady state conditions by the long-term point (Figure 2, 3). In experiments

performed at 4 ºC, silica release less obviously reaches steady state. However, the measured silica concentrations display curvature over time (Figure 2), and long term silica concentrations at 4 ºC are only slightly lower than the long term points measured at 25 ºC and 45 ºC, and therefore likely represent a good approximation of steady state conditions.

In order to calculate dissolution rates that account for the importance of the opposing precipitation reaction, equal to dissolution at steady state, dissolution rates were calculated after Hausrath and Brantley (2010):

$$-m_{ss}\, ln\,(1 - \frac{m}{m_{ss}}) = Ak_{diss}t + C \quad (Eq.\ 2)$$

where m is moles released of silica, calculated by multiplying the change in [SiO_2] by the volume of remaining solution at each time point as described in equation 1, m_{ss} is moles released at steady state based on the long term point(s) measured after 5-179 days, A is the surface area measured by BET analysis as described above, k_{diss} is the dissolution rate in mol m^{-2} s^{-1}, and t is time in seconds. The uncertainty on the dissolution rate was estimated from the standard error on the rate regression (mol s^{-1}) with the 5% uncertainty of the BET surface area (m^2) propagated through, and divided by the stoichiometric coefficient.

Dilute experiments had the highest dissolution rates (1.18×10^{-12} mol mineral m^{-2} s^{-1} $\pm$ 9.30×10^{-14} average for $CaCl_2$ aH_2O=1.00 and $1.89 \times 10^{-12} \pm 9.59 \times 10^{-14}$ mol mineral m^{-2} s^{-1} average for NaCl aH_2O = 1.00). With decreasing activity of water, the dissolution rates decreased for both the NaCl and $CaCl_2$ brines (2.36×10^{-13} mol mineral m^{-2} s^{-1} $\pm 3.07 \times 10^{-14}$ average for $CaCl_2$ aH_2O = 0.75, 2.05×10^{-14} mol mineral m^{-2} s^{-1} $\pm 2.87 \times 10^{-15}$ average for $CaCl_2$ aH_2O = 0.50 and $1.98 \times 10^{-13} \pm 2.26 \times 10^{-14}$ mol mineral m^{-2} s^{-1} average

for NaCl aH$_2$O = 0.75) (Figure 4). Similarly, dissolution rates decreased as temperature decreased with nontronite dissolving in 45 ºC solutions at $4.98 \times 10^{-12} \pm 3.84 \times 10^{-13}$ mol mineral m^{-2} s^{-1}, in 25 ºC solutions at 1.18×10^{-12} mol mineral m^{-2} s^{-1} $\pm$ 9.30×10^{-14} and in 4 ºC solutions at $2.33 \times 10^{-13} \pm 1.25 \times 10^{-14}$ mol mineral m^{-2} s^{-1} (Figure 2). An apparent activation energy was calculated by plotting the natural log of the dissolution rates versus 1000/T, where T is the temperature in K. The apparent activation energy is the negative slope of that line multiplied by the universal gas constant (8.31 J K^{-1} mol^{-1}). In these experiments, dissolution rates from batch reactors with aH$_2$O = 1.0 containing $CaCl_2$ were used to calculate an apparent activation energy (Figure 5) of 54.6 ± 1.00 kJ/mol.

SEM Results

No observations indicated significant alteration or secondary mineral precipitation. Textured surfaces were found in both reacted and unreacted nontronite with no observable difference with changing activity of water and temperature (Figure 6). Nontronite with rounded, rough edges was more common than nontronite with smooth sharp surfaces. Despite being washed, some fine particles are observed on unreacted nontronite, specifically on smooth, flat surfaces (Figure 6A). Fine particles dissolve very quickly and as a result are less visible on reacted nontronite (Figure 6B-F).

IR Results

Changes in the VNIR spectra due to interaction with liquid water or brines are slight if present (Figure 7). A slight shift of about 10nm can be seen between 2.4 and 2.5 μm in samples exposed to saturated $CaCl_2$ brines compared to all other brine and dilute experiments. While subtle, this shift could be explained by an extra absorption caused by differences in water content or crystallinity.

FTIR spectra have more noticeable spectral changes. The Si-O stretch near 1000 cm^{-1} becomes narrower for all reacted samples. A reflectance maximum/emission minimum at 1220 cm^{-1} and a feature at 790 cm^{-1} disappear in reacted samples compared to the unreacted NAu-1 spectra. The Al/Si-O-Si deformations between 600 and 400 cm^{-1} change in shape for all 25º C and 45 ºC experiments. This change is more similar to dioctohedral smectites and could be caused by the removal or transformation of the minor phases detected by Keeling et al. (2000) in NAu-1 (Michalski et al., 2005).

Chapter 4 Discussion

Although the surface of Mars is currently both too cold and too dry to allow pure water to remain liquid (Henderson-Sellers and Meadows, 1976; Brass, 1980; Haberle et al., 2001), brines can remain liquid briefly under specific conditions. There is increasing evidence for liquids present on modern day Mars, many of which are likely brines (Knauth and Burt, 2002; McEwen et al., 2011; Martínez and Renno, 2013; Martín-Torres et al., 2015). Flowing liquid brines have been argued to have formed surface features such as slope streaks (Kreslavsky and Head, 2009), recurring slope lineae (McEwen et al., 2011), and gullies (Knauth and Burt, 2002). Concentrated salt solutions can form by deliquescence and freeze at low temperatures to form ice (Ingersoll, 1970), and melting of such non-pure water ice has been suggested to cause the formation of gullies and depressions (Hecht, 2002). Ice excavated at the Phoenix Lander has also been argued to have formed from a frozen brine because of its softness(Rennó et al., 2009; Smith et al., 2009). Additionally, spheroids on the strut of the Phoenix Lander have been postulated to have grown by deliquescence and eventually dripped off the strut, both of which would suggest that the spheroids were liquid brines (Rennó et al., 2009). Humidity and surface temperatures measured up to 9km from the Bradbury landing over the span of one full martian year by the Mars Curiosity Rover also indicate the likelihood of perchlorate brines at Gale Crater (Martín-Torres et al., 2015).

Evidence for brines has also been observed in martian meteorites. Bridges et al. (2001) suggested that secondary mineral assemblages found in SNC-meteorites including Fe-Mg-Ca carbonates, anhydrite, gypsum, halite, and clays are formed by evaporation of low temperature brines. Salt veins rich in chloride have also been found in nakhlite

meteorites, and are similar to measurements at Gusev crater and Meridiani Planum (Rao et al., 2005).

Although the composition of potential martian brines is not known, they may have contained high chloride concentrations such as those observed in martian meteorites discussed above and used in these experiments. Models of evaporation of putative martian solutions have generated Cl-rich brines (Tosca and McLennan, 2006; Fairen et al., 2009) and chlorides have been detected using Mars Odyssey Thermal Emission Imaging System (THEMIS), Mars Global Surveyor, and Mars Reconnaissance Orbiter data (Osterloo et al., 2008; Osterloo et al., 2010). Chloride solutions are therefore likely throughout martian history, and since chloride solutions can impact mineral dissolution (Hausrath and Brantley, 2010; Pritchett et al., 2012; Dixon et al., 2015), determining the effects of chloride brines on clay mineral dissolution can help interpret the past aqueous history and possible habitability of Mars.

Effect of brines on nontronite dissolution rates

In these experiments, dissolution of nontronite was slower in lower water activity brines than in dilute solutions (Figure 4). Dissolution rates of nontronite in $a H_2O = 0.75$ $CaCl_2$ solutions were 0.20 times as fast when compared to dissolution rates of nontronite in $a H_2O = 1.00$ $CaCl_2$ solutions, while dissolution rates of nontronite in $a H_2O = 0.50$ $CaCl_2$ solutions were 0.017 times as fast when compared to dissolution rates in $a H_2O = 1.00$ $CaCl_2$ solutions. Additionally, dissolution rates for nontronite in $a H_2O = 0.75$ NaCl solutions were 0.11 times as fast when compared to dissolution rates of nontronite in $a H_2O = 1.00$ NaCl solutions.

Previous studies examining mineral dissolution rates in the presence of brines have similarly shown that dissolution rates decrease with decreasing water activity (Hausrath and Brantley, 2010; Pritchett et al., 2012; Dixon et al., 2015; Olsen et al., 2015). Hausrath and Brantley (2010) documented a decrease in olivine dissolution rates of an order of magnitude in $CaCl_2$-NaCl-H_2O near-eutectic brines compared to dilute solutions. Olsen et al. (2015) suggested that dissolution rates of forsterite are slowed in Mg-sulfate-rich brines because the decreased $a H_2O$ decreases the available water that participates as a ligand in the dissolution reaction. Pritchett et al. (2012) documented a decrease in jarosite dissolution rates in early experiments of almost two orders of magnitude in an $a H_2O = 0.35$ brine compared to dilute solutions. The early decrease in jarosite dissolution was then followed by an increase in jarosite dissolution rates following gypsum precipitation allowing Cl^- complexation, although rates were still slower than in dilute solutions. Dixon et al. (2015), who performed batch jarosite dissolution experiments similar to Pritchett et al. (2012) but also performed experiments in flow-through reactors, confirmed the decreased dissolution rates in brines in general, as well as the increase in jarosite dissolution rates in saturated calcium chloride brines over time. Both Olsen et al. (2015) and Pritchett et al. (2012) show a linear decrease in dissolution rates with decreasing activities of water.

Our results also show a linear decrease in dissolution rates with decreasing activities of water, with very similar relationships between the activity of water and dissolution rates as Olsen et al. (2015) and Pritchett et al. (2012) (Figure 8). Solutions used by Olsen et al. (2015) at pH = 2 covered activities from 1.0 to 0.91, and showed a slope of the decreasing rates with decreasing activity of water differing from this study by

11%. In Pritchett et al. (2012) dissolution of jarosite was measured in $CaCl_2$ and NaCl brines (aH_2O = 1.0-0.35) using ultrapure deionized water with a pH of ~ 3-4 (personal communication M. Elwood Madden). These jarosite experiments showed a linear decrease in rates with decreasing activity of water that differed from the slope measured in this study by only 4% (Figure 8). Our results, which are similar to those of Olsen et al. (2015) and Pritchett et al. (2012), are therefore also consistent with the decreased activity of water acting as a ligand (Olsen et al., 2015).

Nontronite dissolution rates in the $CaCl_2$ and NaCl aH_2O = 0.75 brines were within uncertainty of each other, but nontronite dissolution rates in the aH_2O = 1.00 $CaCl_2$ solutions were 0.62 times as fast as the nontronite dissolution rates in the aH_2O = 1.00 NaCl solution. Multiple factors could be contributing to the difference between the dissolution rates in the 0.01 M NaCl and $CaCl_2$ solutions, including differences in the ionic strength and the ions in the solution, as well as the identity of the ions (Ca versus Na) present within the interlayer of the clay mineral. The 0.01 M solutions of $CaCl_2$ and NaCl have different ionic strengths (0.01 mol for the NaCl solutions and 0.02 mol for $CaCl_2$ solution). Icenhower and Dove (2000) have shown that amorphous silica dissolution can increase by as much as 21x in NaCl solutions of up to 0.05 *m* because of enhanced surface reactivity. It was also predicted that other major solutes, including K, Mg, and Ca, would have a similar effect (Icenhower and Dove, 2000). The difference between the ionic strengths of the two solutions would therefore likely cause enhanced dissolution in the $CaCl_2$ solution, and instead we see enhanced dissolution in the presence of the NaCl solution. Therefore, the difference in ionic strengths between the two

solutions is likely not the controlling factor in the differences between the dissolution rates measured in $aH_2O = 1$ solutions.

The presence of the Ca ion in the nontronite interlayer, rather than Na, may cause dissolution to be faster in the presence of the NaCl rather than the $CaCl_2$ solutions. Bibi et al. (2011) have observed increased dissolution when Na/K ion exchange occurs in the interlayer of illite between pH 2-4. The fact that the dissolution rates in these experiments are faster in the presence of the NaCl rather than the $CaCl_2$ solutions suggests that the difference is due to interaction with Ca within the interlayer.

Dissolution of nontronite in dilute 0.01M $CaCl_2$ and NaCl solutions was faster than nontronite dissolution rates previously measured using flow-through reactors at a similar pH (Figure 4) (Gainey et al., 2014). Nontronite used in the Gainey et al. (2014) study was the same NAu-1 as the nontronite used in this study, with the same size fraction (40-125 μm), but Gainey et al. (2014) used the final surface area rather than the initial surface area used in this study. When the Gainey et al. (2014) rates are normalized to the initial surface area of washed nontronite used in this study, dissolution rates were approximately 0.11-0.35x as fast as those measured here (Figure 4). This is consistent with previous studies which have shown that dissolution rates of smectite minerals measured in batch reactors were three times faster than smectite dissolution rates in flow-through reactors (Furrer et al., 1993). The difference in rates measured in batch and mixed flow reactors can be caused by different particle aggregation as a result of the difference in mixing methods (Furrer et al., 1993). In addition, Gainey et al. (2014) calculated rates from the last 5 data points of each steady state condition, whereas in this study we used the solution chemistry over the entire duration of the experiments.

Both the nontronite dissolution rates measured in this study as well as the rates measured by Gainey et al. (2014) are similar to previous measurements of clay mineral dissolution rates in the literature (Wieland and Stumm, 1992; Cama et al., 2002; Rozalén et al., 2008). Wieland and Stumm (1992) measured dissolution rates for kaolinite using Si release of $9.73x10^{-13}$ $\pm 1.07x10^{-13}$ mol m^{-2} s^{-1} at a pH of 2.00 and Cama et al. (2002) measured dissolution rates for kaolinite based on silica of $3.61x10^{-14} \pm 5.77x10^{-15}$ mol m^{-2} s^{-1}at pH 2.04, both in flow-through reactors. Rozalén et al. (2008) measured Si release of $7.76x10^{-14}$ mol m^{-2} s^{-1} (error <15%) for montmorillonite at pH 2.05. Our measured rate of $1.18x10^{-12} \pm 9.30 x10^{-14}$ mol mineral m^{-2} s^{-1} was faster than kaolinite rates measured by Wieland and Stumm (1992) and Cama et al. (2002) but slightly slower than montmorillonite rates measured by Rozalén et al. (2008).

Effect of Temperature

Brines remain liquid at lower temperatures than dilute solutions, including the low temperatures on present day Mars (Brass, 1980; Haberle et al., 2001). Nontronite dissolution rates as a function of temperature are therefore relevant to interpreting past aqueous interactions on Mars. Using nontronite dissolution rates measured in dilute $CaCl_2$ solutions at 4º C, 25º C, and 45º C as described in the methods, an apparent activation energy of 54.6 ± 1.00 kJ/mol was calculated. To the best of our knowledge, this is the first measured apparent activation energy for nontronite dissolution.

This apparent activation energy for nontronite dissolution is similar to previously measured apparent activation energies for clay mineral dissolution. Apparent activation energies for smectite dissolution have been reported as 87 kJ/mol (no error reported, although the error on the rate is reported at 15%) for K-montmorillonite when measured

in flow-through and batch reactors over a pH range of 1.0-5.8 and a temperature range of 25º-70 ºC(Rozalén et al., 2008). Cama et al. (2002) report an apparent activation energy of 78.4 kJ/mol for kaolinite dissolution at pH 2.0 in flow-through reactors at temperatures ranging from 25º-70 ºC (Cama et al., 2002). Palandri and Kharaka (2004) calculated an apparent activation energy of dissolution for smectite of 23.6 kJ/mol, kaolinite of 65.9 kJ/mol and montmorillonite of 48.0 kJ/mol using dissolution data from Carroll and Walther (1990); Nagy et al. (1991); Soong (1993); Ganor et al. (1995); Huertas et al. (1999a); Huertas et al. (1999b) for kaolinite, Nagy (1995) for montmorillonite, and Sverdrup (1990); Zysset and Schindler (1996); Bauer and Berger (1998); Huertas et al. (2001) for smectite.

Implication for Mars

The low temperatures of the present-day martian surface, where only brines are likely to be liquid, make aqueous alteration by brines likely on Mars, and these brines could be habitable environments. Although rare, life on Earth has been found at activities of water as low as 0.61 in a high-sugar food and also in saturated NaCl brines with an $a\mathrm{H_2O} = 0.75$ (Grant, 2004). Gale Crater has shown the potential to support conditions to keep perchlorate brines liquid. These brines have temperatures and activities of water that are too low to support terrestrial life, but areas with high humidity and temperatures could allow brines of other compositions to exist (Martín-Torres et al., 2015). NaCl brines are habitable on Earth and would be stable on Mars at higher temperatures and humidities.

Dissolution rates of nontronite in high ionic strength solutions and low temperatures such as potentially habitable NaCl brines on Mars are significantly slower

than in dilute solutions, suggesting that clay minerals altered by brines on Mars may appear much less altered than clay minerals altered by dilute solutions. In order to quantify this effect, using dissolution data from this study and Gainey et al. (2014) we have calculated rates under a range of pH, temperature, activity of water, and hydrodynamic conditions that are relevant to Mars (Figure 9). Results indicate that dissolution of nontronite on Mars may be very slow, and that the activity of water effect examined in this study has a larger impact on dissolution than the temperature or pH range examined. Weathering of nontronite on Mars would occur much more slowly under conditions of low temperature and low activity of water compared to warmer and more dilute conditions on Earth.

Spectral evidence exists for widespread silica on the surface of Mars (Michalski et al., 2003), which has been attributed to surficial aqueous activity (Kraft et al., 2003). Martian silica coatings may be similar to coatings found on Earth in cold and dry environments (Dorn, 1998; Dixon et al., 2002; Hausrath et al., 2008). The decreased release of silica from the dissolution of nontronite over time in these experiments could be due to the precipitation of amorphous silica, which has been detected in previous dissolution experiments of nontronite (Gainey et al., 2014). Equilibrium with amorphous silica is reached faster and at lower concentrations with decreasing activity of water (Icopini et al., 2005). In previous work, silica concentrations in equilibrium with amorphous silica decreased from an average of 3.76 mmol SiO_2 in dilute solutions to 3.43 mmol SiO_2 in the presence of Na-K-Ca-Cl-HCO_3^- -H_2O solutions ranging from 0.01 molal to 0.24 molal (Icopini et al., 2005). Dissolution of olivine in the presence of Ca-Na-Cl solutions also resulted in decreased steady state silica concentrations in the

presence of increased concentrations of Ca-Na-Cl, with steady state concentrations in near eutectic brines at 22.1 ºC with forsterite, fayalite and basaltic glass ranging from 0.17 to 0.45 m*m* (Hausrath and Brantley, 2010). Precipitated silica would be expected to form a silica-rich coating on the nontronite mineral surfaces. On these samples, silica-rich coatings were not detected using either SEM or VNIR spectroscopy, possibly due to the relatively short duration of the experiments (85-179 days for the final time point), and the low total amount of dissolution (~2-5% for dilute solutions at all temperatures, and < 1% for all brines). FTIR wavelengths show subtle but important differences. Instruments using FTIR on Mars (TES and MiniTES) have difficulty identifying phyllosillicates above background in spectra (Michalski and Fergason, 2009; Michalski et al., 2010). This may be caused by a lack of abundance or the fact that TIR spectral libraries do not contain abundant phyllosillicates(Ehlmann et al., 2011; Ehlmann et al., 2012). In these experiments, FTIR does not change appreciably with dissolution except for the removal of some accessory contaminant phases.

Low Fe/Si ratios also indicate that Fe is less mobile than silica. Fe^{3+} is found in nontronite and is also observed in nanophase hematite on Mars. Our results may result from either non-stoichiometric dissolution, or precipitation of Fe-bearing phases A combination of precipitated Fe-oxides and possible formation of reprecipitated nontronite through an opposing reaction at equilibrium could also explain the similarities between reacted and unreacted nontronite. Metz et al. (2005) observed lower than expected Fe release compared to Al in smectite dissolution caused by preferential Fe reabsorption or precipitation. Smectite can also alter to chlorite when Al and Fe from the octahedral or tetrahedral layers form oxides in the interlayer (Barnhisel and Bertsch, 1989). Low iron

release was also observed in nontronite dissolution by Gainey et al. (2014) at pH 0.9 and 1.7.

Conclusion

There is abundant evidence for past liquid water on Mars observed both by orbiters and rovers as well as in meteorites (Ingersoll, 1970; Brass, 1980; Bridges et al., 2001; Haskin et al., 2005; Rao et al., 2005; Wang et al., 2006; Ming et al., 2008; Rennó et al., 2009; Smith et al., 2009; Cull et al., 2010; Niles et al., 2010; McEwen et al., 2011; Martín-Torres et al., 2015). On Earth, brines can support life at temperatures as low as -30 ºC and activity of water down to 0.61(Jones and Lineweaver, 2010). A saturated NaCl brine with an $a\mathrm{H_2O} = 0.75$, like the one used in this study, can remain liquid down to -21 ºC (Bauer et al., 1988) and has hosted life for a few eukaryotes on Earth (Grant, 2004). Environments on Mars that contain brines may therefore be currently habitable environments.

Nontronite has been detected on the surface of Mars, particularly in ancient terrains that have been exposed at the surface for billions of years (Poulet et al., 2005; Bibring et al., 2006; Bishop et al., 2008; Ehlmann et al., 2009; Milliken et al., 2010; Thomson et al., 2011). To interpret interactions between nontronite and water on Mars, we measured dissolution rates of nontronite in batch reactors with solutions with activities of water ranging from 1.00 to 0.50 and temperatures ranging from 4º-45 ºC. Results indicate that with decreasing activity of water, rates of dissolution for nontronite decrease as well. Dissolution rates also decreased with decreasing temperature and an apparent activation energy of 54.6 ± 1.0 kJ/mol was calculated, similar to other apparent activation energies of smectite dissolution. These results suggest that nontronite reacting

under cold and briny conditions, perhaps similar to present day Mars, would appear much less altered than nontronite reacting with dilute solutions. Perceptibly altered martian nontronite may therefore indicate potentially habitable conditions occurring over very long timescales on Mars.

Appendix A Tables and Figures

Table A. Experimental conditions

T (ºC)[1]	Salt	aH_2O[2]	Duration (days)	Rate (mol mineral m^{-2} s^{-1})	Uncertainty[3]
25.0	$CaCl_2$	1.00	179	$1.23x10^{-12}$	$9.54x10^{-14}$
25.0	$CaCl_2$	1.00	179	$1.13x10^{-12}$	$9.06x10^{-14}$
25.0	$CaCl_2$	0.75	179	$2.13x10^{-13}$	$3.23x10^{-14}$
25.0	$CaCl_2$	0.75	179	$2.59x10^{-13}$	$2.92x10^{-14}$
25.0	$CaCl_2$	0.50	15	$1.41x10^{-14}$	$1.72x10^{-15}$
25.0	$CaCl_2$	0.50	15	$2.69x10^{-14}$	$4.03x10^{-15}$
25.0	NaCl	1.00	105	$1.74x10^{-12}$	$8.75x10^{-14}$
25.0	NaCl	1.00	105	$2.06x10^{-12}$	$1.04x10^{-13}$
25.0	NaCl	0.75	147	$1.94x10^{-13}$	$2.41x10^{-14}$
25.0	NaCl	0.75	147	$2.04x10^{-13}$	$3.45x10^{-14}$
45.0	$CaCl_2$	1.00	85	$5.22x10^{-12}$	$3.84x10^{-13}$
45.0	$CaCl_2$	1.00	85	$4.73x10^{-12}$	$3.85x10^{-13}$
4.0	$CaCl_2$	1.00	105	$2.39x10^{-13}$	$1.31x10^{-14}$
4.0	$CaCl_2$	1.00	105	$2.28x10^{-13}$	$1.18x10^{-14}$

[1]Temperature measured to 0.1 ºC using the internal thermometer on the water bath and cold-room.

[2]aH_2O from Rard and Clegg (1997) for $CaCl_2$ brines, Chirife and Resnik (1984) for NaCl brine, and calculated using PhreeqC (Parkhurst and Appelo (1999)) for all 0.01 M solutions.

[3]Uncertainty is estimated using the standard error of the rate (mol s^{-1}) propagated through the 5% uncertainty of the surface area (m^2) and divided by the stoichiometric coefficient of Si in nontronite to obtain the uncertainty in mol mineral m^{-2} s^{-1}.

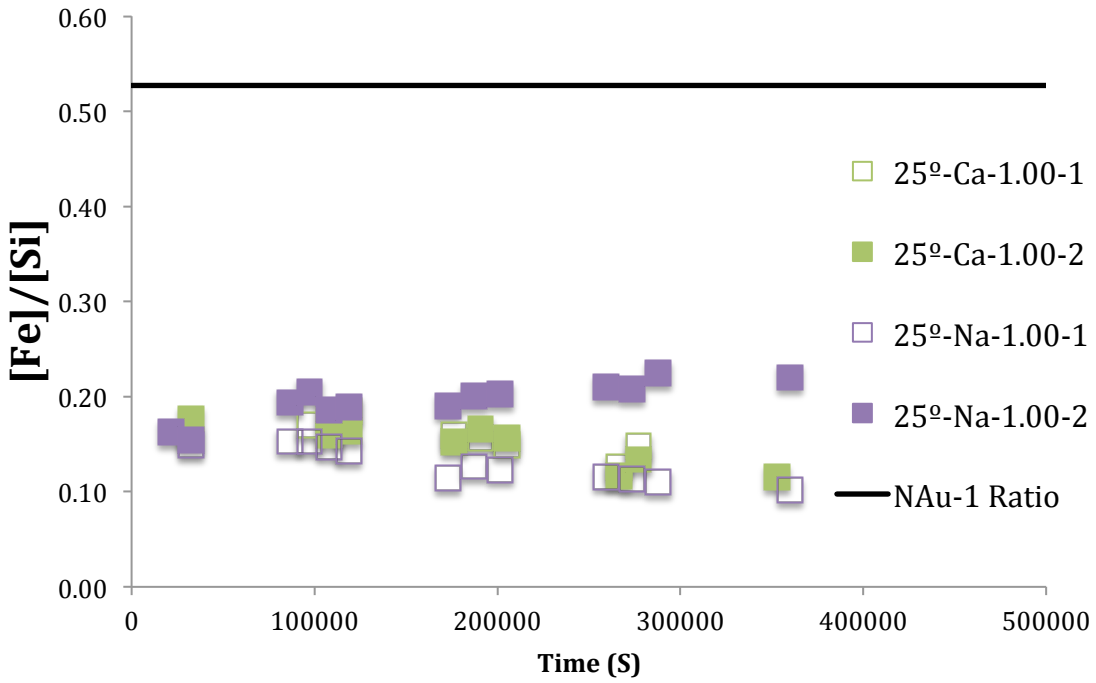

Figure 1.

Fe: Si ratios for experiments at 25 ºC where [Fe] was above detection. The solid line represents the stoichiometric ratio of Fe: Si in the unreacted nontronite (0.52). Experiments at 25 ºC remain relatively stable near 0.20 over time. Analytical uncertainty on solution chemistry is smaller than all points.

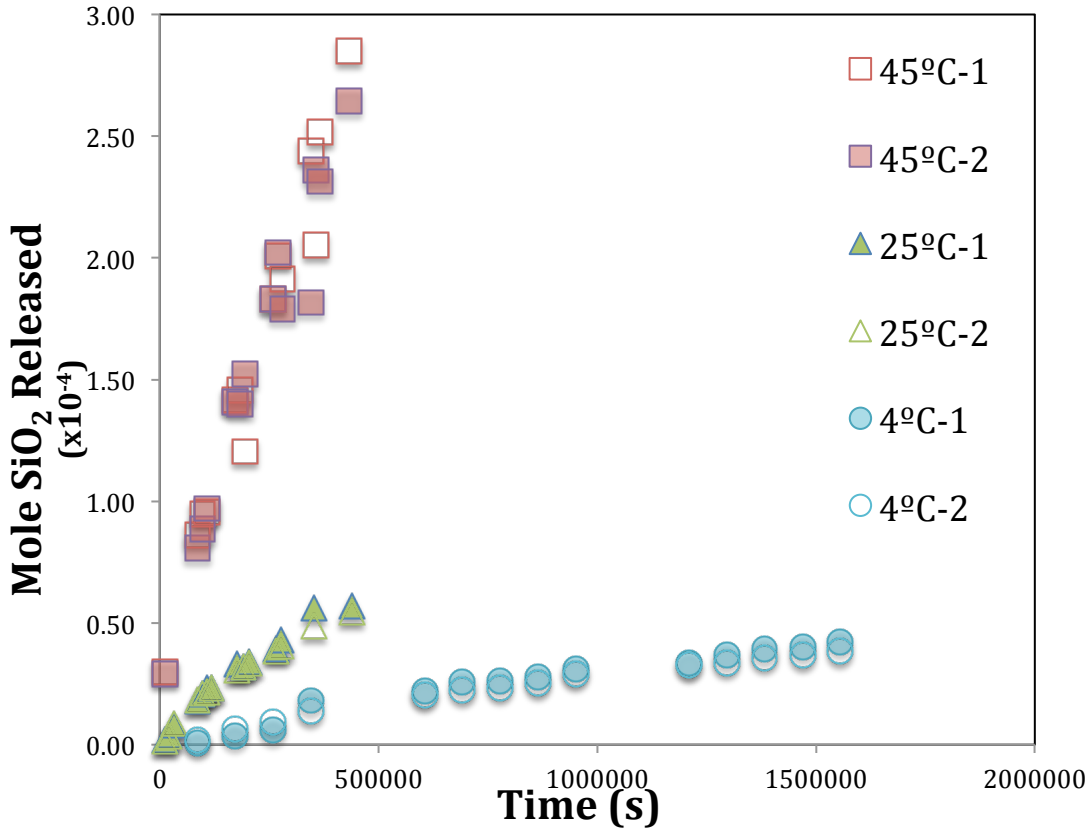

Figure 2.

Moles silica released as a function of time at temperatures of 4º C, 25º C, and 45º C. Steeper slopes indicate faster dissolution rates. These experiments indicate dissolution increased with increasing temperature, and the dissolution rates at different temperatures were used to calculate an apparent activation energy of 54.6 ± 1.0 kJ/mol. Samples were taken at different time intervals to accommodate the different dissolution rates. The 25º and 45º C experiments were sampled 2-3 times a day for one week while the 4º C experiments were sampled daily for three weeks. Analytical uncertainty is smaller than all points.

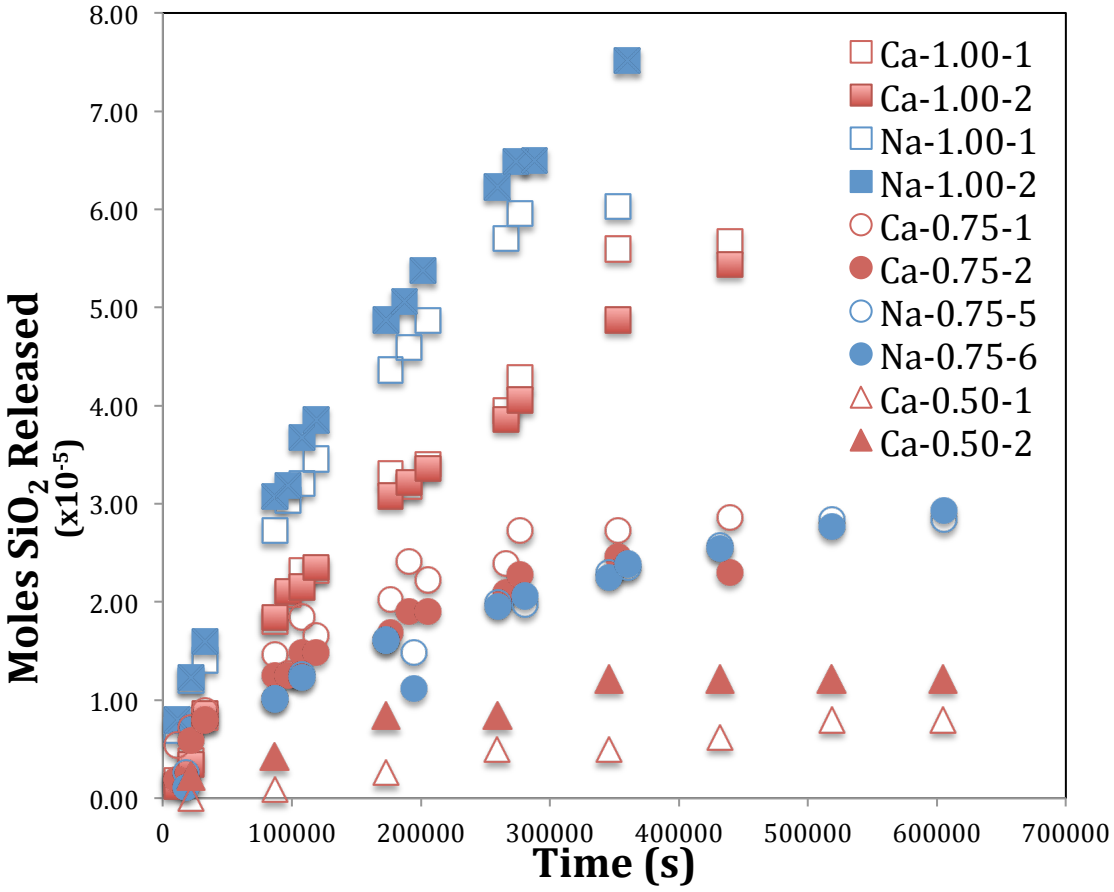

Figure 3.

Moles silica released as a function of time at aH$_2$O of 1.00, 0.75, and 0.50 at 25 ºC. Steeper slopes indicate faster dissolution rates. These experiments indicate dissolution increased with increasing activity of water, and that in very dilute solutions, presence of 0.01 M NaCl solutions increases dissolution over presence of 0.01 M CaCl$_2$ solutions. Samples were taken at different time intervals to accommodate different dissolution rates. The 1.00 aH$_2$O and 0.75 aH$_2$O experiments were sampled 2-3 times a day for one week while the 0.50 aH$_2$O experiments were sampled daily for three weeks. Analytical uncertainty is smaller than all points.

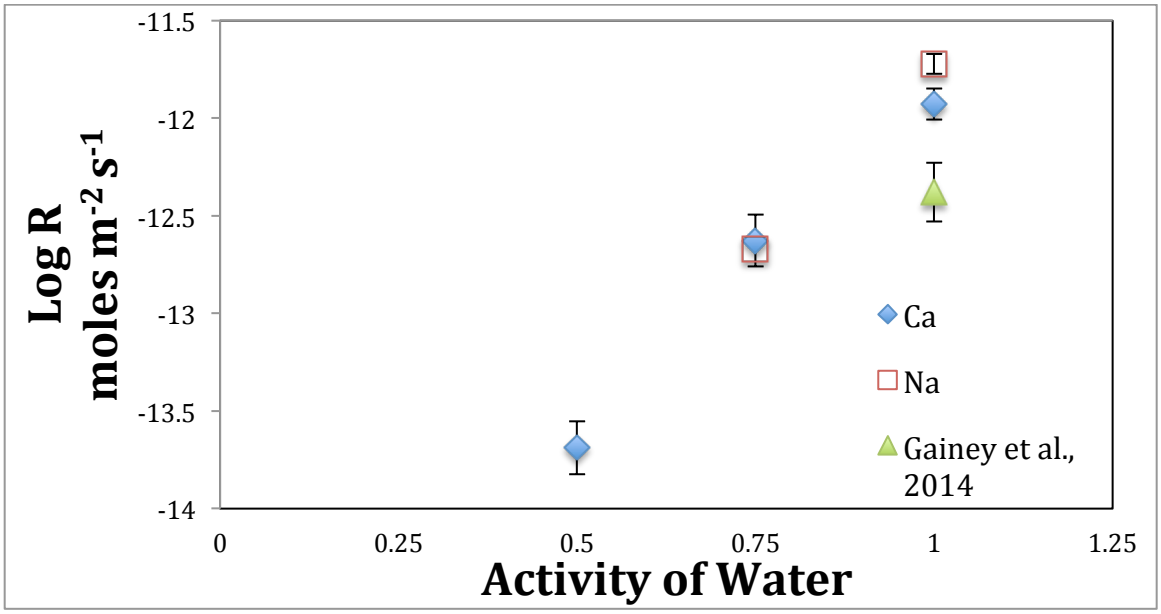

Figure 4.

Log nontronite dissolution rates as a function of activity of water for dilute and brine experiments at 25° C and pH 1.8-2.0 show a linear relationship between activity of water and the dissolution rate. Rates from Gainey et al. (2014) were measured at flow rate = 0.1609 ml/h and pH = 1.8 using the same size fraction NAu-1 as that used in this study. The rate plotted here is the rate reported in Gainey et al. (2014) normalized to the initial surface area (30.865 ± 1.54 m^2 g^{-1}) used in this study ($4.18x10^{-13} \pm 2.79x10^{-14}$ moles mineral m^{-2} s^{-1}) to better compare to our rates.

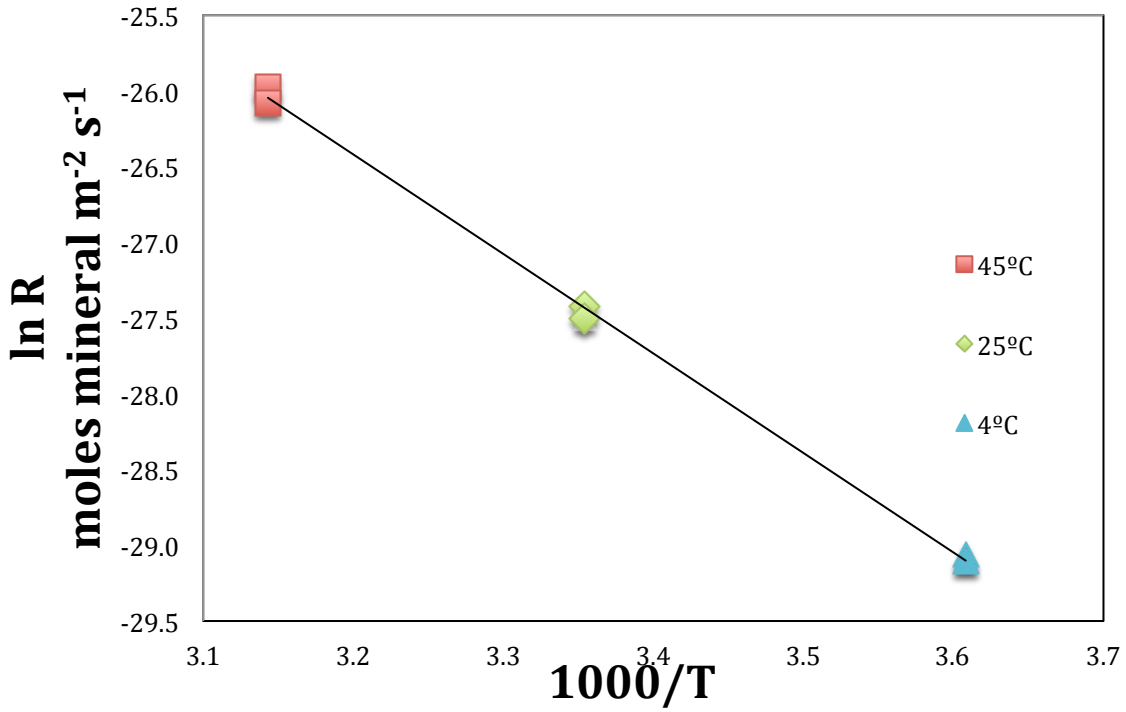

Figure 5.

The natural log of the nontronite dissolution rate versus 1000/T (K). The slope of this line was used to calculate an apparent activation energy. Measured uncertainties are smaller than all points. Final calculated apparent activation energy was 54.6 ± 1.00 kJ/mol.

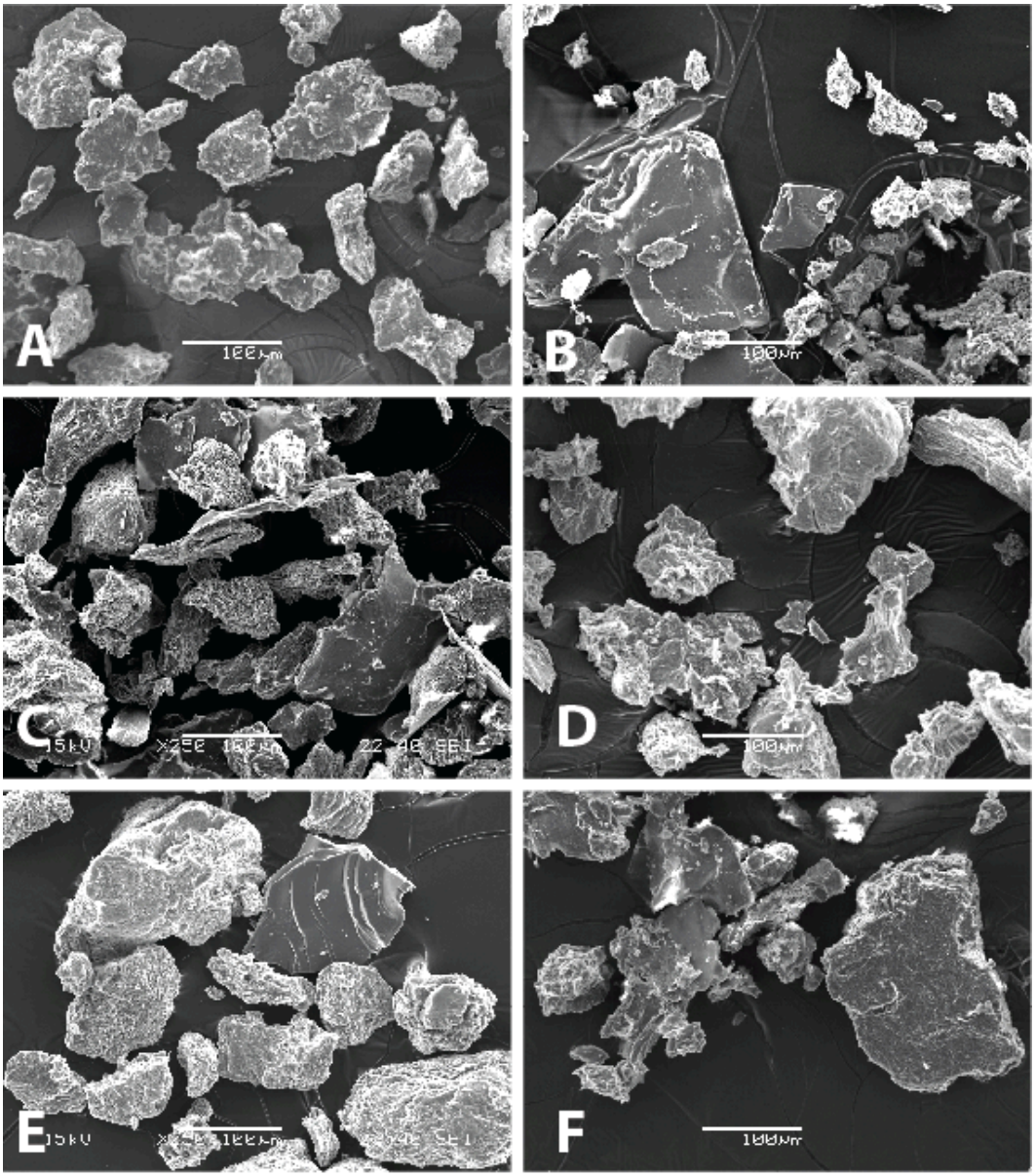

Figure 6.

Unreacted and reacted surfaces of NAu-1. (A) Unreacted sieved and washed NAu-1 observed before dissolution experiments, compared to reacted NAu-1 removed from dissolution experiments conducted at (B) 25º C 1.00 $a$$H_2O$ $CaCl_2$, (C) 25º C 0.75 $a$$H_2O$ $CaCl_2$, (D) 25º C 0.5 $a$$H_2O$ $CaCl_2$, (E) 4º C 1.00 $a$$H_2O$ $CaCl_2$, (F) 45º C 1.00 $a$$H_2O$ $CaCl_2$. Surface textures appear similar for all experiments as well as the unreacted material.

Figure 7.

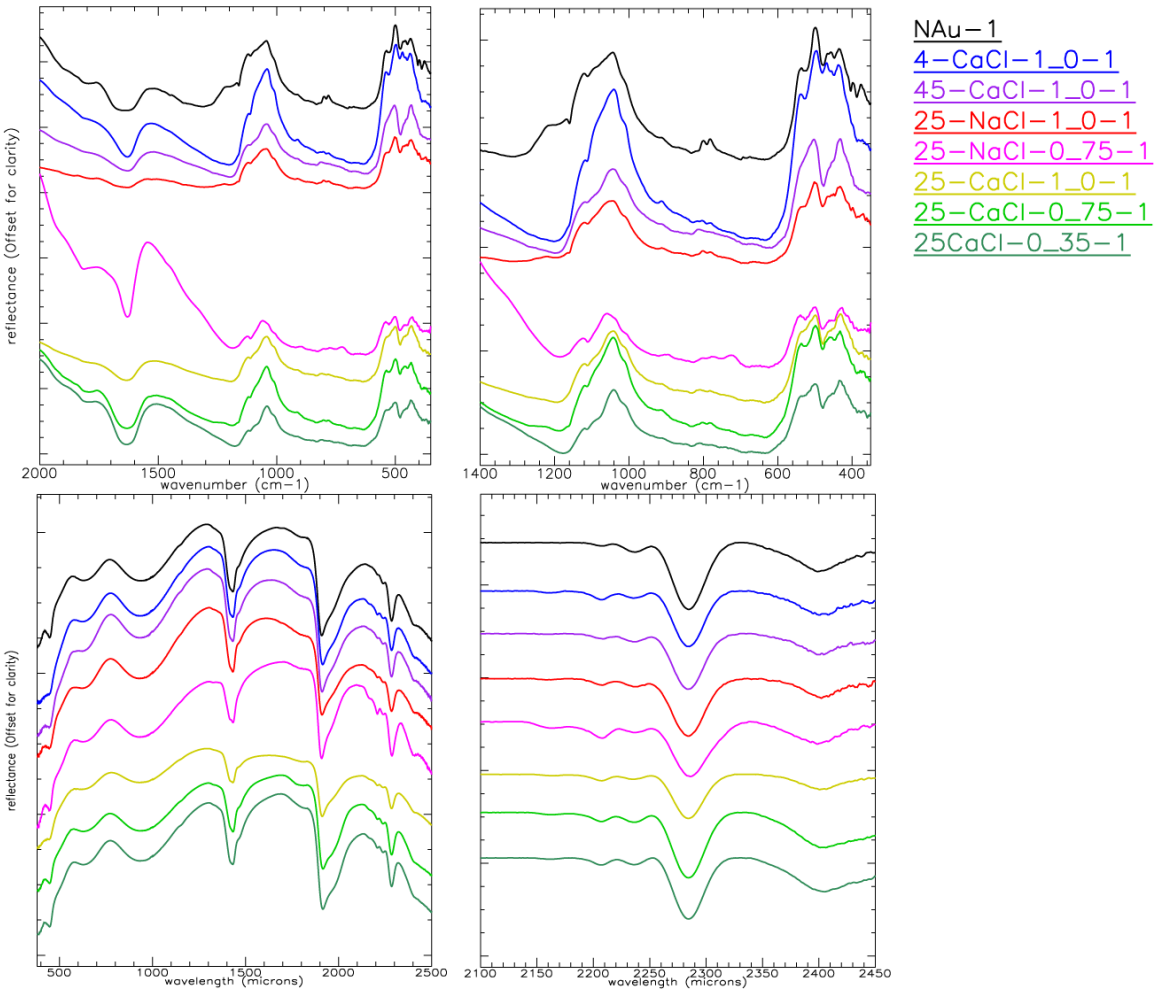

Top: FTIR spectra of unreacted and reacted nontronite, with the whole spectra from wavenumber 2000 – 480 cm^{-1} top left, and enlargement from wavenumber 1400 – 380 cm^{-1} top right. The Si-O stretch near 1000 cm^{-1} becomes narrower for all reacted samples. A reflectance maximum/emission minimum at 1220 cm^{-1} and a feature at 790 cm^{-1} disappear in reacted samples compared to the unreacted NAu-1 spectra. The Al/Si-O-Si deformations between 600 and 400 cm^{-1} change in shape for all 25º C and 45 ºC experiments.

Bottom: IR spectra of unreacted and reacted nontronite at wavelengths from 0.5-2.5 μm, offset for clarity, enlargement from 2.10 μm to 2.45 μm shown to the right. Little change is noted with reaction - for samples treated with the 0.75 $a$$H_2O$ $CaCl_2$ brine, there is a slight change in absorbance near 2.43 μm with a subtle shift of about 10nm near 2.40 μm and 2.45 μm.

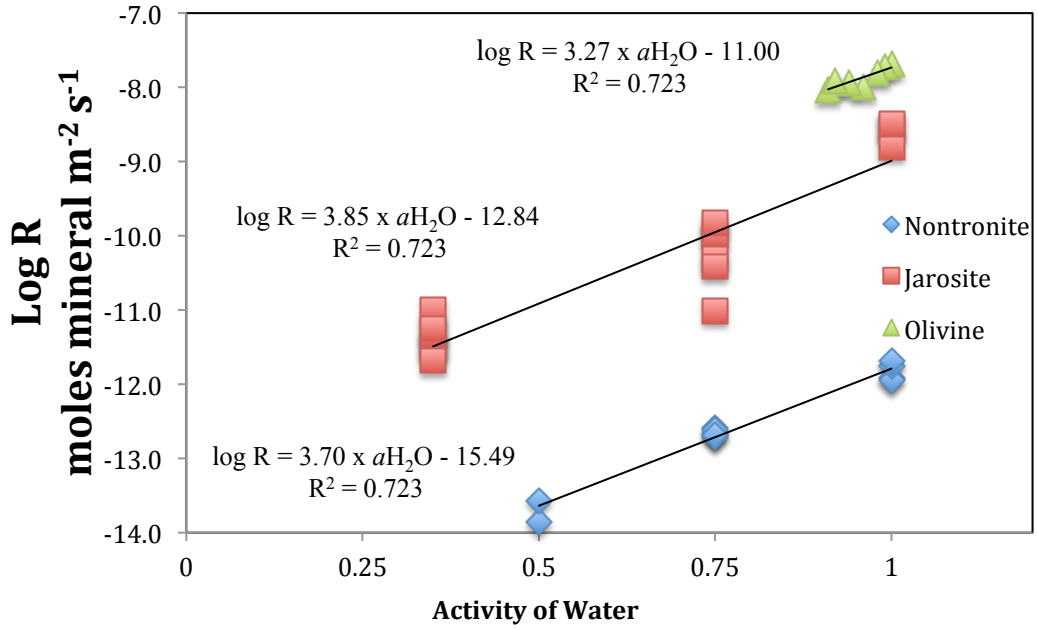

Figure 8.

Comparison of dissolution rates of nontronite, jarosite and olivine as a function of activity of water. Activities cover a range of 1.0-0.5 for nontronite, 1.0-0.35 for K- and Na-jarosite, and 1.0-0.91 at pH 2.00 for olivine. All rates were calculated from experiments performed at temperatures from 23-26º C. For jarosite experiments with $aH_2O < 1.00$ the pH was not measured, but is assumed to be 3-4 (personal communication M. Elwood Madden). Olivine experiments showed decreasing rates with decreasing activity of water differing from this study by 11%. Jarosite experiments showed a decrease in rate with decreasing activity of water that differed from this study by only 4%.

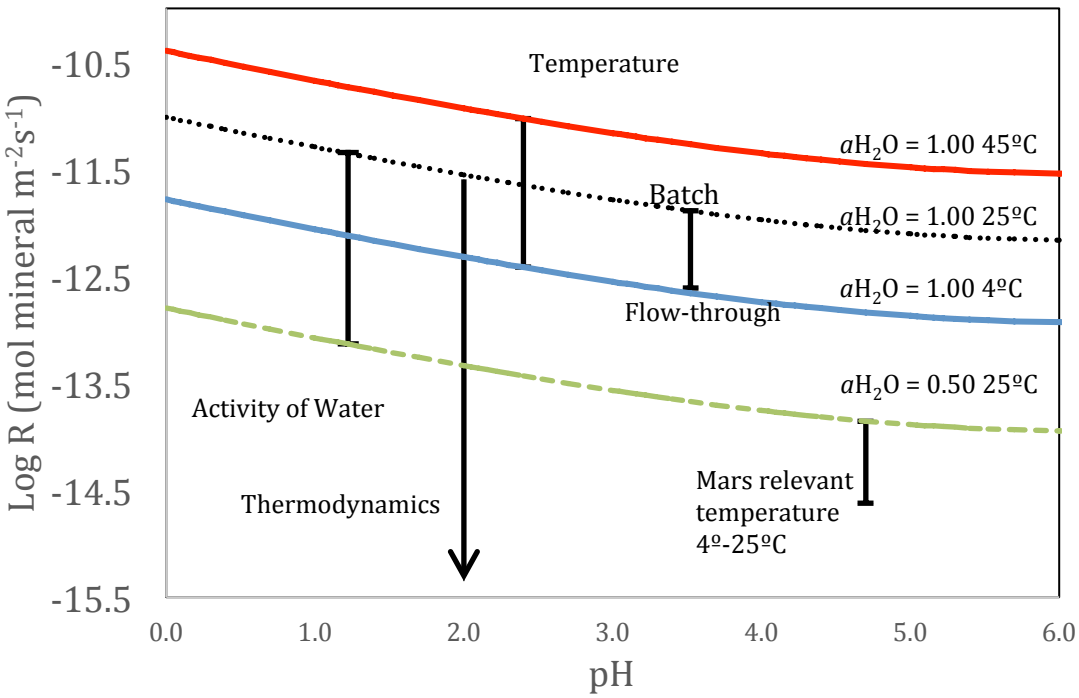

Figure 9.

Nontronite dissolution as a function of pH, temperature, activity of water, thermodynamics and hydrodynamics showing rates likely relevant to martian conditions. Vertical black lines show the range of dissolution rates under each condition. Horizontal lines show dissolution rates from this study with pH dependence under acidic conditions from Gainey et al. (2014). Changes to the rate caused by changes in activity of water measured here have a larger impact than temperature and pH under the range of conditions examined here while use of a either a batch or flow-through reactor is nearly equivalent to a change in temperature from 4º C to 25º C.

Appendix B Supplementary Material

Appendix Table 1. Location of appendix figure by reactor and conditions

					Appendix Figure Location			
Reactor Name	**T (ºC)**	**Salt**	***a*H_2O**	**Duplicate Number**	**Silica Analysis**	**Iron Analysis**	**Silica Duplicate**	**Iron Duplicate**
25-Ca-1.00-1	25.0	$CaCl_2$	1.00	1	1	15	23	30
25-Ca-1.00-2	25.0	$CaCl_2$	1.00	2	2	16	23	30
25-Ca-0.75-1	25.0	$CaCl_2$	0.75	1	3	n/a[1]	24	n/a[1]
25-Ca-0.75-2	25.0	$CaCl_2$	0.75	2	4	n/a[1]	24	n/a[1]
25-Ca-0.50-1	25.0	$CaCl_2$	0.50	1	5	n/a[1]	25	n/a[1]
25-Ca-0.50-2	25.0	$CaCl_2$	0.50	2	6	n/a[1]	25	n/a[1]
45-Ca-1.00-1	45.0	$CaCl_2$	1.00	1	7	17	26	31
45-Ca-1.00-2	45.0	$CaCl_2$	1.00	2	8	18	26	31
4-Ca-1.00-1	4.0	$CaCl_2$	1.00	1	9	19	27	32
4-Ca-1.00-2	4.0	$CaCl_2$	1.00	2	10	20	27	32
25-Na-1.00-1	25.0	NaCl	1.00	1	11	21	28	33
25-Na-1.00-2	25.0	NaCl	1.00	2	12	22	28	33
25-Na-0.75-5	25.0	NaCl	0.75	5	13	n/a[1]	29	n/a[1]
25-Na-0.75-6	25.0	NaCl	0.75	6	14	n/a[1]	29	n/a[1]

[1]Analysis below detection or not performed due to lack of sample.

Appendix Figure 1.

Silica analysis for experiment 25-Ca-1.00-1

Mineral: Nontronite (NAu-1) **Initial pH:** 2.00 **Solution**: 0.01 m $CaCl_2$ **Specific Surf. Area (BET):** 30.865 m^2/g
Batch ID: 25-Ca-1.00-1 ***a*H_2O** = 1.00 **Mineral Mass:** 0.50g **Total Surf. Area (BET):** 15.4325 m^2
NA = no analysis

Batch Results: Shaded data = all data except for the long term steady state point(s).

Time (s)	pH	Volume (ml)	Concentration (ppm)	Si (moles released)	$-m_{ss}$ ln(1-m/m_{ss})
0	2.00	200		0	
10860	2.05	190	0.25	1.79E-06	1.80E-06
21600	1.84	180	0.55	3.78E-06	3.82E-06
32400	1.89	170	1.21	8.02E-06	8.22E-06
86520	1.96	160	2.70	1.71E-05	1.80E-05
97200	2.03	150	3.14	1.96E-05	2.08E-05
108000	2.21	140	3.53	2.17E-05	2.32E-05
118800	2.01	130	3.53	2.17E-05	2.32E-05
176400	2.10	120	5.32	2.99E-05	3.30E-05
190800	2.21	110	5.08	2.89E-05	3.18E-05
205200	2.21	100	5.54	3.07E-05	3.40E-05
266400	2.04	90	6.77	3.51E-05	3.94E-05
277200	2.11	80	7.60	3.77E-05	4.29E-05
352800	2.07	70	11.00	4.74E-05	5.59E-05
439260	2.05	60	11.22	4.80E-05	5.67E-05
15497100	2.33	50	66.05	1.65E-04	

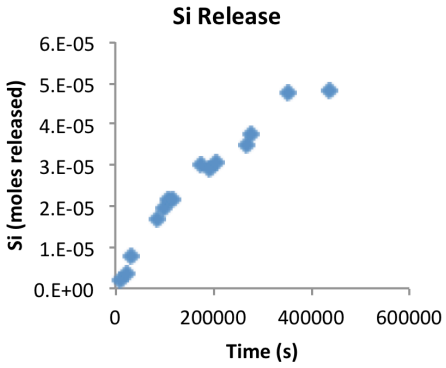

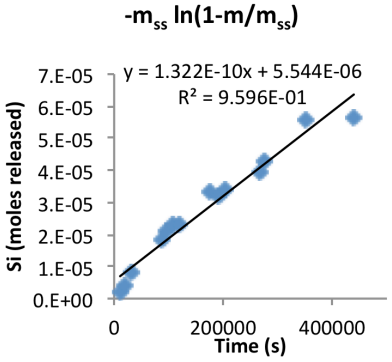

Regression Analysis		*Std.Error*
R Square	0.960	n/a
Si release rate (rSi)	1.32E-10	7.83E-12

Diss. Rate Mineral (K_{diss})	1.23E-12	mol/m^2s
Uncertainty of Fit	9.54E-14	mol/m^2s

Appendix Figure 2.

Silica analysis for experiment 25-Ca-1.00-2

Mineral: Nontronite (NAu-1) **Initial pH:** 2.00 **Solution**: 0.01 m $CaCl_2$ **Specific Surf. Area (BET):** 30.865 m^2/g
Batch ID: 25-Ca-1.00-2 ***a*H_2O** = 1.00 **Mineral Mass:** 0.50g **Total Surf. Area (BET):** 15.4325 m^2

NA = no analysis

Batch Results: Shaded data = all data except for the long term steady state point(s).

Time (s)	pH	Volume (ml)	Concentration (ppm)	Si (moles released)	$-m_{ss}$ ln(1-m/m_{ss})
0		200		0	
10860	2.10	190	0.17	1.24E-06	1.25E-06
21600	1.92	180	0.49	3.38E-06	3.42E-06
32400	2.10	170	1.27	8.37E-06	8.60E-06
86520	2.05	160	2.75	1.73E-05	1.84E-05
97200	2.08	150	3.16	1.97E-05	2.11E-05
108000	2.13	140	3.24	2.01E-05	2.15E-05
118800	2.03	130	3.58	2.18E-05	2.35E-05
176400	2.04	120	4.89	2.79E-05	3.08E-05
190800	2.14	110	5.16	2.90E-05	3.22E-05
205200	2.19	100	5.45	3.01E-05	3.36E-05
266400	2.09	90	6.57	3.41E-05	3.86E-05
277200	2.16	80	7.03	3.56E-05	4.05E-05
352800	2.09	70	9.17	4.17E-05	4.87E-05
439260	2.02	60	10.80	4.58E-05	5.44E-05
15497100	2.43	50	60.84	1.53E-04	

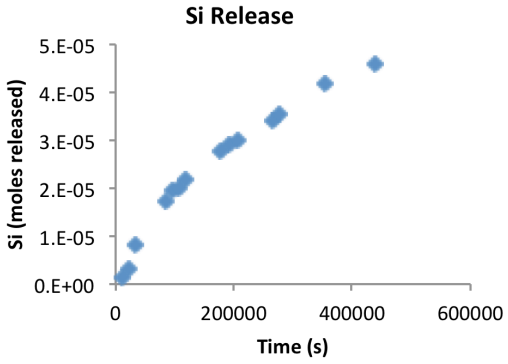

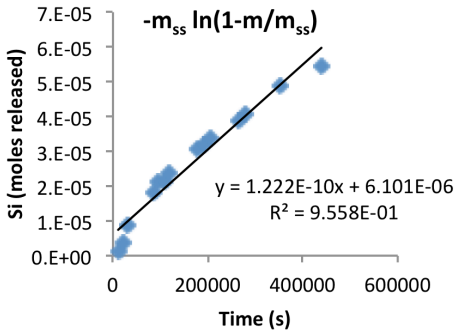

Regression Analysis		*Std.Error*
R Square	0.956	n/a
Si release rate (rSi)	1.22E-10	7.58E-12

Diss. Rate Mineral (K_{diss})	1.13E-12	mol/m^2s
Uncertainty of Fit	9.06E-14	mol/m^2s

Appendix Figure 3.

Silica analysis for experiment 25-Ca-0.75-1

Mineral: Nontronite (NAu-1) **Initial pH:** 2.00 **Solution**: 3.0 m $CaCl_2$ **Specific Surf. Area (BET):** 30.865 m^2/g
Batch ID: 25-Ca-0.75-1 a_{H_2O} = 0.75 **Mineral Mass:** 1.0061g **Total Surf. Area (BET):** 15.4325 m^2
NA = no analysis

Batch Results: Shaded data = all data except for the long term steady state point(s).

Time (s)	pH	Volume (ml)	Concentration (ppm)	Si (moles released)	$-m_{ss}\ln(1-m/m_{ss})$
0	2.00	200		0	
10980	1.92	190	0.69	4.93E-06	5.42E-06
21600	2.00	180	0.90	6.32E-06	7.17E-06
32400	1.96	170	1.10	7.64E-06	8.93E-06
86460	1.95	160	1.72	1.14E-05	1.46E-05
97200	2.07	150	1.51	1.02E-05	1.27E-05
107940	2.27	140	2.13	1.35E-05	1.85E-05
118800	2.27	130	1.93	1.25E-05	1.65E-05
176400	2.26	120	2.34	1.44E-05	2.02E-05
190800	2.24	110	2.75	1.61E-05	2.41E-05
205200	2.27	100	2.54	1.53E-05	2.23E-05
266400	2.33	90	2.75	1.61E-05	2.39E-05
277140	2.25	80	3.16	1.74E-05	2.73E-05
352740	2.39	70	3.16	1.74E-05	2.73E-05
439320	2.13	60	3.37	1.79E-05	2.87E-05
15497040	2.88	50	8.02	2.78E-05	

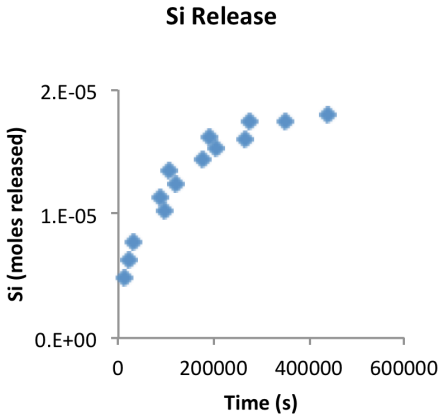

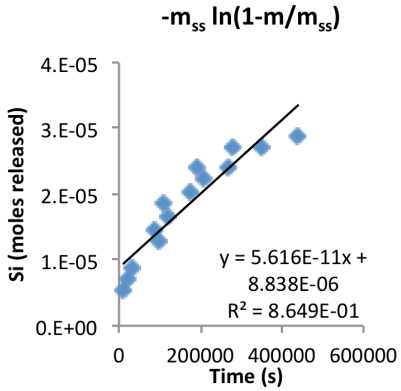

Analytical uncertainty is smaller than the plotted symbol.

Regression Analysis		*Std.Error*
R Square	0.865	n/a
Si release rate (rSi)	5.62E-11	6.41E-12

Diss. Rate Mineral (K_{diss})	2.59E-13	mol/m^2s
Uncertainty of Fit	2.92E-14	mol/m^2s

Appendix Figure 4.

Silica analysis for experiment 25-Ca-0.75-2

Mineral: Nontronite (NAu-1) **Initial pH:** 2.00 **Solution**: 3.0 m $CaCl_2$ **Specific Surf. Area (BET):** 30.865 m^2/g
Batch ID: 25-Ca-0.75-2 ***a*H_2O** = 0.75 **Mineral Mass:** 1.0590g **Total Surf. Area (BET):** 15.4325 m^2
NA = no analysis

Batch Results: Shaded data = all data except for the long term steady state point(s).

Time (s)	pH	Volume (ml)	Concentration (ppm)	Si (moles released)	$-m_{ss}$ ln(1-m/m_{ss})
0		200		0	
10920	1.97	190	0.25	1.81E-06	1.88E-06
21540	1.92	180	0.76	5.27E-06	5.86E-06
32400	1.95	170	1.02	6.90E-06	7.98E-06
86460	2.03	160	1.53	9.99E-06	1.25E-05
97140	2.08	150	1.53	9.99E-06	1.25E-05
107880	2.04	140	1.79	1.14E-05	1.48E-05
118800	2.07	130	1.79	1.14E-05	1.48E-05
176460	2.32	120	2.04	1.25E-05	1.69E-05
190860	2.27	110	2.30	1.36E-05	1.90E-05
205200	2.34	100	2.30	1.36E-05	1.90E-05
266400	1.99	90	2.55	1.45E-05	2.10E-05
277140	2.23	80	2.81	1.54E-05	2.28E-05
352740	2.33	70	3.06	1.61E-05	2.46E-05
439260	2.14	60	2.81	1.54E-05	2.30E-05
15497040	2.94	50	8.10	2.68E-05	#NUM!

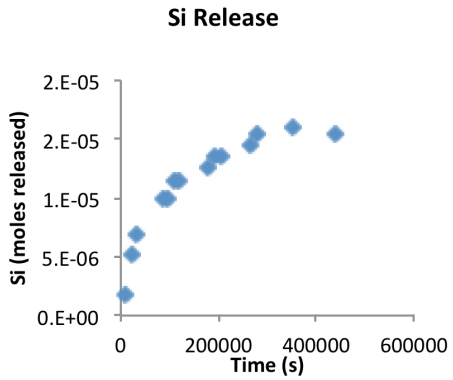

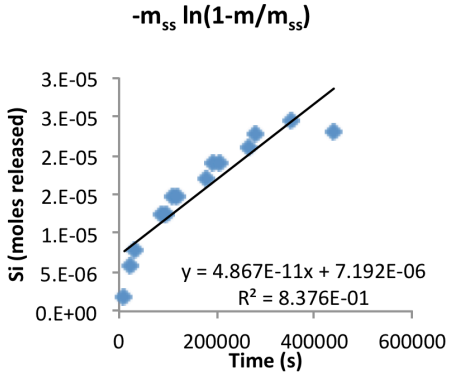

Analytical uncertainty is smaller than the plotted symbol.

Regression Analysis		*Std.Error*
R Square	0.838	n/a
Si release rate (rSi)	4.87E-11	6.19E-12

Diss. Rate Mineral (K_{diss})	2.13E-13	mol/m^2s
Uncertainty of Fit	3.23E-14	mol/m^2s

Appendix Figure 5.

Silica analysis for experiment 25-Ca-0.50-1

Mineral: Nontronite (NAu-1) **Initial pH:** 2.00 **Solution**: 5.0 m $CaCl_2$ **Specific Surf. Area (BET):** 30.865 m^2/g
Batch ID: 25-Ca-0.50-1 ***a*H_2O** = 0.50 **Mineral Mass:** 5.01g **Total Surf. Area (BET):** 15.4325 m^2
NA = no analysis

Batch Results: Shaded data = all data except for the long term steady state point(s).

Time (s)	pH	Volume (ml)	Concentration (ppm)	Si (moles released)	$-m_{ss}$ ln(1-m/m_{ss})
0	2.00	200		0	
21600	2.05	190	0.00	0.00E+00	0.00E+00
86700	n/a	180	0.11	7.63E-07	8.70E-07
172860	1.90	170	0.27	1.80E-06	2.64E-06
259200	2.34	160	0.40	2.54E-06	4.98E-06
345600	2.31	150	0.44	2.54E-06	4.98E-06
431940	2.35	140	0.48	2.76E-06	6.19E-06
518520	2.05	130	0.48	2.96E-06	7.97E-06
604800	2.00	120	0.52	2.96E-06	7.97E-06
691200	2.08	110	0.52	3.13E-06	1.12E-05
777600	2.25	100	0.52	3.13E-06	1.12E-05
864000	2.10	90	0.52	3.13E-06	1.12E-05
950400	2.23	80	0.52	3.13E-06	1.12E-05
1123200	1.97	70	0.56	3.13E-06	1.12E-05
1296000	n/a	60	0.56	3.23E-06	#NUM!

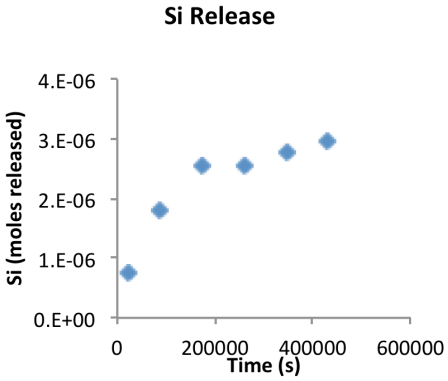

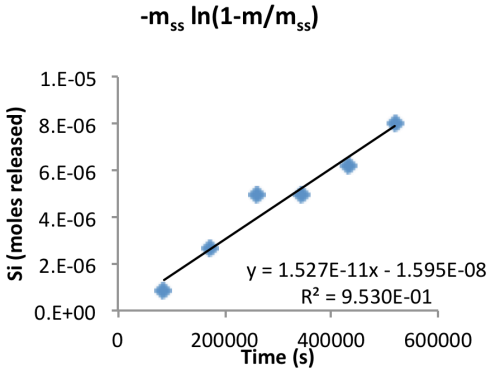

Analytical uncertainty is smaller than the plotted symbol.

Regression Analysis		*Std.Error*
R Square	0.953	n/a
Si release rate (rSi)	1.53E-11	1.69E-12

Diss. Rate Mineral (K_{diss})	1.41E-14	mol/m^2s
Uncertainty of Fit	1.72E-15	mol/m^2s

Appendix Figure 6.

Silica analysis for experiment 25-Ca-0.50-2

Mineral: Nontronite (NAu-1) **Initial pH:** 2.00 **Solution**: 5.0 m $CaCl_2$ **Specific Surf. Area (BET):** 30.865 m^2/g
Batch ID: 25-Ca-0.50-2 ***a*H_2O** = 0.50 **Mineral Mass:** 5.01g **Total Surf. Area (BET):** 15.4325 m^2

NA = no analysis

Batch Results: Shaded data = all data except for the long term steady state point(s).

Time (s)	pH	Volume (ml)	Concentration (ppm)	Si (moles released)	$-m_{ss}\ln(1-m/m_{ss})$
0		200		0	
21540	2.10	190	0.23	1.67E-06	2.23E-06
86520	2.27	180	0.36	2.49E-06	4.21E-06
172800	1.97	170	0.48	3.27E-06	8.39E-06
259140	1.74	160	0.48	3.27E-06	8.39E-06
345540	1.98	150	0.52	3.50E-06	1.21E-05
431880	2.22	140	0.52	3.50E-06	1.21E-05
518460	1.88	130	0.52	3.50E-06	1.21E-05
604800	2.09	120	0.52	3.50E-06	1.21E-05
691140	2.03	110	0.52	3.50E-06	1.21E-05
777540	1.88	100	0.52	3.50E-06	1.21E-05
863940	2.03	90	0.52	3.50E-06	1.21E-05
950340	2.07	80	0.56	3.63E-06	
1123140	2.36	70	0.56	3.63E-06	
1295940	2.60	60	0.48	3.43E-06	

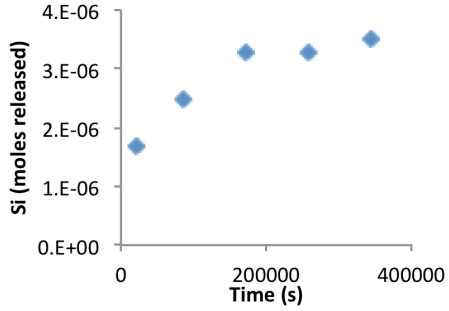

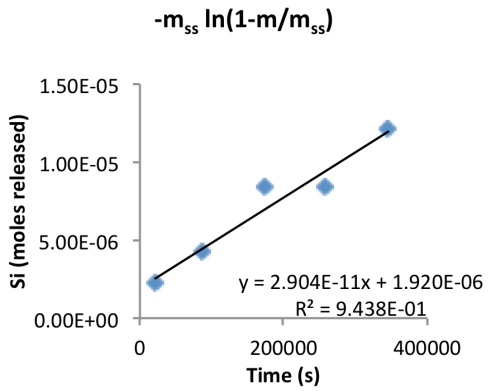

Analytical uncertainty is smaller than the plotted symbol.

Regression Analysis		*Std.Error*
R Square	0.944	n/a
Si release rate (rSi)	2.90E-11	4.09E-12

Diss. Rate Mineral (K_{diss})	2.69E-14	mol/m^2s
Uncertainty of Fit	4.03E-15	mol/m^2s

Appendix Figure 7.

Silica analysis for experiment 45-Ca-1.00-1

Mineral: Nontronite (NAu-1) **Initial pH:** 2.00 **Solution**: 0.01 m $CaCl_2$ **Specific Surf. Area (BET):** 30.865 m^2/g
Batch ID: 45-Ca-1.00-1 ***a*H_2O** = 1.00 **Mineral Mass:** 0.5112g **Total Surf. Area (BET):** 15.4325 m^2
NA = no analysis

Batch Results: Shaded data = all data except for the long term steady state point(s).

Time (s)	pH	Volume (ml)	Concentration (ppm)	Si (moles released)	$-m_{ss}\ln(1-m/m_{ss})$
0	2.00	200		0	
10920	2.08	190	3.96	2.82E-05	3.00E-05
86520	2.05	180	10.46	7.22E-05	8.63E-05
97260	2.05	170	11.34	7.78E-05	9.46E-05
108120	2.07	160	11.48	7.87E-05	9.58E-05
172920	2.09	150	16.36	1.06E-04	1.42E-04
183600	2.08	140	16.74	1.09E-04	1.46E-04
194400	2.07	130	13.88	9.42E-05	1.20E-04
259200	2.08	120	20.99	1.27E-04	1.83E-04
270060	2.07	110	22.83	1.35E-04	2.01E-04
280800	2.08	100	21.76	1.31E-04	1.91E-04
345660	2.13	90	27.63	1.52E-04	2.44E-04
356400	2.08	80	23.00	1.37E-04	2.05E-04
367140	2.07	70	29.14	1.54E-04	2.52E-04
432060	2.10	60	33.41	1.65E-04	2.85E-04
5982180	2.21	50	66.05	2.35E-04	
7347180	n/a	40	68.63	2.39E-04	

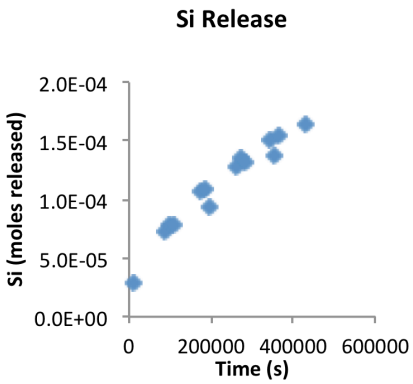

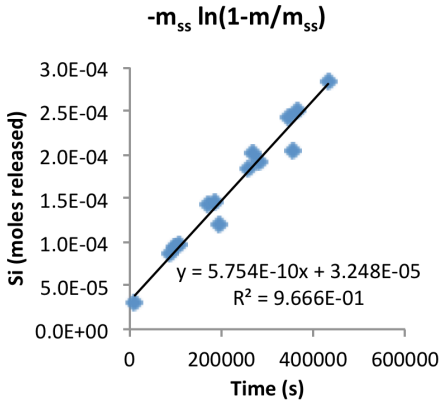

Analytical uncertainty is smaller than the plotted symbol.

Regression Analysis		*Std.Error*
R Square	0.967	n/a
Si release rate (rSi)	5.75E-10	3.09E-11

Diss. Rate Mineral (K_{diss})	5.22E-12	mol/m^2s
Uncertainty of Fit	3.84E-10	mol/m^2s

Appendix Figure 8.

Silica analysis for experiment 45-Ca-1.00-2

Mineral: Nontronite (NAu-1) **Initial pH:** 2.00 **Solution**: 0.01 m $CaCl_2$ **Specific Surf. Area (BET):** 30.865 m^2/g
Batch ID: 45-Ca-1.00-2 ***a*H_2O** = 1.00 **Mineral Mass:** 0.5000g **Total Surf. Area (BET):** 15.4325 m^2
NA = no analysis

Batch Results: Shaded data = all data except for the long term steady state point(s).

Time (s)	pH	Volume (ml)	Concentration (ppm)	Si (moles released)	$-m_{ss}\ln(1-m/m_{ss})$
0	2.00	200		0	
10920	2.02	190	3.88	2.76E-05	2.93E-05
86520	2.05	180	9.97	6.88E-05	8.08E-05
97260	2.02	170	10.82	7.43E-05	8.86E-05
108120	2.07	160	11.78	8.01E-05	9.71E-05
172920	2.08	150	16.52	1.07E-04	1.41E-04
183600	2.08	140	16.41	1.07E-04	1.40E-04
194400	2.07	130	17.76	1.13E-04	1.52E-04
259200	2.07	120	21.12	1.29E-04	1.83E-04
270060	2.07	110	23.16	1.38E-04	2.02E-04
280800	2.06	100	20.46	1.27E-04	1.79E-04
345660	2.13	90	20.79	1.28E-04	1.82E-04
356400	2.10	80	28.04	1.51E-04	2.36E-04
367140	2.11	70	27.41	1.50E-04	2.31E-04
432060	2.10	60	32.20	1.61E-04	2.64E-04
5982180	2.17	50	70.89	2.44E-04	
7347180	n/a	40	73.14	2.48E-04	

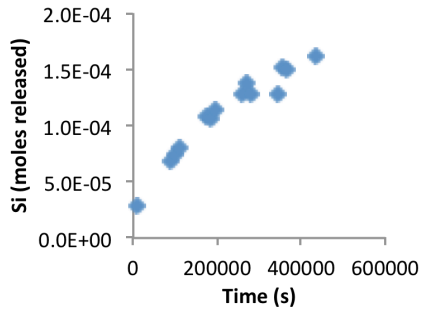

Analytical uncertainty is smaller than the plotted symbol.

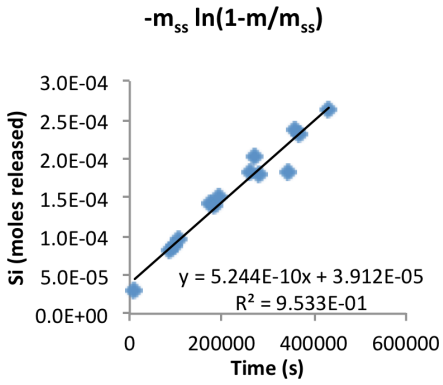

Regression Analysis		*Std.Error*
R Square	0.953	n/a
Si release rate (rSi)	5.24E-10	3.35E-11

Diss. Rate Mineral (K_{diss})	4.74E-12	mol/m^2s
Uncertainty of Fit	3.85E-13	mol/m^2s

Appendix Figure 9.

Silica analysis for experiment 4-Ca-1.00-1

Mineral: Nontronite (NAu-1) **Initial pH:** 2.00 **Solution**: 0.01 m $CaCl_2$ **Specific Surf. Area (BET):** 30.865 m^2/g
Batch ID: 4-Ca-1.00-1 ***a*H$_2$O** = 1.00 **Mineral Mass:** 0.4990g **Total Surf. Area (BET):** 15.4325 m^2

NA = no analysis

Batch Results: Shaded data = all data except for the long term steady state point(s).

Time (s)	pH	Volume (ml)	Concentration (ppm)	Si (moles released)	$-m_{ss}\ln(1-m/m_{ss})$
0	2.00	200		0	
86580	1.98	190	0.13	8.94E-07	8.97E-07
172980	1.98	180	0.55	3.74E-06	3.80E-06
259260	1.99	170	0.89	5.97E-06	6.11E-06
345720	2.01	160	2.70	1.69E-05	1.82E-05
605100	2.02	150	3.30	2.03E-05	2.22E-05
691560	2.02	140	3.84	2.32E-05	2.57E-05
777900	2.04	130	3.94	2.37E-05	2.63E-05
864240	2.04	120	4.21	2.50E-05	2.79E-05
950460	2.03	110	4.81	2.75E-05	3.11E-05
1209540	2.00	100	5.28	2.93E-05	3.35E-05
1296000	2.05	90	5.97	3.18E-05	3.68E-05
1382640	2.04	80	6.51	3.35E-05	3.92E-05
1469160	2.02	70	6.81	3.44E-05	4.03E-05
1555320	2.03	60	7.35	3.57E-05	4.22E-05
6489180	1.98	50	33.74	9.21E-05	1.70E-04
9076320	2.02	40	51.05	1.23E-04	

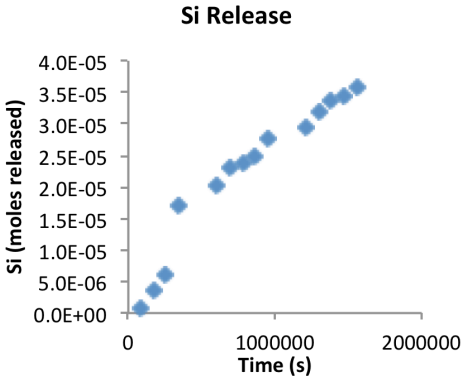

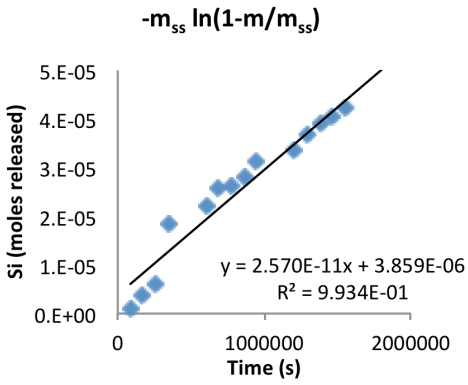

Analytical uncertainty is smaller than the plotted symbol.

Regression Analysis		*Std.Error*
R Square	0.942	n/a
Si release rate (rSi)	2.57E-11	5.81E-13

Diss. Rate Mineral (K_{diss})	2.39E-13	mol/m^2s
Uncertainty of Fit	2.28E-13	mol/m^2s

Appendix Figure 10.

Silica analysis for experiment 4-Ca-1.00-2

Mineral: Nontronite (NAu-1) **Initial pH:** 2.00 **Solution**: 0.01 m $CaCl_2$ **Specific Surf. Area (BET):** 30.865 m^2/g
Batch ID: 4-Ca-1.00-2 ***a*H_2O** = 1.00 **Mineral Mass:** 0.5000g **Total Surf. Area (BET):** 15.4325 m^2

NA = no analysis

Batch Results: Shaded data = all data except for the long term steady state point(s).

Time (s)	pH	Volume (ml)	Concentration (ppm)	Si (moles released)	$-m_{ss}\ln(1-m/m_{ss})$
0		200		0	
86580	1.98	190	0.27	1.95E-06	1.97E-06
172980	2.00	180	0.92	6.31E-06	6.48E-06
259260	1.99	170	1.31	8.85E-06	9.20E-06
345720	2.01	160	1.98	1.29E-05	1.37E-05
605100	2.02	150	3.00	1.87E-05	2.03E-05
691560	2.02	140	3.30	2.03E-05	2.22E-05
777900	2.02	130	3.47	2.11E-05	2.33E-05
864240	2.03	120	3.79	2.26E-05	2.51E-05
950460	2.06	110	4.49	2.56E-05	2.89E-05
1209540	2.06	100	5.20	2.84E-05	3.25E-05
1296060	2.04	90	5.45	2.93E-05	3.37E-05
1382700	2.03	80	5.92	3.08E-05	3.57E-05
1469220	2.04	70	6.19	3.16E-05	3.67E-05
1555380	2.04	60	6.68	3.28E-05	3.84E-05
6489240	2.01	50	32.64	8.82E-05	1.63E-04
9076380	2.00	40	49.12	1.18E-04	

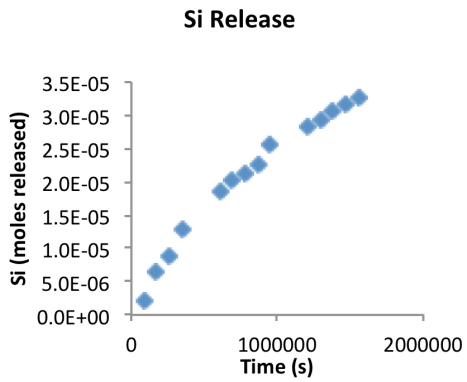

Analytical uncertainty is smaller than the plotted symbol.

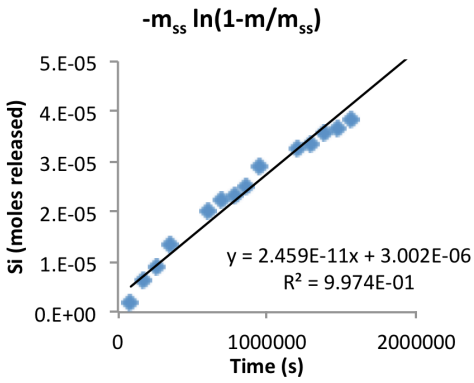

Regression Analysis		*Std.Error*
R Square	0.997	n/a
Si release rate (rSi)	2.46E-11	3.47E-13

Diss. Rate Mineral (K_{diss})	2.28E-13	mol/m^2s
Uncertainty of Fit	1.18E-14	mol/m^2s

Appendix Figure 11.

Silica analysis for experiment 25-Na-1.00-1

Mineral: Nontronite (NAu-1) **Initial pH:** 2.00 **Solution**: 0.01 m NaCl **Specific Surf. Area (BET):** 30.865 m^2/g
Batch ID: 25-Na-1.00-1 ***a*H_2O** = 1.00 **Mineral Mass:** 0.4999g **Total Surf. Area (BET):** 15.4325 m^2
NA = no analysis

Batch Results: Shaded data = all data except for the long term steady state point(s).

Time (s)	pH	Volume (ml)	Concentration (ppm)	Si (moles released)	$-m_{ss}\ln(1-m/m_{ss})$
0	2.00	200		0	
10860	n/a	190	0.95	6.76E-06	6.88E-06
21600	2.03	180	1.67	1.16E-05	1.20E-05
32460	n/a	170	1.98	1.36E-05	1.41E-05
86460	2.23	160	3.94	2.55E-05	2.73E-05
97200	2.01	150	4.42	2.82E-05	3.04E-05
108060	2.18	140	4.68	2.96E-05	3.21E-05
118800	2.19	130	5.11	3.18E-05	3.46E-05
172800	2.18	120	6.72	3.92E-05	4.36E-05
187200	2.19	110	7.15	4.10E-05	4.59E-05
201600	2.18	100	7.70	4.32E-05	4.86E-05
259260	2.17	90	9.52	4.97E-05	5.71E-05
273600	2.19	80	10.09	5.15E-05	5.95E-05
288000	2.21	70	10.31	5.21E-05	6.03E-05
360060	2.21	60	12.87	5.85E-05	6.92E-05
3312480	2.50	50	75.33	1.92E-04	6.29E-04
7282920	2.30	40	80.24	2.01E-04	

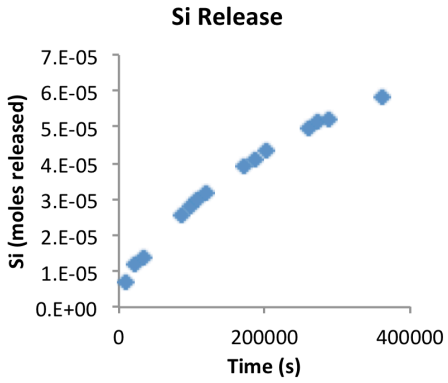

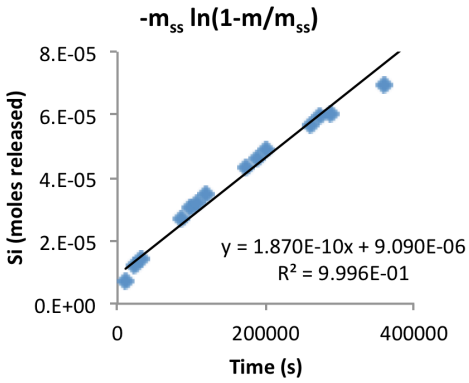

Analytical uncertainty is smaller than the plotted symbol.

Regression Analysis		*Std.Error*
R Square	1.000	n/a
Si release rate (rSi)	1.87E-10	1.01E-12

Diss. Rate Mineral (K_{diss})	1.74E-12	mol/m^2s
Uncertainty of Fit	8.75E-14	mol/m^2s

Appendix Figure 12.

Silica analysis for experiment 25-Na-1.00-2

Mineral: Nontronite (NAu-1) **Initial pH:** 2.00 **Solution**: 0.01 m NaCl **Specific Surf. Area (BET):** 30.865 m^2/g
Batch ID: 25-Na-1.00-2 ***a*H_2O** = 1.00 **Mineral Mass:** 0.5050g **Total Surf. Area (BET):** 15.4325 m^2
NA = no analysis

Batch Results: Shaded data = all data except for the long term steady state point(s).

Time (s)	pH	Volume (ml)	Concentration (ppm)	Si (moles released)	$-m_{ss}$ ln(1-m/m_{ss})
0	2.00	200		0	
10980	2.38	190	1.10	7.83E-06	7.98E-06
21660	2.20	180	1.70	1.19E-05	1.22E-05
32520	n/a	170	2.24	1.54E-05	1.60E-05
86520	2.23	160	4.41	2.85E-05	3.07E-05
97260	2.23	150	4.58	2.95E-05	3.19E-05
108120	2.18	140	5.36	3.36E-05	3.67E-05
118860	2.16	130	5.66	3.51E-05	3.85E-05
172860	2.18	120	7.42	4.33E-05	4.87E-05
187260	2.19	110	7.77	4.48E-05	5.06E-05
201720	2.18	100	8.39	4.72E-05	5.37E-05
259320	2.17	90	10.19	5.36E-05	6.22E-05
273660	2.20	80	10.78	5.55E-05	6.49E-05
288060	2.20	70	10.81	5.56E-05	6.50E-05
360120	2.21	60	13.70	6.28E-05	7.51E-05
3312540	2.28	50	76.80	1.98E-04	7.51E-04
7282980	2.31	40	79.60	2.03E-04	

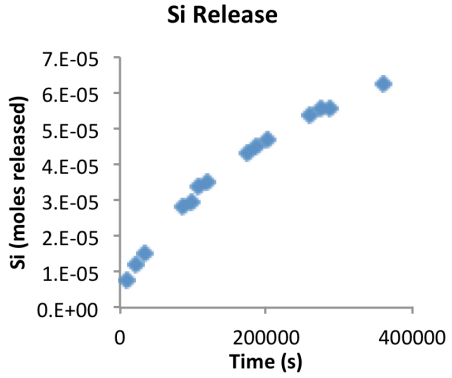

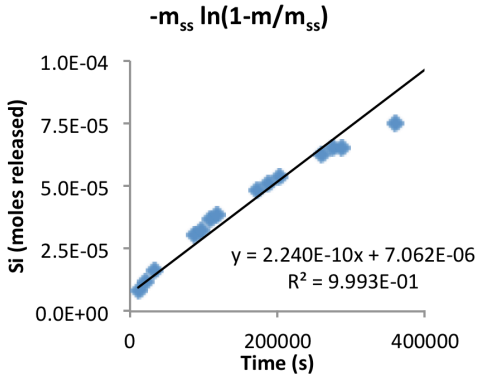

Analytical uncertainty is smaller than the plotted symbol.

Regression Analysis		*Std.Error*
R Square	0.999	n/a
Si release rate (rSi)	2.24E-10	1.63E-12

Diss. Rate Mineral (K_{diss})	2.06E-12	mol/m^2s
Uncertainty of Fit	1.04E-13	mol/m^2s

Appendix Figure 13.

Silica analysis for experiment 25-Na-0.75-5

Mineral: Nontronite (NAu-1) **Initial pH:** 2.00 **Solution**: 6.14 m NaCl **Specific Surf. Area (BET):** 30.865 m^2/g
Batch ID: 25-Na-0.75-5 a_{H_2O} = 0.75 **Mineral Mass:** 0.4990g **Total Surf. Area (BET):** 15.4325 m^2
NA = no analysis

Batch Results: Shaded data = all data except for the long term steady state point(s).

Time (s)	pH	Volume (ml)	Concentration (ppm)	Si (moles released)	$-m_{ss}\ln(1-m/m_{ss})$
0	2.00	200		0	
17940	2.08	190	0.36	2.56E-06	2.63E-06
86400	2.14	180	1.35	9.23E-06	1.02E-05
108000	2.22	170	1.65	1.12E-05	1.26E-05
172980	2.19	160	2.09	1.39E-05	1.61E-05
194580	2.16	150	1.92	1.29E-05	1.48E-05
259800	2.28	140	2.61	1.66E-05	1.99E-05
280740	2.22	130	2.57	1.64E-05	1.97E-05
346020	2.20	120	3.05	1.86E-05	2.30E-05
360420	n/a	110	3.12	1.89E-05	2.35E-05
432000	2.36	100	3.47	2.02E-05	2.57E-05
518940	2.34	90	3.91	2.18E-05	2.83E-05
605460	2.44	80	3.91	2.18E-05	2.83E-05
12708000	2.93	70	14.47	5.19E-05	

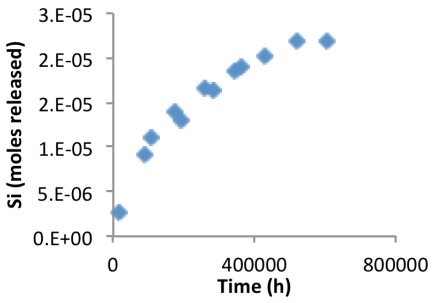

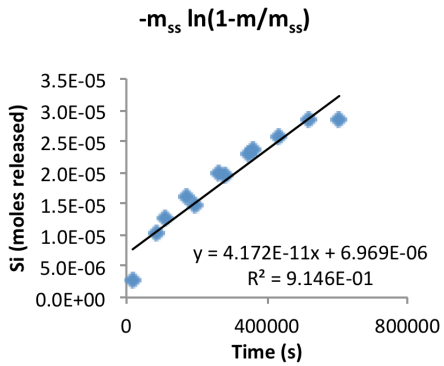

Regression Analysis		*Std.Error*
R Square	0.915	n/a
Si release rate (rSi)	4.17E-11	4.03E-12

Diss. Rate Mineral (K_{diss})	1.94E-13	mol/m^2s
Uncertainty of Fit	2.41E-14	mol/m^2s

Appendix Figure 14.

Silica analysis for experiment 25-Na-0.75-6

Mineral: Nontronite (NAu-1) **Initial pH:** 2.00 **Solution**: 6.14 m NaCl **Specific Surf. Area (BET):** 30.865 m^2/g **Batch ID:** 25-Na-0.75-6 ***a*H_2O** = 0.75 **Mineral Mass:** 0.4990g **Total Surf. Area (BET):** 15.4325 m^2

NA = no analysis

Batch Results: Shaded data = all data except for the long term steady state point(s).

Time (s)	pH	Volume (ml)	Concentration (ppm)	Si (moles released)	$-m_{ss}$ ln(1-m/m_{ss})
0	2.00	200		0	
17940	2.08	190	0.16	1.11E-06	1.12E-06
86400	2.12	180	1.35	9.16E-06	1.01E-05
108000	2.17	170	1.62	1.09E-05	1.22E-05
172980	2.18	160	2.09	1.38E-05	1.60E-05
194580	2.19	150	1.44	1.01E-05	1.12E-05
259800	2.18	140	2.61	1.63E-05	1.96E-05
280740	1.90	130	2.75	1.70E-05	2.06E-05
346020	2.23	120	3.02	1.83E-05	2.25E-05
360420	2.27	110	3.23	1.91E-05	2.39E-05
432000	2.30	100	3.47	2.01E-05	2.54E-05
518940	2.34	90	3.85	2.14E-05	2.77E-05
605460	2.43	80	4.16	2.24E-05	2.94E-05
12708000	3.01	70	14.47	5.18E-05	

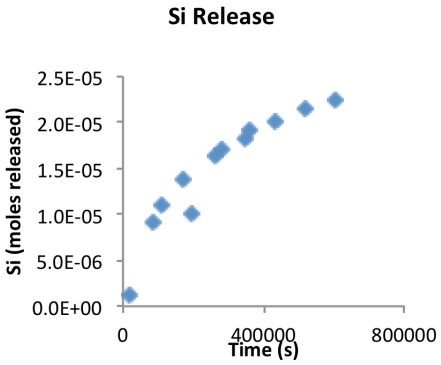

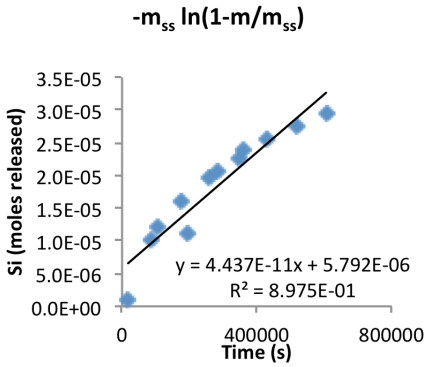

Analytical uncertainty is smaller than the plotted symbol.

Regression Analysis		*Std.Error*
R Square	0.898	n/a
Si release rate (rSi)	4.44E-11	4.74E-12

Diss. Rate Mineral (K_{diss})	2.04E-13	mol/m^2s
Uncertainty of Fit	3.45E-14	mol/m^2s

Appendix Figure 15.

Iron analysis for experiment 25-Ca-1.00-1

Mineral: Nontronite (NAu-1) **Initial pH:** 2.00 **Solution**: 0.01 m $CaCl_2$ **Specific Surf. Area (BET):** 30.865 m^2/g
Batch ID: 25-Ca-1.00-1 αH_2O = 1.00 **Mineral Mass:** 0.50g **Total Surf. Area (BET):** 15.4325 m^2
NA = no analysis

Batch Results: Shaded data = all data except for the long term steady state point(s).

Time (s)	pH	Volume (ml)	Concentration (ppm)	Fe (moles released)	$-m_{ss}$ ln(1-m/m_{ss})
0	2.00	200		0	
97200	2.03	150	0.83	2.97E-06	3.55E-06
108000	2.21	140	0.96	3.32E-06	4.08E-06
118800	2.01	130	1.02	3.47E-06	4.31E-06
176400	2.10	120	1.27	4.05E-06	5.27E-06
190800	2.21	110	1.19	3.89E-06	4.99E-06
205200	2.21	100	1.22	3.93E-06	5.07E-06
266400	2.04	90	1.19	3.88E-06	4.98E-06
277200	2.11	80	1.66	4.63E-06	6.34E-06
15497100	2.33	50	5.09	9.56E-06	

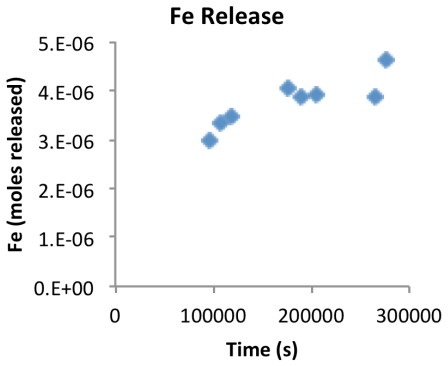

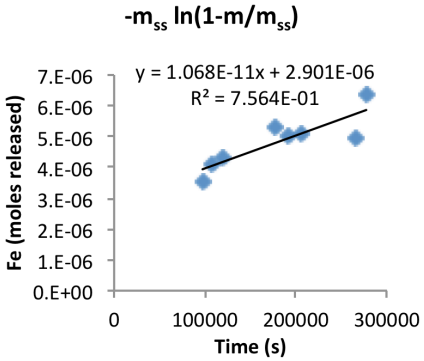

Analytical uncertainty is smaller than the plotted symbol.

Regression Analysis		*Std.Error*
R Square	0.756	n/a
Fe release rate (rFe)	1.07E-11	2.47386E-12

Diss. Rate Mineral (K_{diss})	1.88E-13	mol/m^2s
Uncertainty of Fit	2.36E-14	mol/m^2s

Appendix Figure 16.

Iron analysis for experiment 25-Ca-1.00-2

Mineral: Nontronite (NAu-1) **Initial pH:** 2.00 **Solution**: 0.01 m $CaCl_2$ **Specific Surf. Area (BET):** 30.865 m^2/g
Batch ID: 25-Ca-1.00-2 ***a*H_2O** = 1.00 **Mineral Mass:** 0.5000g **Total Surf. Area (BET):** 15.4325 m^2

NA = no analysis

Batch Results: Shaded data = all data except for the long term steady state point(s).

Time (s)	pH	Volume (ml)	Concentration (ppm)	Fe (moles released)	$-m_{ss}$ ln(1-m/m_{ss})
0		200		0	
32400	2.10	170	0.38	1.37E-06	1.52E-06
108000	2.13	140	0.84	2.75E-06	3.43E-06
118800	2.03	130	0.94	3.00E-06	3.85E-06
176400	2.04	120	1.14	3.48E-06	4.69E-06
190800	2.14	110	1.29	3.80E-06	5.33E-06
205200	2.19	100	1.27	3.76E-06	5.25E-06
266400	2.09	90	1.06	3.38E-06	4.50E-06
277200	2.16	80	1.35	3.86E-06	5.44E-06
352800	2.09	70	1.41	3.93E-06	5.61E-06
15497100	2.43	50	2.11	7.42E-06	

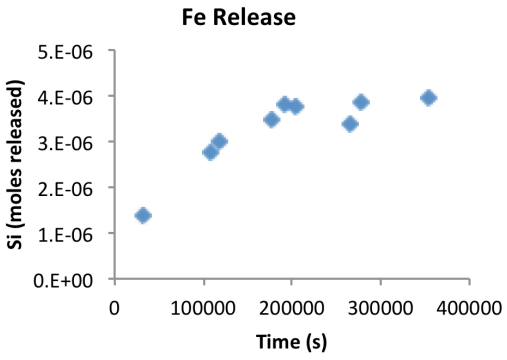

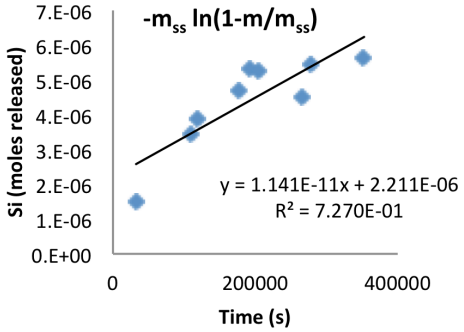

Analytical uncertainty is smaller than the plotted symbol.

Regression Analysis		*Std.Error*
R Square	0.727	n/a
Fe release rate (rFe)	1.14E-11	2.64E-12

Diss. Rate Mineral (K_{diss})	2.01E-13	mol/m^2s
Uncertainty of Fit	2.52E-14	mol/m^2s

Appendix Figure 17.

Iron analysis for experiment 45-Ca-1.00-1

Mineral: Nontronite (NAu-1) **Initial pH:** 2.00 **Solution**: 0.01 m $CaCl_2$ **Specific Surf. Area (BET):** 30.865 m^2/g
Batch ID: 45-Ca-1.00-1 ***a*H_2O** = 1.00 **Mineral Mass:** 0.5112g **Total Surf. Area (BET):** 15.4325 m^2
NA = no analysis

Batch Results: Shaded data = all data except for the long term steady state point(s).

Time (s)	pH	Volume (ml)	Concentration (ppm)	Fe (moles released)	$-m_{ss}\ln(1-m/m_{ss})$
0	2.00	200		0	
10920	2.08	190	0.92	3.28E-06	5.14E-06
86520	2.05	180	1.11	3.94E-06	7.29E-06
97260	2.05	170	1.14	4.04E-06	7.69E-06
108120	2.07	160	1.16	4.09E-06	7.92E-06
172920	2.09	150	1.26	4.37E-06	9.37E-06
183600	2.08	140	1.21	4.24E-06	8.62E-06
194400	2.07	130	1.20	4.22E-06	8.52E-06
259200	2.08	120	1.32	4.49E-06	1.01E-05
270060	2.07	110	1.26	4.37E-06	9.38E-06
280800	2.08	100	1.28	4.42E-06	9.65E-06
345660	2.13	90	1.57	4.94E-06	1.47E-05
356400	2.08	80	1.37	4.61E-06	1.10E-05
367140	2.07	70	1.44	4.71E-06	1.19E-05
432060	2.10	60	1.40	4.66E-06	1.14E-05
5982180	2.21	50	1.96	5.26E-06	

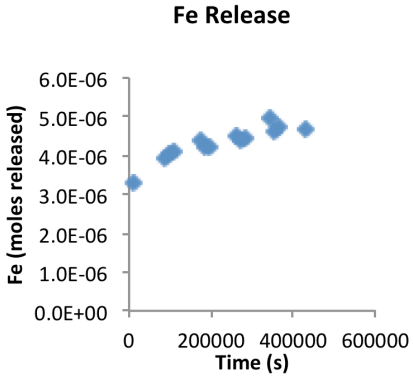

Analytical uncertainty is smaller than the plotted symbol.

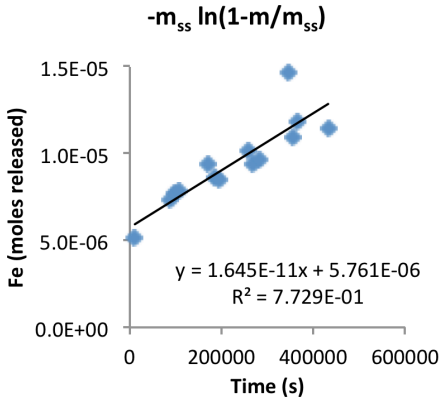

Regression Analysis		*Std.Error*
R Square	0.773	n/a
Fe release rate (rFe)	1.64E-11	2.5735E-12

Diss. Rate Mineral (K_{diss})	2.83E-13	mol/m^2s
Uncertainty of Fit	2.46E-14	mol/m^2s

Appendix Figure 18.

Iron analysis for experiment 45-Ca-1.00-2

Mineral: Nontronite (NAu-1) **Initial pH:** 2.00 **Solution**: 0.01 m $CaCl_2$ **Specific Surf. Area (BET):** 30.865 m^2/g
Batch ID: 45-Ca-1.00-2 ***a*H_2O** = 1.00 **Mineral Mass:** 0.50g **Total Surf. Area (BET):** 15.4325 m^2
NA = no analysis

Batch Results: Shaded data = all data except for the long term steady state point(s).

Time (s)	pH	Volume (ml)	Concentration (ppm)	Fe (moles released)	$-m_{ss}$ ln(1-m/m_{ss})
0		200		0	
10920	2.02	190	0.91	3.26E-06	4.24E-06
86520	2.05	180	1.16	4.12E-06	5.89E-06
97260	2.02	170	1.22	4.31E-06	6.30E-06
108120	2.07	160	1.04	3.75E-06	5.14E-06
172920	2.08	150	1.37	4.71E-06	7.28E-06
183600	2.08	140	1.40	4.79E-06	7.49E-06
194400	2.07	130	1.47	4.95E-06	7.92E-06
259200	2.07	120	1.59	5.24E-06	8.80E-06
270060	2.07	110	1.66	5.39E-06	9.25E-06
280800	2.06	100	1.71	5.48E-06	9.59E-06
345660	2.13	90	1.82	5.69E-06	1.03E-05
356400	2.10	80	1.87	5.76E-06	1.06E-05
367140	2.11	70	1.84	5.72E-06	1.04E-05
432060	2.10	60	1.97	5.89E-06	1.11E-05
5982180	2.17	50	3.66	7.70E-06	
7347180	n/a	40	3.27	7.35E-06	

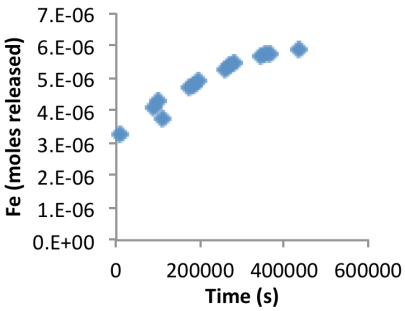

Analytical uncertainty is smaller than the plotted symbol.

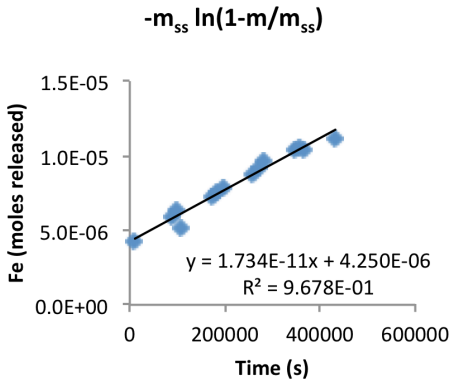

Regression Analysis		*Std.Error*
R Square	0.967	n/a
Fe release rate (rFe)	1.73443E-11	9.1312E-13

Diss. Rate Mineral (K_{diss})	2.97E-13	mol/m^2s
Uncertainty of Fit	1.14E-14	mol/m^2s

Appendix Figure 19.

Iron analysis for experiment 4-Ca-1.00-1

Mineral: Nontronite (NAu-1) **Initial pH:** 2.00 **Solution**: 0.01 m $CaCl_2$ **Specific Surf. Area (BET):** 30.865 m^2/g
Batch ID: 4-Ca-1.00-1 ***a*H_2O** = 1.00 **Mineral Mass:** 0.4990g **Total Surf. Area (BET):** 15.4325 m^2

NA = no analysis

Batch Results: Shaded data = all data except for the long term steady state point(s).

Time (s)	pH	Volume (ml)	Concentration (ppm)	Fe (moles released)	$-m_{ss}$ ln(1-m/m_{ss})
0	2.00	200		0	
86580	1.98	190	0.22	7.83E-07	8.24E-07
172980	1.98	180	0.28	9.85E-07	1.05E-06
259260	1.99	170	0.31	1.10E-06	1.19E-06
345720	2.01	160	0.86	2.75E-06	3.36E-06
605100	2.02	150	1.28	3.96E-06	5.43E-06
691560	2.02	140	1.43	4.37E-06	6.28E-06
777900	2.04	130	1.54	4.65E-06	6.91E-06
864240	2.04	120	1.63	4.84E-06	7.38E-06
950460	2.03	110	1.97	5.58E-06	9.45E-06
1209540	2.00	100	1.64	4.94E-06	7.61E-06
1296000	2.05	90	2.49	6.46E-06	1.29E-05
1382640	2.04	80	2.70	6.80E-06	1.48E-05
1469160	2.02	70	2.62	6.69E-06	1.41E-05
1555320	2.03	60	3.05	7.21E-06	1.79E-05
6489180	1.98	50	3.87	8.10E-06	

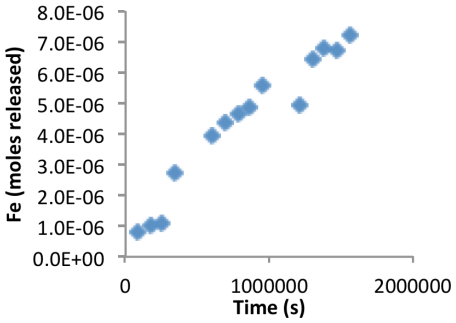

Analytical uncertainty is smaller than the plotted symbol.

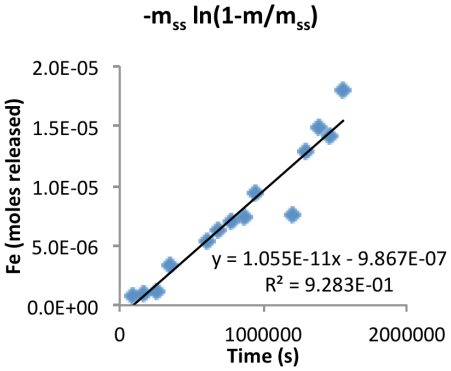

Regression Analysis		*Std.Error*
R Square	0.928	n/a
Fe release rate (rFe)	1.06E-11	8.469E-13

Diss. Rate Mineral (K_{diss})	1.86E-13	mol/m^2s
Uncertainty of Fit	9.31E-15	mol/m^2s

Appendix Figure 20.

Iron analysis for experiment 4-Ca-1.00-2

Mineral: Nontronite (NAu-1) **Initial pH:** 2.00 **Solution**: 0.01 m $CaCl_2$ **Specific Surf. Area (BET):** 30.865 m^2/g
Batch ID: 4-Ca-1.00-2 ***a*H_2O** = 1.00 **Mineral Mass:** 0.5000g **Total Surf. Area (BET):** 15.4325 m^2
NA = no analysis

Batch Results: Shaded data = all data except for the long term steady state point(s).

Time (s)	pH	Volume (ml)	Concentration (ppm)	Fe (moles released)	$-m_{ss}$ ln(1-m/m_{ss})
0		200		0	
86580	1.98	190	0.22	7.96E-07	8.52E-07
172980	2.00	180	0.31	1.09E-06	1.19E-06
259260	1.99	170	0.41	1.40E-06	1.59E-06
345720	2.01	160	0.57	1.91E-06	2.29E-06
605100	2.02	150	1.14	3.55E-06	5.27E-06
691560	2.02	140	0.62	2.13E-06	2.62E-06
777900	2.02	130	0.75	2.45E-06	3.13E-06
864240	2.03	120	0.47	1.82E-06	2.16E-06
950460	2.06	110	1.00	2.95E-06	4.01E-06
1209540	2.06	100	0.71	2.39E-06	3.01E-06
1296060	2.04	90	1.97	4.64E-06	8.59E-06
1382700	2.03	80	2.09	4.84E-06	9.43E-06
1469220	2.04	70	2.11	4.85E-06	9.52E-06
1555380	2.04	60	2.13	4.89E-06	9.67E-06
6489240	2.01	50	3.33	6.18E-06	

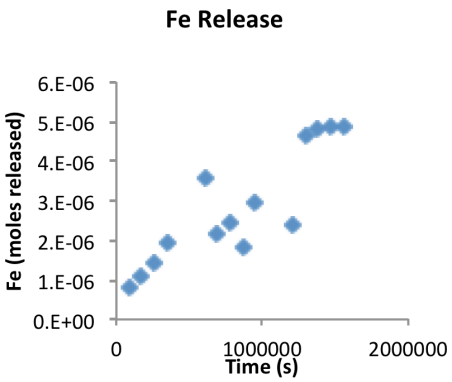

Analytical uncertainty is smaller than the plotted symbol.

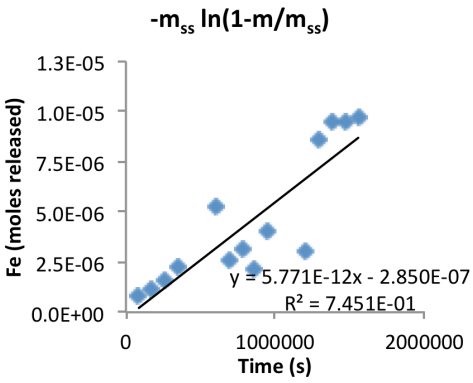

Regression Analysis		*Std.Error*
R Square	0.745	n/a
Fe release rate (rFe)	5.77E-12	9.7448E-13

Diss. Rate Mineral (K_{diss})	1.02E-13	mol/m^2s
Uncertainty of Fit	9.46E-15	mol/m^2s

Appendix Figure 21.

Iron analysis for experiment 25-Na-1.00-1

Mineral: Nontronite (NAu-1) **Initial pH:** 2.00 **Solution**: 0.01 m NaCl **Specific Surf. Area (BET):** 30.865 m^2/g
Batch ID: 25-Na-1.00-1 $a H_2O$ = 1.00 **Mineral Mass:** 0.4999g **Total Surf. Area (BET):** 15.4325 m^2
NA = no analysis

Batch Results: Shaded data = all data except for the long term steady state point(s).

Time (s)	pH	Volume (ml)	Concentration (ppm)	Fe (moles released)	$-m_{ss}$ ln(1-m/m_{ss})
0	2.00	200		0	
10860	n/a	190	0.15	1.06E-06	1.08E-06
21600	2.03	180	0.23	1.59E-06	1.64E-06
32460	n/a	170	0.29	2.01E-06	2.10E-06
86460	2.23	160	0.59	3.83E-06	4.17E-06
97200	2.01	150	0.66	4.23E-06	4.65E-06
108060	2.18	140	0.68	4.30E-06	4.73E-06
118800	2.19	130	0.71	4.47E-06	4.94E-06
172800	2.18	120	0.72	4.51E-06	4.98E-06
187200	2.19	110	0.87	5.17E-06	5.81E-06
201600	2.18	100	0.91	5.32E-06	6.00E-06
259260	2.17	90	1.04	5.79E-06	6.60E-06
273600	2.19	80	1.07	5.88E-06	6.72E-06
288000	2.21	70	1.05	5.83E-06	6.65E-06
360060	2.21	60	1.18	6.13E-06	7.05E-06
3312480	2.50	50	9.06	2.30E-05	6.77E-05
7282920	2.30	40	9.93	2.45E-05	#NUM!

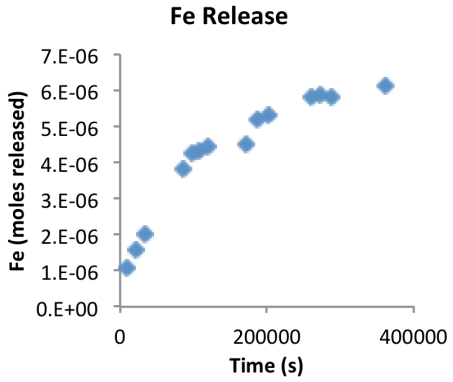

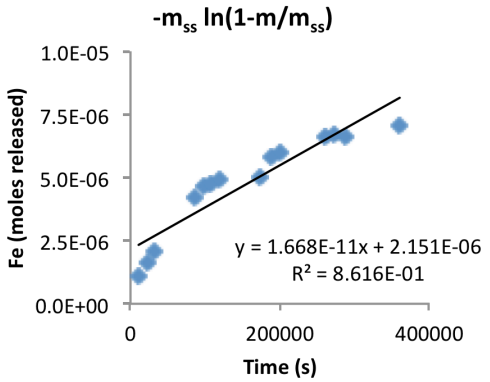

Analytical uncertainty is smaller than the plotted symbol.

Regression Analysis		*Std.Error*
R Square	0.862	n/a
Fe release rate (rFe)	1.66E-11	1.93E-12

Diss. Rate Mineral (K_{diss})	2.67E-13	mol/m^2s
Uncertainty of Fit	1.86E-14	mol/m^2s

Appendix Figure 22.

Iron analysis for experiment 25-Na-1.00-2

Mineral: Nontronite (NAu-1) **Initial pH:** 2.00 **Solution**: 0.01 m NaCl **Specific Surf. Area (BET):** 30.865 m^2/g
Batch ID: 25-Na-1.00-2 a_{H_2O} = 1.00 **Mineral Mass:** 0.5050g **Total Surf. Area (BET):** 15.4325 m^2

NA = no analysis

Batch Results: Shaded data = all data except for the long term steady state point(s).

Time (s)	pH	Volume (ml)	Concentration (ppm)	Fe (moles released)	$-m_{ss}$ ln(1-m/m_{ss})
0	2.00	200		0	
10980	2.38	190	0.17	1.23E-06	1.25E-06
21660	2.20	180	0.25	1.76E-06	1.82E-06
32520	n/a	170	0.31	2.13E-06	2.21E-06
86520	2.23	160	0.65	4.18E-06	4.51E-06
97260	2.23	150	0.69	4.44E-06	4.82E-06
108120	2.18	140	0.72	4.57E-06	4.97E-06
118860	2.16	130	0.76	4.76E-06	5.20E-06
172860	2.18	120	0.91	5.46E-06	6.04E-06
187260	2.19	110	0.97	5.72E-06	6.36E-06
201720	2.18	100	1.02	5.91E-06	6.59E-06
259320	2.17	90	1.15	6.38E-06	7.20E-06
273660	2.20	80	1.18	6.47E-06	7.30E-06
288060	2.20	70	1.24	6.66E-06	7.55E-06
360120	2.21	60	1.35	6.93E-06	7.90E-06
3312540	2.28	50	10.82	2.72E-05	7.57E-05
7282980	2.31	40	12.08	2.94E-05	

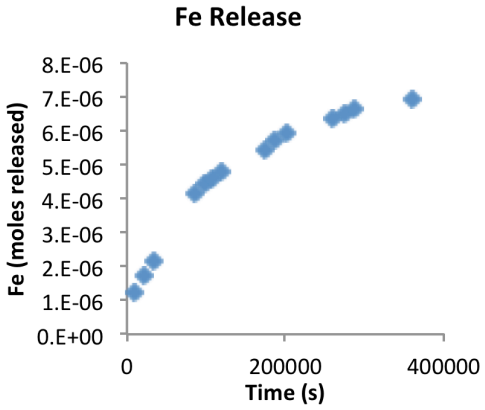

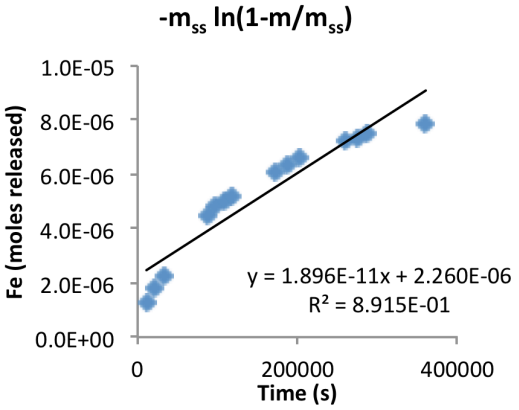

Analytical uncertainty is smaller than the plotted symbol.

Regression Analysis		*Std.Error*
R Square	0.892	n/a
Fe release rate (rFe)	1.90E-11	1.39E-12

Diss. Rate Mineral (K_{diss})	3.30E-13	mol/m^2s
Uncertainty of Fit	2.41E-15	mol/m^2s

Appendix Figure 23.

Duplicate silica analysis for experiment 25-Ca-1.00-1 and 25-Ca-1.00-2

Mineral: Nontronite (NAu-1) **Initial pH:** 2.00 **Solution**: 0.01 m $CaCl_2$ **Specific Surf. Area (BET):** 30.865 m^2
Si Duplicate: 25-Ca-1.00 ***a*H_2O** = 1.00 **Mineral Mass:** 0.5000g **Total Surf. Area (BET):** 15.4325 m^2

	25-Ca-1.00-1				25-Ca-1.00-2			
Sample #	Time (sec)	Moles Released	$-m_{ss}$ ln(1-m/m_{ss})	pH	Time (sec)	Moles Released	$-m_{ss}$ ln(1-m/m	pH
0	0	0		2.00		0		2.00
1	10860	1.79E-06	1.80E-06	2.05	10860	1.24E-06	1.25E-06	2.10
2	21600	3.78E-06	3.82E-06	1.84	21600	3.38E-06	3.42E-06	1.92
3	32400	8.02E-06	8.22E-06	1.89	32400	8.37E-06	8.60E-06	2.10
4	86520	1.71E-05	1.80E-05	1.96	86520	1.73E-05	1.84E-05	2.05
5	97200	1.96E-05	2.08E-05	2.03	97200	1.97E-05	2.11E-05	2.08
6	108000	2.17E-05	2.32E-05	2.21	108000	2.01E-05	2.15E-05	2.13
7	118800	2.17E-05	2.32E-05	2.01	118800	2.18E-05	2.35E-05	2.03
8	176400	2.99E-05	3.30E-05	2.10	176400	2.79E-05	3.08E-05	2.04
9	190800	2.89E-05	3.18E-05	2.21	190800	2.90E-05	3.22E-05	2.14
10	205200	3.07E-05	3.40E-05	2.21	205200	3.01E-05	3.36E-05	2.19
11	266400	3.51E-05	3.94E-05	2.04	266400	3.41E-05	3.86E-05	2.09
12	277200	3.77E-05	4.29E-05	2.11	277200	3.56E-05	4.05E-05	2.16
13	352800	4.74E-05	5.59E-05	2.07	352800	4.17E-05	4.87E-05	2.09
14	439260	4.80E-05	5.67E-05	2.05	439260	4.58E-05	5.44E-05	2.02
15	15497100	1.65E-04		2.33	15497100	1.53E-04		2.43

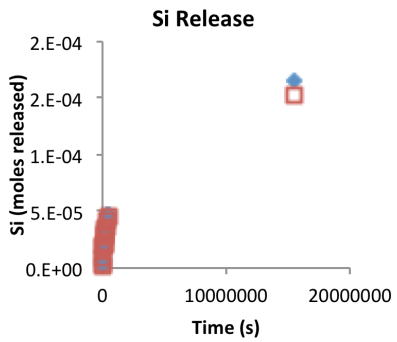

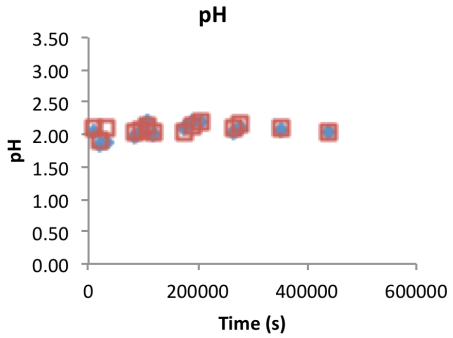

Analytical uncertainty is smaller than the plotted symbol.

Appendix Figure 24.

Duplicate silica analysis for experiment 25-Ca-0.75-1 and 25-Ca-0.75-2

Mineral: Nontronite (NAu-1) **Initial pH:** 2.00 **Solution**: 3.0 m $CaCl_2$ **Specific Surf. Area (BET):** 30.865 m^2
Si Duplicate: 25-Ca-0.75 a_{H_2O} = 0.75 **Mineral Mass:** 1.0061g **Total Surf. Area (BET):** 15.4325 m^2

	25-Ca-0.75-1				25-Ca-0.75-2			
Sample #	Time (sec)	Moles Released	$-m_{ss}\ln(1-m/m_{ss})$	pH	Time (sec)	Moles Released	$-m_{ss}\ln(1-m/m_{ss})$	pH
0	0	0		2.00		0		2.00
1	10980	4.93E-06	5.42E-06	1.92	10920	1.81E-06	1.88E-06	1.97
2	21600	6.32E-06	7.17E-06	2.00	21540	5.27E-06	5.86E-06	1.92
3	32400	7.64E-06	8.93E-06	1.96	32400	6.90E-06	7.98E-06	1.95
4	86460	1.14E-05	1.46E-05	1.95	86460	9.99E-06	1.25E-05	2.03
5	97200	1.02E-05	1.27E-05	2.07	97140	9.99E-06	1.25E-05	2.08
6	107940	1.35E-05	1.85E-05	2.27	107880	1.14E-05	1.48E-05	2.04
7	118800	1.25E-05	1.65E-05	2.27	118800	1.14E-05	1.48E-05	2.07
8	176400	1.44E-05	2.02E-05	2.26	176460	1.25E-05	1.69E-05	2.32
9	190800	1.61E-05	2.41E-05	2.24	190860	1.36E-05	1.90E-05	2.27
10	205200	1.53E-05	2.23E-05	2.27	205200	1.36E-05	1.90E-05	2.34
11	266400	1.61E-05	2.39E-05	2.33	266400	1.45E-05	2.10E-05	1.99
12	277140	1.74E-05	2.73E-05	2.25	277140	1.54E-05	2.28E-05	2.23
13	352740	1.74E-05	2.73E-05	2.39	352740	1.61E-05	2.46E-05	2.33
14	439320	1.79E-05	2.87E-05	2.13	439260	1.54E-05	2.30E-05	2.14
15	15497040	2.78E-05		2.88	15497040	2.68E-05		2.94

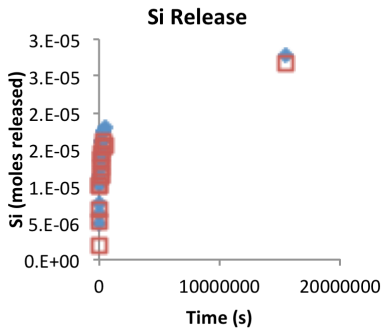

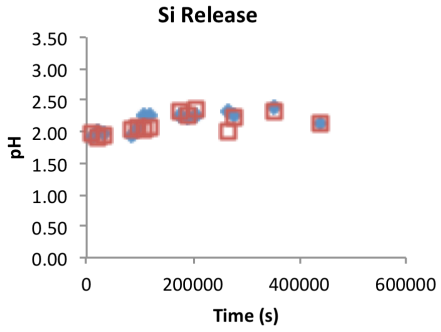

Analytical uncertainty is smaller than the plotted symbol.

Appendix Figure 25.

Duplicate silica analysis for experiment 25-Ca-0.50-1 and 25-Ca-0.50-2

Mineral: Nontronite (NAu-1) **Initial pH:** 2.00 **Solution**: 5.0 m $CaCl_2$ **Specific Surf. Area (BET):** 30.865 m^2
Si Duplicate: 25-Ca-0.50 ***a*H_2O** = 0.50 **Mineral Mass:** 5.01g **Total Surf. Area (BET):** 15.4325 m^2

	25-Ca-0.50-1				25-Ca-0.50-2			
Sample #	Time (sec)	Moles Released	$-m_{ss}\ln(1-m/m_{ss})$	pH	Time (sec)	Moles Released	$-m_{ss}\ln(1-m/m_{ss})$	pH
0	0	0		2.00		0		2.00
1	21600	0.00E+00		2.05	21540	1.67E-06	2.23E-06	2.10
2	86700	7.63E-07	8.70E-07	n/a	86520	2.49E-06	4.21E-06	2.27
3	172860	1.80E-06	2.64E-06	1.90	172800	3.27E-06	8.39E-06	1.97
4	259200	2.54E-06	4.98E-06	2.34	259140	3.27E-06	8.39E-06	1.74
5	345600	2.54E-06	4.98E-06	2.31	345540	3.50E-06	1.21E-05	1.98
6	431940	2.76E-06	6.19E-06	2.35	431880	3.50E-06	1.21E-05	2.22
7	518520	2.96E-06	7.97E-06	2.05	518460	3.50E-06	1.21E-05	1.88
8	604800	2.96E-06	7.97E-06	2.00	604800	3.50E-06	1.21E-05	2.09
9	691200	3.13E-06	1.12E-05	2.08	691140	3.50E-06	1.21E-05	2.03
10	777600	3.13E-06	1.12E-05	2.25	777540	3.50E-06	1.21E-05	1.88
11	864000	3.13E-06	1.12E-05	2.10	863940	3.50E-06	1.21E-05	2.03
12	950400	3.13E-06	1.12E-05	2.23	950340	3.63E-06		2.07
13	1123200	3.13E-06	1.12E-05	1.97	1123140	3.63E-06		2.36
14	1296000	3.23E-06		n/a	1295940	3.43E-06		2.60

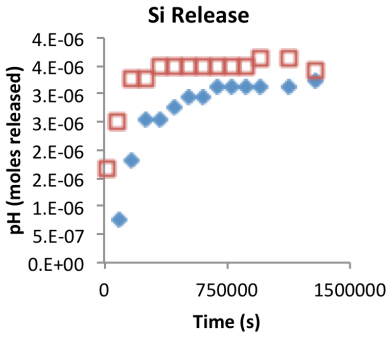

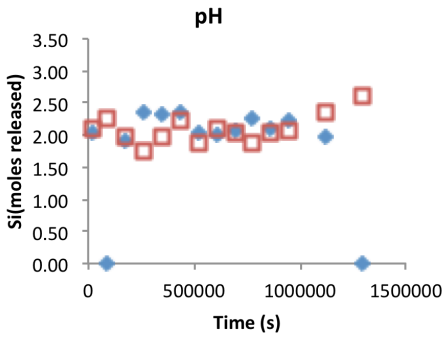

Analytical uncertainty is smaller than the plotted symbol.

Appendix Figure 26.

Duplicate silica analysis for experiment 45-Ca-0.50-1 and 45-Ca-0.50-2

Mineral: Nontronite (NAu-1) **Initial pH:** 2.00 **Solution**: 0.01 mol $CaCl_2$ **Specific Surf. Area (BET):** 30.865 m^2
Si Duplicate: 45-Ca-1.00 ***a*H_2O** = 1.00 **Mineral Mass:** 0.5112g **Total Surf. Area (BET):** 15.4325 m^2

	45-Ca-1.00-1				45-Ca-1.00-2			
Sample #	Time (h)	Moles Released	$-m_{ss}\ln(1-m/m_{ss})$	pH	Time (sec)	Moles Released	$-m_{ss}\ln(1-m/m_{ss})$	pH
0	0	0		2.00		0		2.00
1	10920	2.82E-05	3.00E-05	2.08	10920	2.76E-05	2.93E-05	2.02
2	86520	7.22E-05	8.63E-05	2.05	86520	6.88E-05	8.08E-05	2.05
3	97260	7.78E-05	9.46E-05	2.05	97260	7.43E-05	8.86E-05	2.02
4	108120	7.87E-05	9.58E-05	2.07	108120	8.01E-05	9.71E-05	2.07
5	172920	1.06E-04	1.42E-04	2.09	172920	1.07E-04	1.41E-04	2.08
6	183600	1.09E-04	1.46E-04	2.08	183600	1.07E-04	1.40E-04	2.08
7	194400	9.42E-05	1.20E-04	2.07	194400	1.13E-04	1.52E-04	2.07
8	259200	1.27E-04	1.83E-04	2.08	259200	1.29E-04	1.83E-04	2.07
9	270060	1.35E-04	2.01E-04	2.07	270060	1.38E-04	2.02E-04	2.07
10	280800	1.31E-04	1.91E-04	2.08	280800	1.27E-04	1.79E-04	2.06
11	345660	1.52E-04	2.44E-04	2.13	345660	1.28E-04	1.82E-04	2.13
12	356400	1.37E-04	2.05E-04	2.08	356400	1.51E-04	2.36E-04	2.10
13	367140	1.54E-04	2.52E-04	2.07	367140	1.50E-04	2.31E-04	2.11
14	432060	1.65E-04	2.85E-04	2.10	432060	1.61E-04	2.64E-04	2.10
15	5982180	2.35E-04		2.21	5982180	2.44E-04		2.17
	7347180	2.39E-04		n/a	7347180	2.48E-04		n/a

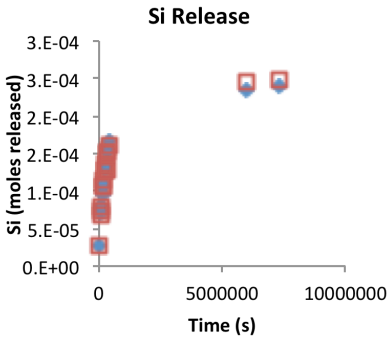

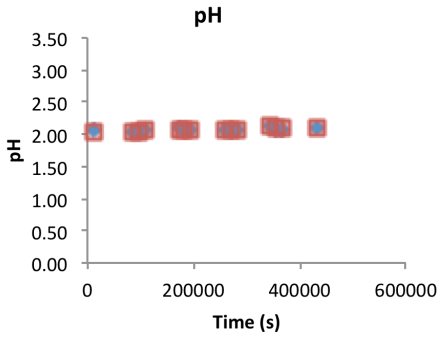

Analytical uncertainty is smaller than the plotted symbol.

Appendix Figure 27.

Duplicate silica analysis for experiment 4-Ca-0.50-1 and 4-Ca-0.50-2

Mineral: Nontronite (NAu-1) **Initial pH:** 2.00 **Solution**: 0.01 m $CaCl_2$ **Specific Surf. Area (BET):** 30.865 m^2
Si Duplicate: 4-Ca-1.00 a_{H_2O} = 1.00 **Mineral Mass:** 0.4990g **Total Surf. Area (BET):** 15.4325 m^2

	4-Ca-1.00-1				4-Ca-1.00-2			
Sample #	Time (sec)	Moles Released	$-m_{ss}\ln(1-m/m_{ss})$	pH	Time (sec)	Moles Released	$-m_{ss}\ln(1-m/m_{ss})$	pH
0	0	0				0		
1	86580	8.94E-07	8.97E-07	1.98	86580	1.95E-06	1.97E-06	1.98
2	172980	3.74E-06	3.80E-06	1.98	172980	6.31E-06	6.48E-06	2.00
3	259260	5.97E-06	6.11E-06	1.99	259260	8.85E-06	9.20E-06	1.99
4	345720	1.69E-05	1.82E-05	2.01	345720	1.29E-05	1.37E-05	2.01
5	605100	2.03E-05	2.22E-05	2.02	605100	1.87E-05	2.03E-05	2.02
6	691560	2.32E-05	2.57E-05	2.02	691560	2.03E-05	2.22E-05	2.02
7	777900	2.37E-05	2.63E-05	2.04	777900	2.11E-05	2.33E-05	2.02
8	864240	2.50E-05	2.79E-05	2.04	864240	2.26E-05	2.51E-05	2.03
9	950460	2.75E-05	3.11E-05	2.03	950460	2.56E-05	2.89E-05	2.06
10	1209540	2.93E-05	3.35E-05	2.00	1209540	2.84E-05	3.25E-05	2.06
11	1296000	3.18E-05	3.68E-05	2.05	1296060	2.93E-05	3.37E-05	2.04
12	1382640	3.35E-05	3.92E-05	2.04	1382700	3.08E-05	3.57E-05	2.03
13	1469160	3.44E-05	4.03E-05	2.02	1469220	3.16E-05	3.67E-05	2.04
14	1555320	3.57E-05	4.22E-05	2.03	1555380	3.28E-05	3.84E-05	2.04
15	6489180	9.21E-05	1.70E-04	1.98	6489240	8.82E-05	1.63E-04	2.01
16	9076320	1.23E-04		2.02	9076380	1.18E-04		2.00

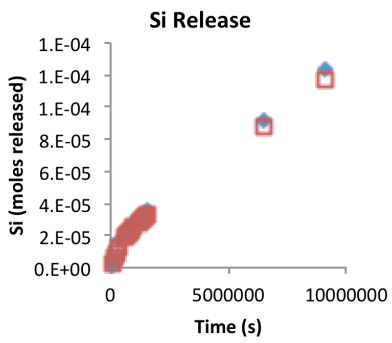

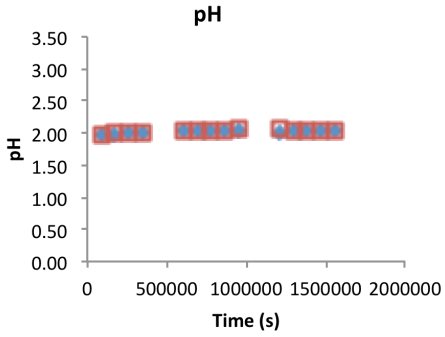

Analytical uncertainty is smaller than the plotted symbol.

Appendix Figure 28.

Duplicate silica analysis for experiment 25-Na-1.00-1 and 25-Na-1.00-2

Mineral: Nontronite (NAu-1) **Initial pH:** 2.00 **Solution**: 0.01 m NaCl **Specific Surf. Area (BET):** 30.865 m^2
Si Duplicate: 25-Na-1.00 ***a*H_2O** = 1.00 **Mineral Mass:** 0.4999g **Total Surf. Area (BET):** 15.4325 m^2

	25-Na-1.00-1				25-Na-1.00-2			
Sample #	Time (sec)	Moles Released	$-m_{ss}\ln(1-m/m_{ss})$	pH	Time (sec)	Moles Released	$-m_{ss}\ln(1-m/m_{ss})$	pH
0	0	0			0	0		
1	10860	6.76E-06	6.88E-06	n/a	10980	7.83E-06	7.98E-06	2.38
2	21600	1.16E-05	1.20E-05	2.03	21660	1.19E-05	1.22E-05	2.20
3	32460	1.36E-05	1.41E-05	n/a	32520	1.54E-05	1.60E-05	n/a
4	86460	2.55E-05	2.73E-05	2.23	86520	2.85E-05	3.07E-05	2.23
5	97200	2.82E-05	3.04E-05	2.01	97260	2.95E-05	3.19E-05	2.23
6	108060	2.96E-05	3.21E-05	2.18	108120	3.36E-05	3.67E-05	2.18
7	118800	3.18E-05	3.46E-05	2.19	118860	3.51E-05	3.85E-05	2.16
8	172800	3.92E-05	4.36E-05	2.18	172860	4.33E-05	4.87E-05	2.18
9	187200	4.10E-05	4.59E-05	2.19	187260	4.48E-05	5.06E-05	2.19
10	201600	4.32E-05	4.86E-05	2.18	201720	4.72E-05	5.37E-05	2.18
11	259260	4.97E-05	5.71E-05	2.17	259320	5.36E-05	6.22E-05	2.17
12	273600	5.15E-05	5.95E-05	2.19	273660	5.55E-05	6.49E-05	2.20
13	288000	5.21E-05	6.03E-05	2.21	288060	5.56E-05	6.50E-05	2.20
14	360060	5.85E-05	6.92E-05	2.21	360120	6.28E-05	7.51E-05	2.21
15	3312480	1.92E-04	6.29E-04	2.50	3312540	1.98E-04	7.51E-04	2.28
16	7282920	2.01E-04		2.30	7282980	2.03E-04		2.31

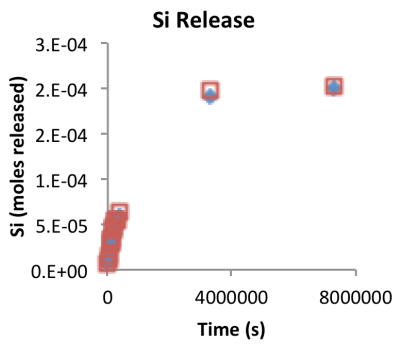

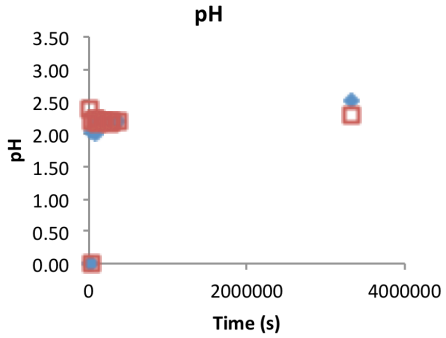

Analytical uncertainty is smaller than the plotted symbol.

Appendix Figure 29.

Duplicate silica analysis for experiment 25-Na-0.75-5 and 25-Na-0.75-6

Mineral: Nontronite (NAu-1) **Initial pH:** 2.00 **Solution**: 6.14 m NaCl **Specific Surf. Area (BET):** 30.865 m^2
Si Duplicate: 25-Na-0.75 ***a*H_2O** = 1.00 **Mineral Mass:** 0.4990g **Total Surf. Area (BET):** 15.4325 m^2

	25-Na-0.75-5				25-Na-0.75-6			
Sample #	Time (sec)	Moles Released	$-m_{ss}\ln(1-m/m_{ss})$	pH	Time (sec)	Moles Released	$-m_{ss}\ln(1-m/m_{ss})$	pH
0	0	0			0	0		
1	17940	1.11E-06	1.12E-06	2.08	17940	2.56E-06	2.63E-06	2.08
2	86400	9.16E-06	1.01E-05	2.14	86400	9.23E-06	1.02E-05	2.14
3	108000	1.09E-05	1.22E-05	2.22	108000	1.12E-05	1.26E-05	2.22
4	172980	1.38E-05	1.60E-05	2.19	172980	1.39E-05	1.61E-05	2.19
5	194580	1.01E-05	1.12E-05	2.16	194580	1.29E-05	1.48E-05	2.16
6	259800	1.63E-05	1.96E-05	2.28	259800	1.66E-05	1.99E-05	2.28
7	280740	1.70E-05	2.06E-05	2.22	280740	1.64E-05	1.97E-05	2.22
8	346020	1.83E-05	2.25E-05	2.20	346020	1.86E-05	2.30E-05	2.20
9	360420	1.91E-05	2.39E-05	n/a	360420	1.89E-05	2.35E-05	n/a
10	432000	2.01E-05	2.54E-05	2.36	432000	2.02E-05	2.57E-05	2.36
11	518940	2.14E-05	2.77E-05	2.34	518940	2.18E-05	2.83E-05	2.34
12	605460	2.24E-05	2.94E-05	2.44	605460	2.18E-05	2.83E-05	2.44
13	12708000	5.19E-05		2.93	12708000	5.18E-05		3.01

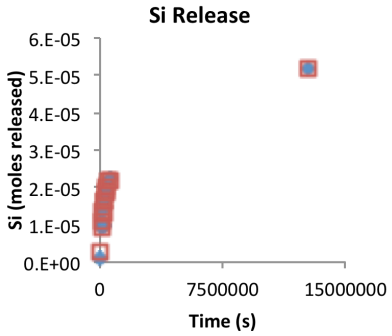

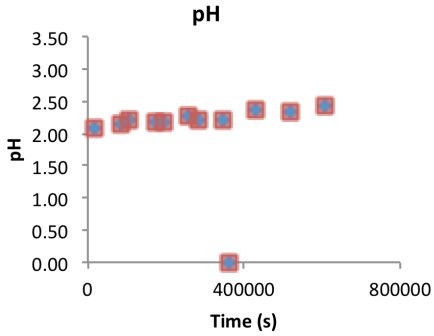

Analytical uncertainty is smaller than the plotted symbol.

Appendix Figure 30.

Duplicate iron analysis for experiment 25-Ca-1.00-1 and 25-Ca-1.00-2

Mineral: Nontronite (NAu-1) **Initial pH:** 2.00 **Solution**: 0.01 m $CaCl_2$ **Specific Surf. Area (BET):** 30.865 m^2
Fe Duplicate: 25-Ca-1.00 ***a*H_2O** = 1.00 **Mineral Mass:** 0.50g **Total Surf. Area (BET):** 15.4325 m^2

	25-Ca-1.00-1				25-Ca-1.00-2			
Sample #	Time (sec)	Moles Released	$-m_{ss}$ ln(1-m/m_{ss})	pH	Time (sec)	Moles Released	$-m_{ss}$ ln(1-m/m	pH
0	0	0		2.00	0	0		2.00
3					32400.00	1.37E-06	1.52E-06	2.10
5	97200	2.97E-06	3.55E-06	2.03				
6	108000	3.32E-06	4.08E-06	2.21	108000.00	2.75E-06	3.43E-06	2.13
7	118800	3.47E-06	4.31E-06	2.01	118800.00	3.00E-06	3.85E-06	2.03
8	176400	4.05E-06	5.27E-06	2.1	176400.00	3.48E-06	4.69E-06	2.04
9	190800	3.89E-06	4.99E-06	2.21	190800.00	3.80E-06	5.33E-06	2.14
10	205200	3.93E-06	5.07E-06	2.21	205200.00	3.76E-06	5.25E-06	2.19
11	266400	3.88E-06	4.98E-06	2.04	266400.00	3.38E-06	4.50E-06	2.09
12	277200	4.63E-06	6.34E-06	2.11	277200.00	3.86E-06	5.44E-06	2.16
13					352800.00	3.93E-06	5.61E-06	2.09
15	15497100	9.56E-06		2.33	15497100.00	7.42E-06		2.43

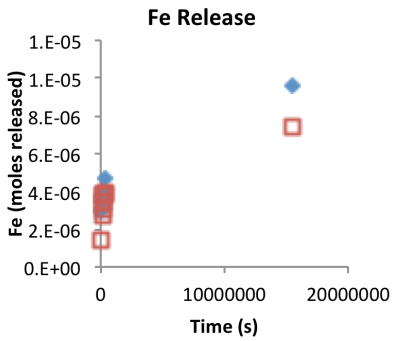

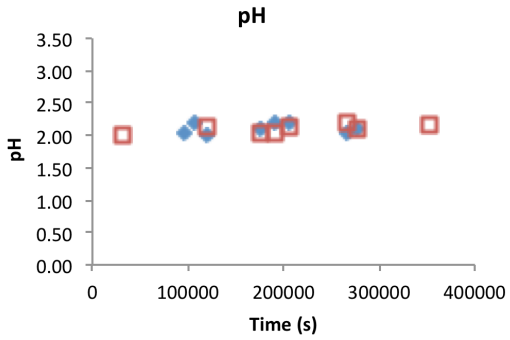

Analytical uncertainty is smaller than the plotted symbol.

Appendix Figure 31.

Duplicate iron analysis for experiment 45-Ca-1.00-1 and 45-Ca-1.00-2

Mineral: Nontronite (NAu-1) **Initial pH:** 2.00 **Solution**: 0.01 m $CaCl_2$ **Specific Surf. Area (BET):** 30.865 m^2
Fe Duplicate: 45-Ca-1.00 ***a*H_2O** = 1.00 **Mineral Mass:** 0.5112g **Total Surf. Area (BET):** 15.4325 m^2

	45-Ca-1.00-1				45-Ca-1.00-2			
Sample #	Time (h)	Moles Released	$-m_{ss}\ln(1-m/m_{ss})$	pH	Time (sec)	Moles Released	$-m_{ss}\ln(1-m/m_{ss})$	pH
0	0	0		2.00	0	0		2.00
1	10920	3.28E-06	5.14E-06	2.08	10920	3.2608E-06	4.24E-06	2.02
2	86520	3.94E-06	7.29E-06	2.05	86520	4.12E-06	5.89E-06	2.05
3	97260	4.04E-06	7.69E-06	2.05	97260	4.31E-06	6.30E-06	2.02
4	108120	4.09E-06	7.92E-06	2.07	108120	3.75E-06	5.14E-06	2.07
5	172920	4.37E-06	9.37E-06	2.09	172920	4.71E-06	7.28E-06	2.08
6	183600	4.24E-06	8.62E-06	2.08	183600	4.79E-06	7.49E-06	2.08
7	194400	4.22E-06	8.52E-06	2.07	194400	4.95E-06	7.92E-06	2.07
8	259200	4.49E-06	1.01E-05	2.08	259200	5.24E-06	8.80E-06	2.07
9	270060	4.37E-06	9.38E-06	2.07	270060	5.39E-06	9.25E-06	2.07
10	280800	4.42E-06	9.65E-06	2.08	280800	5.48E-06	9.59E-06	2.06
11	345660	4.94E-06	1.47E-05	2.13	345660	5.69E-06	1.03E-05	2.13
12	356400	4.61E-06	1.10E-05	2.08	356400	5.76E-06	1.06E-05	2.10
13	367140	4.71E-06	1.19E-05	2.07	367140	5.72E-06	1.04E-05	2.11
14	432060	4.66E-06	1.14E-05	2.10	432060	5.89E-06	1.11E-05	2.10
15	5982180	5.26E-06		2.21	5982180	7.70E-06		2.17
16					7347180	7.35E-06		n/a

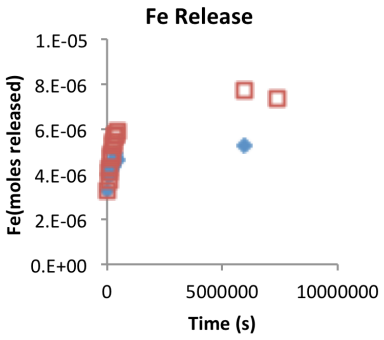

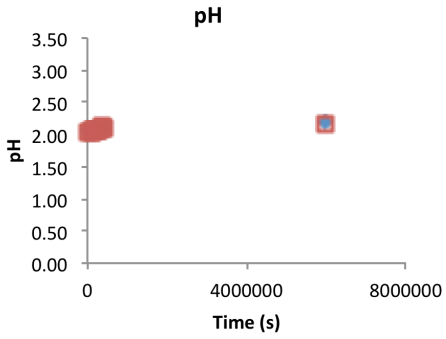

Analytical uncertainty is smaller than the plotted symbol.

Appendix Figure 32.

Duplicate iron analysis for experiment 4-Ca-1.00-1 and 4-Ca-1.00-2

Mineral: Nontronite (NAu-1) **Initial pH:** 2.00 **Solution**: 0.01 m $CaCl_2$ **Specific Surf. Area (BET):** 30.865 m^2
Fe Duplicate: 4-Ca-1.00 αH_2O = 1.00 **Mineral Mass:** 0.4990g **Total Surf. Area (BET):** 15.4325 m^2

	4-Ca-1.00-1				4-Ca-1.00-2			
Sample #	Time (sec)	Moles Released	$-m_{ss}\ln(1-m/m_{ss})$	pH	Time (sec)	Moles Released	$-m_{ss}\ln(1-m/m_{ss})$	pH
0	0	0		2.00	0	0		2.00
1	86580	7.83E-07	8.24E-07	1.98	86580	7.96E-07	8.52E-07	1.98
2	172980	9.85E-07	1.05E-06	1.98	172980	1.09E-06	1.19E-06	2.00
3	259260	1.10E-06	1.19E-06	1.99	259260	1.40E-06	1.59E-06	1.99
4	345720	2.75E-06	3.36E-06	2.01	345720	1.91E-06	2.29E-06	2.01
5	605100	3.96E-06	5.43E-06	2.02	605100	3.55E-06	5.27E-06	2.02
6	691560	4.37E-06	6.28E-06	2.02	691560	2.13E-06	2.62E-06	2.02
7	777900	4.65E-06	6.91E-06	2.04	777900	2.45E-06	3.13E-06	2.02
8	864240	4.84E-06	7.38E-06	2.04	864240	1.82E-06	2.16E-06	2.03
9	950460	5.58E-06	9.45E-06	2.03	950460	2.95E-06	4.01E-06	2.06
10	1209540	4.94E-06	7.61E-06	2.00	1209540	2.39E-06	3.01E-06	2.06
11	1296000	6.46E-06	1.29E-05	2.05	1296060	4.64E-06	8.59E-06	2.04
12	1382640	6.80E-06	1.48E-05	2.04	1382700	4.84E-06	9.43E-06	2.03
13	1469160	6.69E-06	1.41E-05	2.02	1469220	4.85E-06	9.52E-06	2.04
14	1555320	7.21E-06	1.79E-05	2.03	1555380	4.89E-06	9.67E-06	2.04
15	6489180	8.10E-06		1.98	6489240	6.18E-06		2.01

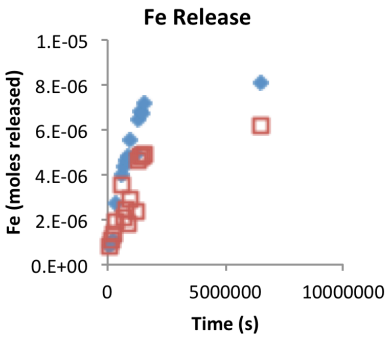

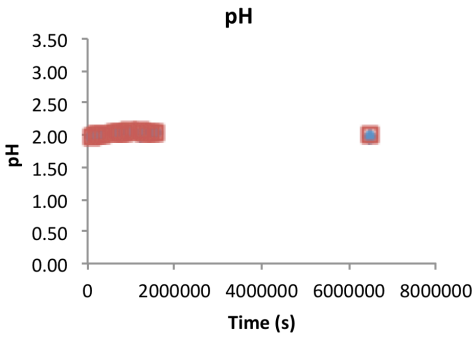

Analytical uncertainty is smaller than the plotted symbol.

Appendix Figure 33.

Duplicate iron analysis for experiment 25-Na-1.00-1 and 25-Na-1.00-2

Mineral: Nontronite (NAu-1) **Initial pH:** 2.00 **Solution**: 0.01 m NaCl **Specific Surf. Area (BET):** 30.865 m^2
Fe Duplicate: 25-Na-1.00 **αH_2O** = 1.00 **Mineral Mass:** 0.4999g **Total Surf. Area (BET):** 15.4325 m^2

	25-Na-1.00-1				25-Na-1.00-2			
Sample #	Time (sec)	Moles Released	$-m_{ss}\ln(1-m/m_{ss})$	pH	Time (sec)	Moles Released	$-m_{ss}\ln(1-m/m_{ss})$	pH
0	0	0		2.00	0	0		2.00
1	10860	1.06E-06	1.08E-06	n/a	10980	1.23E-06	1.25E-06	2.38
2	21600	1.59E-06	1.64E-06	2.03	21660	1.76E-06	1.82E-06	2.20
3	32460	2.01E-06	2.10E-06	n/a	32520	2.13E-06	2.21E-06	n/a
4	86460	3.83E-06	4.17E-06	2.23	86520	4.18E-06	4.51E-06	2.23
5	97200	4.23E-06	4.65E-06	2.01	97260	4.44E-06	4.82E-06	2.23
6	108060	4.30E-06	4.73E-06	2.18	108120	4.57E-06	4.97E-06	2.18
7	118800	4.47E-06	4.94E-06	2.19	118860	4.76E-06	5.20E-06	2.16
8	172800	4.51E-06	4.98E-06	2.18	172860	5.46E-06	6.04E-06	2.18
9	187200	5.17E-06	5.81E-06	2.19	187260	5.72E-06	6.36E-06	2.19
10	201600	5.32E-06	6.00E-06	2.18	201720	5.91E-06	6.59E-06	2.18
11	259260	5.79E-06	6.60E-06	2.17	259320	6.38E-06	7.20E-06	2.17
12	273600	5.88E-06	6.72E-06	2.19	273660	6.47E-06	7.30E-06	2.20
13	288000	5.83E-06	6.65E-06	2.21	288060	6.66E-06	7.55E-06	2.20
14	360060	6.13E-06	7.05E-06	2.21	360120	6.93E-06	7.90E-06	2.21
15	3312480	2.30E-05	6.77E-05	2.50	3312540	2.72E-05	7.57E-05	2.28
16	7282920	2.45E-05		2.30	7282980	2.94E-05		2.31

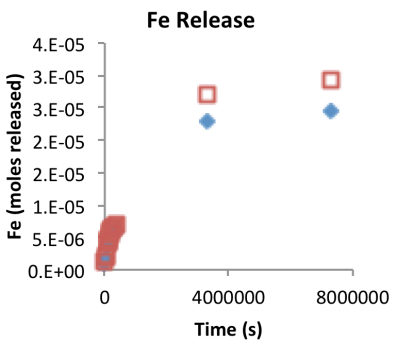

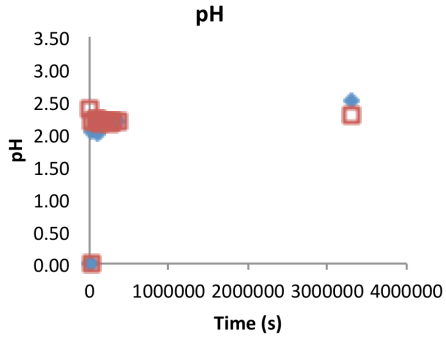

Analytical uncertainty is smaller than the plotted symbol.

References

ASTM D859-10 Standard Test Method for Silica in Water. ASTM International, West Conshohocken, PA.

Barnhisel, R.I. and Bertsch, P.M. (1989) Chlorites and hydroxy-interlayered vermiculite and smectite. Minerals in soil environments, 729-788.

Bauer, A. and Berger, G. (1998) Kaolinite and smectite dissolution rate in high molar KOH solutions at 35°and 80°C. Applied Geochemistry 13, 905-916.

Bauer, K., Garbe, D. and Surburg, H. (1988) Ullmann's encyclopedia of industrial chemistry. Ullmann's Encyclopedia of Industrial Chemistry 11.

Bibi, I., Singh, B. and Silvester, E. (2011) Dissolution of illite in saline–acidic solutions at 25 C. Geochimica et Cosmochimica Acta 75, 3237-3249.

Bibring, J.-P., Langevin, Y., Mustard, J.F., Poulet, F., Arvidson, R., Gendrin, A., Gondet, B., Mangold, N., Pinet, P. and Forget, F. (2006) Global mineralogical and aqueous Mars history derived from OMEGA/Mars Express data. Science 312, 400-404.

Bishop, J.L., Dobrea, E.Z.N., McKeown, N.K., Parente, M., Ehlmann, B.L., Michalski, J.R., Milliken, R.E., Poulet, F., Swayze, G.A. and Mustard, J.F. (2008) Phyllosilicate diversity and past aqueous activity revealed at Mawrth Vallis, Mars. Science 321, 830-833.

Bowen, B.B. and Benison, K.C. (2009) Geochemical characteristics of naturally acid and alkaline saline lakes in southern Western Australia. Applied Geochemistry 24, 268-284.

Brass, G.W. (1980) Stability of brines on Mars. Icarus 42, 20-28.

Bridges, J.C., Catling, D.C., Saxton, J.M., Swindle, T.D., Lyon, I.C. and Grady, M.M. (2001) Alteration assemblages in Martian meteorites: Implications for near-surface processes. Space Science Reviews 96, 365-392.

Brunauer, S., Emmett, P.H. and Teller, E. (1938) Adsorption of gases in multimolecular layers. Journal of the American Chemical Society 60, 309-319.

Cama, J., Metz, V. and Ganor, J. (2002) The effect of pH and temperature on kaolinite dissolution rate under acidic conditions. Geochimica et Cosmochimica Acta 66, 3913-3926.

Carroll, S.A. and Walther, J.V. (1990) Kaolinite dissolution at 25°, 60° and 80°C. American Journal of Science 290, 797-810.

Chirife, J. and Resnik, S.L. (1984) Unsaturated solutions of sodium chloride as reference sources of water activity at various temperatures. Journal of Food Science 49, 1486-1488.

Cull, S.C., Arvidson, R.E., Catalano, J.G., Ming, D.W., Morris, R.V., Mellon, M.T. and Lemmon, M. (2010) Concentrated perchlorate at the Mars Phoenix landing site: Evidence for thin film liquid water on Mars. Geophysical Research Letters 37.

Dixon, E., Elwood Madden, A., Hausrath, E.M. and Elwood Madden, M.E. (2015) Assesing Hydrodynamic effects on jarosite dissolution rates, reaction products, and preservation on Mars. Journal of Geophysical Research Planets.

Dixon, J.C., Thorn, C.E., Darmody, R.G. and Campbell, S.W. (2002) Weathering rinds and rock coatings from an Arctic alpine environment, northern Scandinavia. Geological Society of America Bulletin 114, 226-238.

Dorn, R.I. (1998) Rock coatings. Elsevier.

Eaton, A.D., Clesceri, L.S., Rice, E.W., Greenberg, A.E. and Franson, M.A.H. (2005) Standard Methods for the Examination of Water and Wastewater: Centennial Edition, 21st ed. American Public Health Association., Washington, D.C.

Ehlmann, B.L., Bish, D.L., Ruff, S.W. and Mustard, J.F. (2012) Mineralogy and chemistry of altered Icelandic basalts: Application to clay mineral detection and understanding aqueous environments on Mars. Journal of Geophysical Research 117.

Ehlmann, B.L., Mustard, J.F., Murchie, S.L., Bibring, J.P., Meunier, A., Fraeman, A.A. and Langevin, Y. (2011) Subsurface water and clay mineral formation during the early history of Mars. Nature 479, 53-60.

Ehlmann, B.L., Mustard, J.F., Swayze, G.A., Clark, R.N., Bishop, J.L., Poulet, F., Des Marais, D.J., Roach, L.H., Milliken, R.E., Wray, J.J., Barnouin-Jha, O. and Murchie, S.L. (2009) Identification of hydrated silicate minerals on Mars using MRO-CRISM: Geologic context near Nili Fossae and implications for aqueous alteration. Journal of Geophysical Research: Planets 114, E00D08.

Fairen, A.G., Davila, A.F., Gago-Duport, L., Amils, R. and McKay, C.P. (2009) Stability against freezing of aqueous solutions on early Mars. Nature 459, 401-404.

Fishman, M. and Friedman, L.C. (1989) Techniques of water-resources investigations of the United States Geological Survey. Chapter A1: Methods for Determination of Inorganic Substances in Water and Fluvial Sediments, TWRI, 5-A1.

Furrer, G., Zysset, M. and Schindler, P. (1993) Weathering kinetics of montmorillonite: Investigations in batch and mixed-flow reactors. Geochemistry of clay-pore fluid interaction 4, 243-262.

Gainey, S.R., Hausrath, E.M., Hurowitz, J.A. and Milliken, R.E. (2014) Nontronite dissolution rates and implications for Mars. Geochimica et Cosmochimica Acta 126, 192-211.

Ganor, J., Mogollón, J.L. and Lasaga, A.C. (1995) The effect of pH on kaolinite dissolution rates and on activation energy. Geochimica et Cosmochimica Acta 59, 1037-1052.

Govett, G. (1961) Critical factors in the colorimetric determination of silica. Analytica Chimica Acta 25, 69-80.

Grant, W.D. (2004) Life at low water activity. Philosophical transactions of the Royal Society of London. Series B, Biological sciences 359, 1249-1266; discussion 1266-1247.

Haberle, R.M., McKay, C.P., Schaeffer, J., Cabrol, N.A., Grin, E.A., Zent, A.P. and Quinn, R. (2001) On the possibility of liquid water on present-day Mars. Journal of Geophysical Research E: Planets 106, 23317-23326.

Harter, R.D. and Naidu, R. (2001) An assessment of environmental and solution parameter impact on trace-metal sorption by soils. Soil Science Society of America Journal 65, 597-612.

Haskin, L.A., Wang, A., Jolliff, B.L., McSween, H.Y., Clark, B.C., Des Marais, D.J., McLennan, S.M., Tosca, N.J., Hurowitz, J.A. and Farmer, J.D. (2005) Water alteration of rocks and soils on Mars at the Spirit rover site in Gusev crater. Nature 436, 66-69.

Hausrath, E., Treiman, A., Vicenzi, E., Bish, D., Blake, D., Sarrazin, P., Hoehler, T., Midtkandal, I., Steele, A. and Brantley, S. (2008) Short-and long-term olivine weathering in Svalbard: implications for Mars. Astrobiology 8, 1079-1092.

Hausrath, E.M. and Brantley, S.L. (2010) Basalt and olivine dissolution under cold, salty, and acidic conditions: What can we learn about recent aqueous weathering on Mars? Journal of Geophysical Research 115.

Hecht, M.H. (2002) Metastability of Liquid Water on Mars. Icarus 156, 373-386.

Henderson-Sellers, A. and Meadows, A.J. (1976) The evolution of the surface temperature of Mars. Planetary and Space Science 24, 41-44.

Huertas, F.J., Caballero, E., Jiménez De Cisneros, C., Huertas, F. and Linares, J. (2001) Kinetics of montmorillonite dissolution in granitic solutions. Applied Geochemistry 16, 397-407.

Huertas, F.J., Chou, L. and Wollast, R. (1999a) Mechanism of kaolinite dissolution at room temperature and pressure Part II: kinetic study. Geochimica et Cosmochimica Acta 63, 3261-3275.

Huertas, F.J., Fiore, S., Huertas, F. and Linares, J. (1999b) Experimental study of the hydrothermal formation of kaolinite. Chemical Geology 156, 171-190.

Icenhower, J.P. and Dove, P.M. (2000) The dissolution kinetics of amorphous silica into sodium chloride solutions: Effects of temperature and ionic strength. Geochimica et Cosmochimica Acta 64, 4193-4203.

Icopini, G.A., Brantley, S.L. and Heaney, P.J. (2005) Kinetics of silica oligomerization and nanocolloid formation as a function of pH and ionic strength at 25 C. Geochimica et Cosmochimica Acta 69, 293-303.

Iler, R.K. (1979) The chemistry of silica.

Ingersoll, A.P. (1970) Mars: Occurrence of Liquid Water. Science 168, 972-973.

Jones, E.G. and Lineweaver, C.H. (2010) To what extent does terrestrial life "follow the water"? Astrobiology 10, 349-361.

Keeling, J.L., Raven, M.D. and Gates, W.P. (2000) Geology and characterization of two hydrothermal nontronites from weathered metamorphic rocks at the Uley Graphite Mine, South Australia. Clays and Clay Minerals 48, 537-548.

Knauth, L.P. and Burt, D.M. (2002) Eutectic Brines on Mars: Origin and Possible Relation to Young Seepage Features. Icarus 158, 267-271.

Kraft, M.D., Michalski, J.R. and Sharp, T.G. (2003) Effects of pure silica coatings on thermal emission spectra of basaltic rocks: Considerations for Martian surface mineralogy. Geophysical Research Letters 30.

Kreslavsky, M.A. and Head, J.W. (2009) Slope streaks on Mars: A new "wet" mechanism. Icarus 201, 517-527.

Loizeau, D., Mangold, N., Poulet, F., Ansan, V., Hauber, E., Bibring, J.-P., Gondet, B., Langevin, Y., Masson, P. and Neukum, G. (2010) Stratigraphy in the Mawrth Vallis region through OMEGA, HRSC color imagery and DTM. Icarus 205, 396-418.

Martín-Torres, F.J., Zorzano, M.-P., Valentín-Serrano, P., Harri, A.-M., Genzer, M., Kemppinen, O., Rivera-Valentin, E.G., Jun, I., Wray, J., Bo Madsen, M., Goetz, W., McEwen, A.S., Hardgrove, C., Renno, N., Chevrier, V.F., Mischna, M., Navarro-González, R., Martínez-Frías, J., Conrad, P., McConnochie, T., Cockell, C., Berger, G., R. Vasavada, A., Sumner, D. and Vaniman, D. (2015) Transient liquid water and water activity at Gale crater on Mars. Nature Geoscience.

Martínez, G.M. and Renno, N.O. (2013) Water and Brines on Mars: Current Evidence and Implications for MSL. Space Science Reviews 175, 29-51.

Marty, N.C.M., Cama, J., Sato, T., Chino, D., Villiéras, F., Razafitianamaharavo, A., Brendlé, J., Giffaut, E., Soler, J.M., Gaucher, E.C. and Tournassat, C. (2011) Dissolution kinetics of synthetic Na-smectite. An integrated experimental approach. Geochimica et Cosmochimica Acta 75, 5849-5864.

McEwen, A.S., Ojha, L., Dundas, C.M., Mattson, S.S., Byrne, S., Wray, J.J., Cull, S.C., Murchie, S.L., Thomas, N. and Gulick, V.C. (2011) Seasonal flows on warm Martian slopes. Science 333, 740-743.

McKeown, N.K., Bishop, J.L., Noe Dobrea, E.Z., Ehlmann, B.L., Parente, M., Mustard, J.F., Murchie, S.L., Swayze, G.A., Bibring, J.P. and Silver, E.A. (2009) Characterization of phyllosilicates observed in the central Mawrth Vallis region, Mars, their potential formational processes, and implications for past climate. Journal of Geophysical Research: Planets (1991–2012) 114.

Metz, V., Amram, K. and Ganor, J. (2005) Stoichiometry of smectite dissolution reaction. Geochimica et Cosmochimica Acta 69, 1755-1772.

Michalski, J. and Fergason, R. (2009) Composition and thermal inertia of the Mawrth Vallis region of Mars from TES and THEMIS data. Icarus 199, 25-48.

Michalski, J., Poulet, F., Bibring, J.-P. and Mangold, N. (2010) Analysis of phyllosilicate deposits in the Nili Fossae region of Mars: Comparison of TES and OMEGA data. Icarus 206, 269-289.

Michalski, J.R., Kraft, M.D., Diedrich, T., Sharp, T.G. and Christensen, P.R. (2003) Thermal emission spectroscopy of the silica polymorphs and considerations for remote sensing of Mars. Geophysical research letters 30.

Michalski, J.R., Kraft, M.D., Sharp, T.G., Williams, L.B. and Christensen, P.R. (2005) Mineralogical constraints on the high-silica martian surface component observed by TES. Icarus 174, 161-177.

Milliken, R., Grotzinger, J. and Thomson, B. (2010) Paleoclimate of Mars as captured by the stratigraphic record in Gale Crater. Geophysical Research Letters 37.

Ming, D.W., Gellert, R., Morris, R.V., Arvidson, R.E., Brückner, J., Clark, B.C., Cohen, B.A., D'Uston, C., Economou, T., Fleischer, I., Klingelhöfer, G., McCoy, T.J., Mittlefehldt, D.W., Schmidt, M.E., Schröder, C., Squyres, S.W., Tréguier, E., Yen, A.S. and Zipfel, J. (2008) Geochemical properties of rocks and soils in Gusev Crater, Mars: Results of the Alpha Particle X-Ray Spectrometer from Cumberland Ridge to Home Plate. Journal of Geophysical Research E: Planets 113.

Murchie, S.L., Mustard, J.F., Ehlmann, B.L., Milliken, R.E., Bishop, J.L., McKeown, N.K., Noe Dobrea, E.Z., Seelos, F.P., Buczkowski, D.L., Wiseman, S.M., Arvidson, R.E., Wray, J.J., Swayze, G., Clark, R.N., Des Marais, D.J., McEwen, A.S. and Bibring, J.P. (2009) A synthesis of Martian aqueous mineralogy after 1 Mars year of observations from the Mars Reconnaissance Orbiter. Journal of Geophysical Research E: Planets 114.

Mustard, J.F., Murchie, S.L., Pelkey, S.M., Ehlmann, B.L., Milliken, R.E., Grant, J.A., Bibring, J.P., Poulet, F., Bishop, J., Dobrea, E.N., Roach, L., Seelos, F., Arvidson, R.E., Wiseman, S., Green, R., Hash, C., Humm, D., Malaret, E., McGovern, J.A., Seelos, K., Clancy, T., Clark, R., Des Marais, D., Izenberg, N., Knudson, A., Langevin, Y., Martin, T., McGuire, P., Morris, R., Robinson, M., Roush, T., Smith, M., Swayze, G., Taylor, H., Titus, T. and Wolff, M. (2008) Hydrated silicate minerals on Mars observed by the Mars Reconnaissance Orbiter CRISM instrument. Nature 454, 305-309.

Nagy, K. (1995) Dissolution and precipitation kinetics of sheet silicates. Reviews in Mineralogy and Geochemistry 31, 173-233.

Nagy, K.L., Blum, A.E. and Lasaga, A.C. (1991) Dissolution and precipitation kinetics of kaolinite at 80°C and pH 3: the dependence on solution saturation state. American Journal of Science 291, 649-686.

Niles, P.B., Boynton, W.V., Hoffman, J.H., Ming, D.W. and Hamara, D. (2010) Stable isotope measurements of martian atmospheric CO2 at the Phoenix landing site. Science 329, 1334-1337.

Noe Dobrea, E., Bishop, J., McKeown, N., Fu, R., Rossi, C., Michalski, J., Heinlein, C., Hanus, V., Poulet, F. and Mustard, R. (2010) Mineralogy and stratigraphy of phyllosilicate‐bearing

and dark mantling units in the greater Mawrth Vallis/west Arabia Terra area: Constraints on geological origin. Journal of Geophysical Research: Planets (1991–2012) 115.

Olsen, A.A., Hausrath, E.M. and Rimstidt, J.D. (2015) Forsterite dissolution rates in Mg-sulfate-rich Mars-analog brines, and implications the aqueous history of Mars.

Osterloo, M.M., Anderson, F.S., Hamilton, V.E. and Hynek, B.M. (2010) Geologic context of proposed chloride-bearing materials on Mars. Journal of Geophysical Research E: Planets 115.

Osterloo, M.M., Hamilton, V.E., Bandfield, J.L., Glotch, T.D., Baldridge, A.M., Christensen, P.R., Tornabene, L.L. and Anderson, F.S. (2008) Chloride-Bearing Materials in the Southern Highlands of Mars. Science 319, 1651-1654.

Palandri, J.L. and Kharaka, Y.K. (2004) A compilation of rate parameters of water-mineral interaction kinetics for application to geochemical modeling. DTIC Document.

Parkhurst, D.L. and Appelo, C. (1999) User's guide to PHREEQC (Version 2): A computer program for speciation, batch-reaction, one-dimensional transport, and inverse geochemical calculations.

Poulet, F., Bibring, J.P., Mustard, J.F., Gendrin, A., Mangold, N., Langevin, Y., Arvidson, R.E., Gondet, B., Gomez, C., Berthe, M., Erard, S., Forni, O., Manaud, N., Poulleau, G., Soufflot, A., Combes, M., Drossart, P., Encrenaz, T., Fouchet, T., Melchiorri, R., Bellucci, G., Altieri, F., Formisano, V., Fonti, S., Capaccioni, F., Cerroni, P., Coradini, A., Korablev, O., Kottsov, V., Ignatiev, N., Titov, D., Zasova, L., Pinet, P., Schmitt, B., Sotin, C., Hauber, E., Hoffmann, H., Jaumann, R., Keller, U., Forget, F. and Omega, T. (2005) Phyllosilicates on Mars and implications for early martian climate. Nature 438, 623-627.

Pritchett, B.N., Elwood Madden, M.E. and Madden, A.S. (2012) Jarosite dissolution rates and maximum lifetimes in high salinity brines: Implications for Earth and Mars. Earth and Planetary Science Letters 357-358, 327-336.

Rao, M.N., Sutton, S.R., McKay, D.S. and Dreibus, G. (2005) Clues to Martian brines based on halogens in salts from nakhlites and MER samples. Journal of Geophysical Research E: Planets 110, 1-12.

Rard, J.A. and Clegg, S.L. (1997) Critical Evaluation of the Thermodynamic Properties of Aqueous Calcium Chloride. 1. Osmotic and Activity Coefficients of 0-10.77 mol⊙ kg-1 Aqueous Calcium Chloride Solutions at 298.15 K and Correlation with Extended Pitzer Ion-Interaction Models. Journal of Chemical & Engineering Data 42, 819-849.

Rennó, N.O., Bos, B.J., Catling, D., Clark, B.C., Drube, L., Fisher, D., Goetz, W., Hviid, S.F., Keller, H.U., Kok, J.F., Kounaves, S.P., Leer, K., Lemmon, M., Madsen, M.B., Markiewicz, W.J., Marshall, J., McKay, C., Mehta, M., Smith, M., Zorzano, M.P., Smith, P.H., Stoker, C. and Young, S.M.M. (2009) Possible physical and thermodynamical evidence for liquid water at the Phoenix landing site. Journal of Geophysical Research 114.

Rozalén, M.L., Huertas, F.J., Brady, P.V., Cama, J., García-Palma, S. and Linares, J. (2008) Experimental study of the effect of pH on the kinetics of montmorillonite dissolution at 25°C. Geochimica et Cosmochimica Acta 72, 4224-4253.

Smith, P.H., Tamppari, L.K., Arvidson, R.E., Bass, D., Blaney, D., Boynton, W.V., Carswell, A., Catling, D.C., Clark, B.C., Duck, T., DeJong, E., Fisher, D., Goetz, W., Gunnlaugsson, H.P., Hecht, M.H., Hipkin, V., Hoffman, J., Hviid, S.F., Keller, H.U., Kounaves, S.P., Lange, C.F., Lemmon, M.T., Madsen, M.B., Markiewicz, W.J., Marshall, J., McKay, C.P., Mellon, M.T., Ming, D.W., Morris, R.V., Pike, W.T., Renno, N., Staufer, U., Stoker, C., Taylor, P., Whiteway, J.A. and Zent, A.P. (2009) H20 at the phoenix landing site. Science 325, 58-61.

Soong, C. (1993) Hydrothermal kinetics of kaolinite-water interaction at pH 4.2 and 7.3, 130 C to 230 C. Pennsylvania State University.

Sverdrup, H.U. (1990) The kinetics of base cation release due to chemical weathering.

Thomson, B.J., Bridges, N.T., Milliken, R., Baldridge, A., Hook, S.J., Crowley, J.K., Marion, G.M., de Souza Filho, C.R., Brown, A.J. and Weitz, C.M. (2011) Constraints on the origin and evolution of the layered mound in Gale Crater, Mars using Mars Reconnaissance Orbiter data. Icarus 214, 413-432.

Tosca, N.J. and McLennan, S.M. (2006) Chemical divides and evaporite assemblages on Mars. Earth and Planetary Science Letters 241, 21-31.

Tu, V.M., Hausrath, E.M., Tschauner, O., Iota, V. and Egeland, G.W. (2014) Dissolution rates of amorphous Al-and Fe-phosphates and their relevance to phosphate mobility on Mars. American Mineralogist 99, 1206-1215.

Velde, B. (1995) Composition and mineralogy of clay minerals, Origin and mineralogy of clays. Springer, pp. 8-42.

Wang, A., Haskin, L.A., Squyres, S.W., Jolliff, B.L., Crumpler, L., Gellert, R., Schröder, C., Herkenhoff, K., Hurowitz, J., Tosca, N.J., Farrand, W.H., Anderson, R. and Knudson, A.T. (2006) Sulfate deposition in subsurface regolith in Gusev crater, Mars. Journal of Geophysical Research E: Planets 111.

Welch, S.A. and Ullman, W.J. (2000) The temperature dependence of bytownite feldspar dissolution in neutral aqueous solutions of inorganic and organic ligands at low temperature (5–35 C). Chemical Geology 167, 337-354.

Wieland, E. and Stumm, W. (1992) Dissolution kinetics of kaolinite in acidic aqueous solutions at 25°C. Geochimica et Cosmochimica Acta 56, 3339-3355.

Wray, J., Ehlmann, B., Squyres, S., Mustard, J. and Kirk, R. (2008) Compositional stratigraphy of clay‐bearing layered deposits at Mawrth Vallis, Mars. Geophysical Research Letters 35.

Zysset, M. and Schindler, P.W. (1996) The proton promoted dissolution kinetics of K-montmorillonite. Geochimica et Cosmochimica Acta 60, 921-931.

Curriculum Vitae

Michael Steiner

University of Nevada, Las Vegas
Department of Geoscience
4505 South Maryland Parkway
Las Vegas, NV 89154

Steine18@unlv.nevada.edu
Phone: (313) 350-7694

EDUCATION

University of Nevada, Las Vegas, 2013-Present
M.S. in Geology
Advisor Dr. Elisabeth Hausrath

University of Nevada, Las Vegas, 2008-2013
B.S. in Geology

CERTIFICATIONS

40-Hour HAZWOPER

EMPLOYMENT AND RESEARCH EXPERIENCE

Graduate Teaching Assistant, January 2014- Present

- Geology 101 Online Lab Instructor
  - Maintain communication between 150 students through email and discussion boards.
  - Evaluate and grade assignments on a weekly basis.
  - Be available for additional instruction during office hour periods.

Graduate Research Assistant, July 2013-Present

- Dissolution of Nontronite in High Ionic Strength Brines and Implications for Habitable Environments on Mars.
- Train and supervise undergraduate lab assistants.

Undergraduate Research Assistant , March 2012 - June 2013

- Hausrath Geochemistry Lab
  - Perform analysis for master's and Ph.D students.
  - Conduct research for an independent study investigating potential biosignature phosphate minerals relevant to Mars.
  - Laboratory maintenance and upkeep.

Research Experiences for Undergraduates (REU), University of Nevada, Las Vegas, June-August 2012 (research mentor: Dr. Elisabeth Hausrath, program director: Dr. Kurt Regner)

- Investigation of potential phosphate biominerals in Mars analog solutions.
- Possible "sign of life" to be used by the Mars Science Laboratory on its current mission.

Resident Assistant , August 2010 - May 2012

- UNLV Housing and Residential Life
  - Facilitate a living environment for a floor of 40 student residents ranging from freshmen to graduate.
  - Oversee a student committee that planned and executed programs that benefited both students and neighboring communities.
  - Trained as a mediator to resolve student conflicts.

PRESENTATIONS AND ABSTRACTS

Steiner, M., Schofield, R., Hausrath, E. Dissolution of Nontronite in High Ionic Strength Brines and Implications for Mars Habitability. Poster presented at: 9th Annual UNLV Geosymposium. 2014 April 18; Las Vegas, NV.

Steiner, M., Schofield, R., Hausrath, E. Dissolution of Nontronite in High Ionic Strength Brines and Implications for Mars Habitability. Poster presented at: 45th Lunar and Planetary Science Conference. 2014 March 20; The Woodlands, TX.

Schofield, R. **Steiner, M.** Hausrath, E. Dissolution of nontronite: Implications for habitable environments on Mars. Poster session presented at: UNLV Undergraduate Research Symposium. 2013 August 8; Las Vegas, NV.

Steiner, M. Hausrath, E. Sun, H. Synthesis of potential phosphate biosignature minerals from Mars analog solutions. Poster presented at: 44th Lunar and Planetary Science Conference. 2013 March 21; The Woodlands, TX.

Steiner, M. Hausrath, E. Sun, H. Biosignature minerals and Mars analog solutions. Poster session presented at: UNLV Undergraduate Research Symposium. 2012 August 7; Las Vegas, NV.

AWARDS AND HONORS

UNLV Graduate and Professional Student Association Research Forum Poster – Honorable Mention (2015)
UNLV Geosymposium Best Graduate Poster - 2nd Place (2014)
Edwards and Olswang Geology Scholarship (2014)
UNLV Graduate and Professional Student Association Sponsorship Funding (2013)
Nevada NASA Space Grant Consortium Undergraduate Scholarship (2013)

UNLV Geosymposium Best Undergraduate Poster - 2nd Place (2013)
NSF Bio REU Travel Scholarship (2013)
Beranda French Scholarship (2012, 2013, 2014)
National Residence Hall Honorary Outstanding Leadership Service Award (2011)
Resident Assistant of the Year (2011) awarded by UNLV Housing and Residential Life

MEMBERSHIPS AND PROFFESIONAL ASSOCIATIONS

- Geologic Society of America, July 2012-present
- American Geophysical Union, July 2012-present
- Geologic Society of Nevada, January 2012-present